Adaptive Coarse Spaces for FETI-DP and BDDC Methods

INAUGURAL-DISSERTATION

zur

Erlangung des Doktorgrades

der Mathematisch-Naturwissenschaftlichen Fakultät

der Universität zu Köln

vorgelegt von

Patrick Radtke

aus Bottrop

Berichterstatter: Prof. Dr. Axel Klawonn, Universität zu Köln

Prof. Dr. Oliver Rheinbach, TU Bergakademie Freiberg

Prof. Dr. Olof B. Widlund, New York University

Tag der mündlichen Prüfung: 23. 10. 2015

Contents

List of Figures

List of Tables

Abstract

Iterative substructuring methods are well suited for the parallel iterative solution of elliptic partial differential equations. These methods are based on subdividing the computational domain into smaller nonoverlapping subdomains and solving smaller problems on these subdomains. The solutions are then joined to a global solution in an iterative process. In case of a scalar diffusion equation or the equations of linear elasticity with a diffusion coefficient or Young modulus, respectively, constant on each subdomain, the numerical scalability of iterative substructuring methods can be proven. However, the convergence rate deteriorates significantly if the coefficient in the underlying partial differential equation (PDE) has a high contrast across and along the interface of the substructures. Even sophisticated scalings often do not lead to a good convergence rate. One possibility to enhance the convergence rate is to choose appropriate primal constraints. In the present work three different adaptive approaches to compute suitable primal constraints are discussed. First, we discuss an adaptive approach introduced by Dohrmann and Pechstein that draws on the operator P_D which is an important ingredient in the analysis of iterative substructuring methods like the dual-primal Finite Element Tearing and Interconnecting (FETI-DP) method and the closely related Balancing Domain Decomposition by Constraints (BDDC) method. We will also discuss variations of the method by Dohrmann and Pechstein introduced by Klawonn, Radtke, and Rheinbach. Secondly, we describe an adaptive method introduced by Mandel and Sousedík which is also based on the P_D-operator. Recently, a proof for the condition number bound in this method was provided by Klawonn, Radtke, and Rheinbach. Thirdly, we discuss an adaptive approach introduced by Klawonn, Radtke, and Rheinbach that enforces a Poincaré- or Korn-like inequality and an extension theorem. In all approaches generalized eigenvalue problems are used to compute a coarse space that leads to an upper bound of the condition number which is

independent of the jumps in the coefficient and depend on an a priori prescribed tolerance. Proofs and numerical tests for all approaches are given in two dimensions. Finally, all approaches are compared.

Übersicht

Nichtüberlappende Gebietszerlegungsverfahren sind geeignete Methoden zur parallelen iterativen Lösung elliptischer partieller Differentialgleichungen. In diesen Verfahren wird das Gebiet in kleinere Teilgebiete zerlegt und es werden kleinere Probleme auf den Teilgebieten gelöst. Anschließend werden in einem iterativen Prozeßdie Lösungen zu einer globalen Lösung zusammengefügt. Im Fall von skalaren Diffusionsproblemen oder linearer Elastizität mit einem Koeffizienten oder einem Elastizitätsmodul der konstant auf jedem Teilgebiet ist, kann die numerische Skalierbarkeit dieser Verfahren bewiesen werden. Jedoch verschlechtert sich die Konvergenzrate beträchtlich, falls der Koeffizient der zugrundeliegenden partiellen Differentialgleichung (PDGL) sowohl entlang als auch über Teilgebietsgrenzen hinweg einen hohen Kontrast aufweist. Auch anspruchsvolle Skalierungen führen häufig nicht zu einer guten Konvergenz. Eine Möglichkeit die Konvergenz zu verbessern besteht darin, passende primale Bedingungen zu wählen. In der vorliegenden Arbeit werden drei verschiedene Herangehensweisen vorgestellt um adäquate Bedingungen zu berechnen. Zuerst wird ein adaptiver Ansatz von Dohrmann und Pechstein dargestellt. Dieser Ansatz nutzt den P_D-Operator, welcher eine wichtige Rolle in der Analysis von iterativen Substrukturierungsmethoden wie der dual-primal Finite Element Tearing and Interconnecting (FETI-DP) Methode und der eng verwandten Balancing Domain Decomposition by Constraints (BDDC) Methode spielt. Außerdem werden Varianten des Algorithmus von Dohrmann und Pechstein diskutiert, welche von Klawonn, Radtke und Rheinbach eingeführt wurden. Zweitens wird ein adaptiver Algorithmus von Mandel und Sousedík vorgestellt, der auch am P_D-Operator ansetzt. Kürzlich wurde eine Konditionszahlabschätzung für diesen Algorithmus in zwei Raumdimensionen von Klawonn, Radtke und Rheinbach bewiesen. Drittens wird ein adaptiver Algorithmus bewiesen, welcher von Klawonn, Radtke und Rheinbach eingeführt wurde und Bedingungen berechnet,

die eine Poincaré ähnliche Ungleichung und einen Fortsetzungssatz ermöglicht. In allen Ansätzen werden verallgemeinerte Eigenwertprobleme verwendet um einen Grobgitterraum auszurechnen, der zu einer oberen Schranke der Konditionszahl führt, welche unabhängig von Sprüngen im Koeffizienten ist und von einer a priori vorgegebenen Toleranz abhängt. Es werden Beweise aller Verfahren und numerische Tests für zwei Raumdimensionen dargelegt. Abschließend werden alle Verfahren verglichen.

Acknowledgements

First, I would like to thank my advisor Prof. Dr. Klawonn for the interesting topic and the time he devoted to me and my work. I am also grateful for the possibility to research in his group and for the scientific guidance and many fruitful discussions we had during the last years. I like to thank Prof. Dr. Rheinbach for all his support and I am also thankful for his implementations of the FETI-DP algorithm. I am happy to thank all of my former and current colleagues, Dres. Sabrina Gippert, Martin Lanser, Andreas Fischle and Alexander Heinlein, Martin Kühn, with whom I had a great time discussing scientific issues as well as spending free time together. I owe special thanks to Sabrina Gippert, Alexander Heinlein, and Martin Kühn for the good time sharing an office together. I would not be at this point without the support of my family, especially my parents to whom I would like to express my gratitude for all the support and encouragement. I am also happy to thank my wife for her encouragement and support.

Introduction

Many physical processes in nature can be modeled by partial differential equations (PDEs). In engineering applications, e.g., structural mechanics, in particular elliptic partial differential equations play an important role. Under certain conditions, e.g., on the boundary and the underlying domain, the existence and uniqueness of a solution can be proven. Solutions to these equations on specific domains can be impossible to derive analytically. However, numerical algorithms can often solve the equations approximately up to a sufficient precision. With an increasing computational effort the accuracy of the solution will be improved. One of these methods is the Finite Element Method. The precision is mainly limited by the available computational resources and the condition of the problem. Usually, the required precision of the approximate solution dictates the size of a system of linear equations that has to be solved, either by direct or iterative methods. In Finite Element Methods the dimension of the space of finite element functions V^h determines the accuracy of the solution. This results in very large systems of equations. Additionally, these systems are mostly ill-conditioned. Direct methods have a complexity which depends polynomially on the number of unknowns and have a high demand of memory. At a certain size, a linear system is therefore not solvable in a reasonable time with a direct method and iterative algorithms are needed. Since the convergence of iterative methods applied to elliptic systems heavily depends on the condition number, they need good preconditioners.

Modern computers have an increasingly parallel architecture and require

new algorithms that perform efficiently in these environments. An efficient approach to parallelize the finite element method for the use on modern parallel computers are domain decomposition methods (DDMs). These methods are based on subdivision of the computational domain of the PDE into many subdomains which makes it possible to solve many smaller problems on many processors at the same time instead of solving one big problem in a sequential way. The subdivision can be either overlapping or nonoverlapping. Unfortunately, communication is still needed between the subproblems such that the parallelism is not trivial. A small global problem needs to be solved additionally, to join the solutions of the subproblems to a global solution of the PDE.

The concept of scalability of a parallel algorithm was introduced to denote if an algorithm performs well on parallel machines. The performance of DDMs is mainly driven by two kinds of scalability, i.e., numerical and parallel scalability. Numerical scalability is achieved if a domain decomposition algorithm solves problems of different sizes with the same number of iterations. A DDM is weakly parallel scalable if the runtime to solution remains constant while increasing the number of unknowns and the number of processors by the same factor. Strong parallel scalability is attained if a problem with constant size is solved in half the time by doubling the number of processors. Two very successful nonoverlapping decomposition methods are the FETI-DP and BDDC algorithms, which have been introduced in [23] and [14], respectively. These algorithms have been proven to be numerical scalable for different partial differential equations under certain assumptions [61, 56, 49, 52, 83, 53, 66] and achieve strong parallel scalability in simulations; see, e.g., [23, 14, 43, 44, 55].

The preconditioned system obtained by solving elliptic problems by DDMs is usually positive definite and solved by the preconditioned conjugate gradients method (PCG). The convergence rate of PCG is determined by the con-

dition number. Thus it is an important indicator for the numerical scalability. The condition number in FETI-DP and BDDC highly depends on the chosen primal variables and the underlying equation. For scalar elliptic equations in two dimensions with constant coefficients on each subdomain it suffices to choose constraints associated with the vertices at the cross points of subdomains as primal variables, e.g., the cross points of the subdomain interfaces. This results in a condition number which is bounded by $C\left(1+\log\left(\frac{H}{h}\right)\right)^2$, where H/h is a measure for the number of degrees of freedom in each subdomain and the constant is often independent of critical parameters, such as coefficient jumps. The iteration counts grow only weakly in a logarithmical sense with the number of unknowns in each subdomain. In three dimensions edge averages over edges of the subdomains need to be chosen primal to obtain the same bound.

However, for a general distribution of coefficient jumps, the constant in the condition number bound can depend on the contrast of the coefficient function if the coarse space is not chosen appropriately. In the classical theory the constant in the condition number bound depends, among others, on constants in the Poincaré or Korn inequality and in the extension theorem [72, 82]. In [72] a detailed analysis of constants in weighted Poincaré inequalities for different coefficient functions is given. Certain coefficient functions that satisfy a quasimonotonicity condition result in a Poincaré constant that is independent of the contrast in the coefficient function. An application to iterative substructuring methods can result in a condition number bound independent of the contrast in the coefficient if weighted edge averages are used [71, 45]. However, in many cases the Poincaré constant depends on the jump in the coefficient.

Adaptive coarse spaces have been developed to obtain robust condition number estimates in these cases. Typically these coarse spaces are selected by computing certain eigenvectors of local generalized eigenvalue problems. In

[4] an adaptive coarse space construction for a two-level Neumann-Neumann method was discussed where low energy modes related to the substructure are included in the Neumann-Neumann coarse solve. In [3] this approach was considered in the context of a large scale industrial finite element solver and applied to industrial problems. In [59, 60, 58] localized indicators of the condition number depending on a localization of the P_D-operator, used in the analysis of iterative substructuring, on two neighboring subdomains are heuristically developed. An adaptive coarse space was designed to guarantee that this indicators are small. An abstract coarse space for overlapping Schwarz algorithms has been developed in [79, 80]. Recently, in [81] a variant for FETI and BDD based on this Schwarz coarse space was established. This coarse space relies on the solution of eigenvalue problems that have the size of one subdomain interface which are based on a localization of the preconditioner to the neighborhood of the subdomains. Some related block strategies to this adaptive coarse space were considered in [30]. In a recent paper [78] an adaptive strategy without explicitly solving generalized eigenvalue problems but using an adaptive strategy inside of a multi-preconditioned conjugate gradients algorithm has been proposed. An adaptive coarse space for two-level Schwarz preconditioners that is based on certain eigenvalue problems with stiffness and mass matrices was analyzed in [28, 27]. In [32] generalized eigenvalue problems with stiffness and mass matrices have been used for the computation of a special finite element discretization instead of for the enrichment of the coarse space. This computation has been carried out in parallel. In [42], we introduced a coarse space designed to replace weighted Poincaré inequalities and an extension theorem. A coarse space related to a local P_D-estimate and an extension theorem was developed in [35]. Recently, Dohrmann and Pechstein [68] proposed an adaptive coarse space for BDDC methods which is based on a localization of P_D-estimates to equivalence classes. We proposed a variant of this method using different kinds

of scalings in [39]. In [38], we presented a comparison of the approaches in [59, 68, 39, 42] as well as a proof of the condition number estimate in two dimensions for the coarse space given in [59], new variants of the algorithms in [68, 39, 42] based on eigenvalue problems on slabs instead of subdomains, and a new scaling for the coarse space from [42].

This thesis has the following outline: In Chapter 1, we first introduce various model problems and their variational formulations. We review the FETI-DP and BDDC domain decomposition methods and give an overview on how to implement arbitrary primal constraints using a transformation of basis or projector preconditioning. In the last section of this chapter, we provide some spectral estimates that we will use throughout the thesis.

In the following three chapters we elaborate on three different approaches to compute adaptive primal constraints in the FETI-DP and BDDC methods for difficult problems, e.g., a high contrast in the coefficient of the underlying PDE. In Chapter 2, we describe approaches recently introduced in [68] with variants developed in [39, 38]. In Chapter 3, we briefly sketch an adaptive coarse space developed in [59] and give a condition number estimate for this coarse space in two dimensions; see also [38]. We also give an example for an application to a Newton-Krylov algorithm for perfect plasticity. In Chapter 4, we provide an adaptive approach, designed closely on the classical theory of substructuring methods for elliptic equations aiming at replacing certain inequalities such that the constants in these inequalities become independent of critical parameters. The Poincaré inequality and an extension theorem are replaced by estimates obtained from the solution of appropriate eigenvalue problems. We introduced this approach in [42, 36]. In Chapter 5, we compare the different approaches regarding computational cost and give numerical examples.

1 Fundamentals

The present chapter contains concepts which will be frequently used throughout this thesis. In Section 1.1, we will introduce different model problems. Then, we will briefly recapitulate the Galerkin method for the discretization of the variational formulations in Section 1.1.1. In Sections 1.2 and 1.3, we will review two well known nonoverlapping domain decomposition algorithms, the FETI-DP and BDDC methods. Section 1.4 gives a brief exposition of how to transform the finite element basis in this methods to obtain arbitrary primal constraints. In Section 1.5, we will describe another possibility how to introduce additional primal constraints in a second coarse level. Finally, in Section 1.6, we will review two lemmas from linear algebra regarding eigenvectors of generalized eigenvalue problems.

1.1 Model Problems and Finite Elements

Let $\Omega \subset \mathbb{R}^d$, $d = 2, 3$ be a Lipschitz domain and $\partial\Omega_D \subset \partial\Omega$ a closed subset of positive measure where we impose Dirichlet boundary conditions. We denote by $\partial\Omega_N = \partial\Omega \setminus \partial\Omega_D$ the Neumann boundary. In the following we will introduce the Galerkin method and various model problems considered throughout this thesis.

1.1.1 The Galerkin Method

We define the Sobolev space

$$H_0^1(\Omega, \partial\Omega_D) := \{v \in H^1(\Omega) : v = 0 \text{ on } \partial\Omega_D\}.$$

Let $V = H_0^1(\Omega, \partial\Omega_D)$ in the scalar case or $V = H_0^1(\Omega, \partial\Omega_D)^d$ in the vector valued case. Consider a bilinear form $a(\cdot, \cdot)$, a linear functional $F(\cdot)$, and the variational problem: Find $u \in V$, such that

$$a(u, v) = F(v) \quad \forall\, v \in V.$$

The classical Galerkin approach is to replace the infinite dimensional space V by a finite dimensional subspace $V^h \subset V$, e.g. the space of conforming piecewise linear finite element functions. By replacement of $v \in V$ by $v_h \in V^h$ we obtain

$$a(u_h, v_h) = F(v_h) \qquad \forall v_h \in V^h. \tag{1.1}$$

Expressing $u_h = \sum_{i=1}^n u_i \varphi_i$ by the basis φ_i, $i = 1, \ldots, n$ of V^h and replacing v_h by the basis functions yields

$$\sum_{i=1}^{n} u_i a(\varphi_i, \varphi_j) = F(\varphi_j) \qquad \forall j = 1, \ldots, n$$

or equivalently

$$\mathbf{A}\mathbf{u} = \mathbf{b}, \tag{1.2}$$

with $\mathbf{A} = (a_{ij})_{i,j}$, $a_{ij} = a(\varphi_i, \varphi_j)$, $\mathbf{u} = (u_i)_i$, and $\mathbf{b} = (b_i)_i$, where $b_i = F(\varphi_i)$. In order to solve (1.1) we have to solve (1.2) for $\mathbf{u}$.

1.1.2 Diffusion Equation

Let $\rho(x) \in L^\infty(\Omega)$ be piecewise constant on Ω and constant on any finite element $T \in \mathcal{T}_h$ with $\rho(x) > 0$. We consider the scalar elliptic boundary

value problem

$$\begin{aligned} -\nabla \cdot (\rho \nabla u) &= f \quad \text{in} \quad \Omega, \\ \rho \nabla u \cdot \mathbf{n} &= 0 \quad \text{on } \partial\Omega_N, \\ u &= 0 \quad \text{on} \quad \partial\Omega_D, \end{aligned}$$

where $\mathbf{n}$ denotes the outer unit normal on Ω_N. We obtain the weak formulation: Find $u \in H_0^1(\Omega, \partial\Omega_D)$, such that

$$a(u, v) = F(v) \qquad \forall v \in H_0^1(\Omega, \partial\Omega_D),$$

where

$$a(u, v) = \int_\Omega \rho \, \nabla u \cdot \nabla v \, dx \quad \text{and} \quad F(v) = \int_\Omega f v \, dx.$$

1.1.3 Linear Elasticity

In linear elasticity, Ω can be interpreted as a body which is exposed to a volume force $\mathbf{f} \in L_2(\Omega)^d$ and a surface force $\mathbf{g} \in L_2(\partial\Omega_N)^d$, and deforms under their influence. The difference between the starting configuration and the deformed configuration is denoted as the displacement and can be expressed by a function $\mathbf{u} : \mathbb{R}^d \to \mathbb{R}^d$. The linear elastic strain is then given by the symmetric gradient

$$\varepsilon(\mathbf{u}) = \frac{1}{2} \left(\nabla(\mathbf{u}) + \nabla(\mathbf{u})^T \right).$$

In the linear elastic model the displacement $\mathbf{u}$ is the solution of the boundary value problem

$$\begin{aligned} -\text{div } \sigma(\mathbf{u}) &= \mathbf{f} \quad \text{in } \Omega, \\ \sigma(\mathbf{u}) \cdot \mathbf{n} &= \mathbf{g} \quad \text{on } \partial\Omega_N, \\ \mathbf{u} &= 0 \quad \text{on } \partial\Omega_D, \end{aligned}$$

where $\mathbf{n}$ denotes the outer unit normal on $\partial\Omega_N$. The tension tensor $\sigma(\mathbf{u})$ is given by $\sigma(\mathbf{u}) = \mathbb{C}\varepsilon(\mathbf{u})$ with the fourth order elasticity tensor $\mathbb{C}$ and can be

alternatively expressed by

$$\sigma(\mathbf{u}) = \lambda \mathrm{tr}\, \varepsilon(\mathbf{u}) I + 2\mu\varepsilon(\mathbf{u})$$

with the Lamé constants λ and μ. The Lamé constants of a material can easily be derived from Young's modulus E and Poisson's ratio ν by

$$\lambda = \frac{\nu E}{(1+\nu)(1-2\nu)} \quad \text{and} \quad \mu = \frac{E}{2(1+\nu)}.$$

In the following, we assume the material parameters to be piecewise constant on Ω and constant on any finite element $T \in \mathcal{T}_h$. By multiplication with a test function we obtain the variational formulation in the case of compressible linear elasticity: Find $\mathbf{u} \in H_0^1(\Omega, \partial\Omega_D)^d$, such that

$$a(u,v) = F(v) \quad \text{for all } v \in H_0^1(\Omega, \partial\Omega_D)^d,$$

$$\text{where} \quad a(u,v) = \int_\Omega \lambda \,\mathrm{div}(\mathbf{u})\,\mathrm{div}(\mathbf{v})\, dx + \int_\Omega 2\mu\varepsilon(\mathbf{u}) : \varepsilon(\mathbf{v})\, dx,$$

$$\text{and} \quad F(v) = \int_\Omega \mathbf{f}\cdot\mathbf{v}\, dx + \int_{\partial\Omega_N} \mathbf{g}\cdot\mathbf{v}\, ds.$$

For more details on linear elasticity in the finite element context, see, e.g., [5].

1.1.4 Almost Incompressible Linear Elasticity

For Poisson's ratio approaching 1/2, locking phenomena will occur in the standard displacement formulation. A well known remedy is to introduce a displacement-pressure saddle point formulation and its mixed finite element discretization. With the bilinear forms

$$a(\mathbf{u},\mathbf{v}) = \int_\Omega \mu\, \varepsilon(\mathbf{u}) : \varepsilon(\mathbf{v})\, dx,$$

$$b(\mathbf{v},p) = \int_\Omega \mathrm{div}(\mathbf{v}) p\, dx,$$

$$c(p,q) = \int_\Omega \frac{1}{\lambda} pq\, dx,$$

and the linear functional

$$F(\mathbf{v}) = \int_\Omega \mathbf{f} \cdot \mathbf{v}\, dx + \int_{\partial\Omega_N} \mathbf{g} \cdot \mathbf{v}\, ds$$

the saddle point variational formulation is of the form:
Find $(\mathbf{u}, p) \in H_0^1(\Omega, \partial\Omega_D)^d \times L^2(\Omega)$, such that

$$\begin{aligned} a(\mathbf{u}, \mathbf{v}) + b(\mathbf{v}, p) &= F(\mathbf{v}) \quad \forall\, \mathbf{v} \in H_0^1(\Omega, \partial\Omega_D)^d, \\ b(\mathbf{u}, q) - c(p, q) &= 0 \qquad \forall\, q \in L_2(\Omega). \end{aligned}$$

For a stable mixed finite element discretization, special care has to be taken of the choice of the finite element basis functions for the displacement and pressure. Only pairs of basis functions should be chosen that fulfill the discrete Babuška-Brezzi condition. For more details, see, e.g., [5]. The discretization results in the linear system

$$\begin{pmatrix} A & B^T \\ B & -C \end{pmatrix} \begin{pmatrix} u \\ p \end{pmatrix} = \begin{pmatrix} f \\ 0 \end{pmatrix}.$$

In our numerical examples we use $\mathbb{P}2 - \mathbb{P}0$ elements. These elements are inf-sup stable [7]. We can eliminate the discontinuous pressure elementwise to obtain the Schur complement $A + B^T C^{-1} B$.

1.1.5 Perfect Elastoplastic Material Model

First, we will introduce the locally nonlinear variational formulation. In the second paragraph, we will linearize this formulation by a Newton scheme with a globalization strategy. The presentation here is based on [40].

Variational Formulation

The material model is derived from the quasistatic equation of equilibrium

$$\operatorname{div} \sigma(x, t) = f(x, t);$$

see, e.g., [10, 75, 31]. Multiplying the equation with $\mathbf{v} \in H_0^1(\Omega, \partial\Omega_D)^d$ and application of the Gauss theorem yields the weak formulation:

Find $\mathbf{u} \in H_0^1(\Omega, \partial\Omega_D)^d$, such that for all $\mathbf{v} \in H_0^1(\Omega, \partial\Omega_D)^d$

$$\int_\Omega \sigma(\mathbf{u}) : \varepsilon(\mathbf{v}) dx = \int_\Omega \mathbf{f} \cdot \mathbf{v} dx + \int_{\partial\Omega_N} \mathbf{g} \cdot \mathbf{v} ds.$$

By discretization in time using the implicit Euler method, we obtain in the n-th timestep:

Find $\mathbf{u}_n \in H_0^1(\Omega, \partial\Omega_D)^d$, such that for all $\mathbf{v} \in H_0^1(\Omega, \partial\Omega_D)^d$

$$\int_\Omega \sigma_n : \varepsilon(\mathbf{v})\, dx = \int_\Omega \mathbf{f}_n \cdot \mathbf{v}\, dx + \int_{\partial\Omega_N} \mathbf{g}_n \cdot \mathbf{v}\, ds,$$

where σ_n is dependent on the displacement $\mathbf{u}_n$. This dependency is determined by the von Mises flow function and the chosen type of hardening. In this thesis, we consider perfect elastoplastic material behavior and hardening effects are absent. In this case, the von Mises flow function is given by

$$\Phi(\sigma) = |\mathrm{dev}(\sigma)| - \sigma_y,$$

where σ_y is the yield point of the material and the deviator of a tensor is defined by

$$\mathrm{dev}\,(\sigma) = \sigma - \frac{1}{d}\mathrm{tr}\,(\sigma)\mathrm{I}_{d\times d}.$$

The tension tensor in the n-th timestep is then linear elastic if $\Phi(\sigma_n) \leq 0$ and plastic otherwise. In the first case, we have

$$\sigma_n = (\lambda+\mu)\mathrm{tr}\left(\varepsilon(\mathbf{u}_n - \mathbf{u}_{n-1}) + \mathbb{C}^{-1}\sigma_{n-1}\right) + 2\mu\,\mathrm{dev}\left(\varepsilon(\mathbf{u}_n - \mathbf{u}_{n-1}) + \mathbb{C}^{-1}\sigma_{n-1}\right)$$

with the Lamé constants λ and μ and the fourth order elasticity tensor $\mathbb{C}$. In the second case, the tension tensor in the n-th timestep reads

$$\sigma_n = (\lambda+\mu)\mathrm{tr}\left(\varepsilon(\mathbf{u}_n - \mathbf{u}_{n-1}) + \mathbb{C}^{-1}\sigma_{n-1}\right)$$

$$+ \sigma_y \frac{\mathrm{dev}\left(\varepsilon(\mathbf{u}_n - \mathbf{u}_{n-1}) + \mathbb{C}^{-1}\sigma_{n-1}\right)}{|\mathrm{dev}\left(\varepsilon(\mathbf{u}_n - \mathbf{u}_{n-1}) + \mathbb{C}^{-1}\sigma_{n-1}\right)|}.$$

Note that in the first case, we have a linear relationship between the tension and the displacement, while in the second case, we have a nonlinearity introduced by normalizing the deviatoric term. Here, by $|\cdot|$ we denote the Frobenius norm. For a more detailed description how to obtain the time discrete tension tensor explicitly for different types of hardening, see [10].

Linearization

The nonlinear discrete problem has to be linearized in every time step. Thus, we will represent the problem as a root finding problem. We define the p-th component of the vector field F by

$$F_p(\mathbf{u}_n) = \int_\Omega \sigma_n : \varepsilon(\varphi_p)\,dx - \int_\Omega \mathbf{f}_n \cdot \varphi_p\,dx - \int_{\partial\Omega_N} \mathbf{g}_n \cdot \varphi_p\,ds.$$

Then, the nonlinear problem reads: Solve $F(\mathbf{u}_n) = 0$. Using Newton's method, the Newton update in the $(k+1)$-th Newton step is

$$\mathbf{u}_n^{k+1} = \mathbf{u}_n^k + \tau \Delta \mathbf{u}_n^{k+1}$$

where τ is a step length parameter and with $\Delta\mathbf{u}_n^{k+1}$ defined as the solution of

$$DF\left(\mathbf{u}_n^k\right)\Delta\mathbf{u}_n^{k+1} = -F\left(\mathbf{u}_n^k\right).$$

Here, the tangential stiffness matrix DF is given componentwise by

$$\left(DF\left(\mathbf{u}_n^k\right)\right)_{pq} = \frac{\partial F_p\left(\mathbf{u}_n^k\right)}{\partial u_{n,q}^k}.$$

Let $\mathbf{u}_{n-1}$ be the solution and σ_{n-1} the resulting tension tensor in the $(n-1)$-th timestep, respectively. Following [10], we obtain for the derivative

$$\begin{aligned}\frac{\partial F_p\left(\mathbf{u}_n^k\right)}{\partial u_{n,q}^k} = &\int_\Omega (\lambda+\mu)\mathrm{tr}\left(\varepsilon(\varphi_p)\right)\mathrm{tr}\left(\varepsilon(\varphi_q)\right) + \kappa_1 \mathrm{dev}\left(\varepsilon(\varphi_p)\right) : \mathrm{dev}\left(\varepsilon(\varphi_q)\right) \\ &- \kappa_2(\mathrm{dev}\left(\varepsilon(\varphi_p)\right) : \mathrm{dev}\left(\varepsilon(\mathbf{v})\right))(\mathrm{dev}\left(\varepsilon(\mathbf{v})\right) : \mathrm{dev}\left(\varepsilon(\varphi_q)\right))\,dx,\end{aligned}$$

where $\mathbf{v} = \varepsilon\left(\mathbf{u}_n^k - \mathbf{u}_{n-1}\right) + \mathbb{C}^{-1}\sigma_{n-1}$,

$$\kappa_1 = \begin{cases} \frac{\sigma_y}{|\mathrm{dev}\,(\mathbf{v})|}, & \text{if} \quad |\mathrm{dev}\,(\mathbf{v})| - \frac{\sigma_y}{2\mu} > 0, \\ 2\mu, & \text{else}, \end{cases}$$

and

$$\kappa_2 = \begin{cases} \frac{\sigma_y}{|\mathrm{dev}\,(\mathbf{v})|^3}, & \text{if} \quad |\mathrm{dev}\,(\mathbf{v})| - \frac{\sigma_y}{2\mu} > 0, \\ 0, & \text{else}. \end{cases}$$

In our numerical examples, we iterate in each timestep until the residual satisfies the mixed stopping criterion

$$||F(\mathbf{u}_n^k)||_2 \leq 10^{-10} + 10^{-6}||F(\mathbf{u}_n^0)||_2,$$

where $\mathbf{u}_n^0 := 0$; for the stopping criterion, see, e.g. [10, p. 171, l. 34 of the source code], [34, p. 73, (5.4)]. To guarantee the convergence we will use the Armijo rule, see, e.g., [34], as a line search algorithm. In each Newton iteration, we will assemble local stiffness matrices $K^{(i)} = DF\left(\mathbf{u}_n^{k,(i)}\right)$ and right-hand sides $f^{(i)} = F\left(\mathbf{u}_n^{k,(i)}\right)$, $i = 1, \ldots, N$. Then we solve the linearized system

$$DF\left(\mathbf{u}_n^k\right)\Delta\mathbf{u}_n^{k+1} = -F\left(\mathbf{u}_n^k\right)$$

using FETI-DP as described in Section 1.2. We set $\tau = 1$ as an initial step length. Our trial update is given by $\mathbf{u}_{n,\tau}^{k+1} = \mathbf{u}_n^k + \tau\Delta\mathbf{u}_n^{k+1}$. We test if the Armijo condition

$$\left|\left|F\left(\mathbf{u}_{n,\tau}^{k+1}\right)\right|\right|_2 < \left(1 - 10^{-4}\cdot\tau\right)\left|\left|F\left(\mathbf{u}_n^k\right)\right|\right|_2 \tag{1.3}$$

is satisfied. In this case we update $\mathbf{u}_n^{k+1,(i)} \leftarrow \mathbf{u}_{n,\tau}^{k+1,(i)}$. Otherwise we halve the step length $\tau \leftarrow \tau/2$ until (1.3) holds.

1.2 The FETI-DP Algorithm

In this section, which is based on the presentation in [42], we briefly review an algorithmic description of the dual-primal Finite Element Tearing and

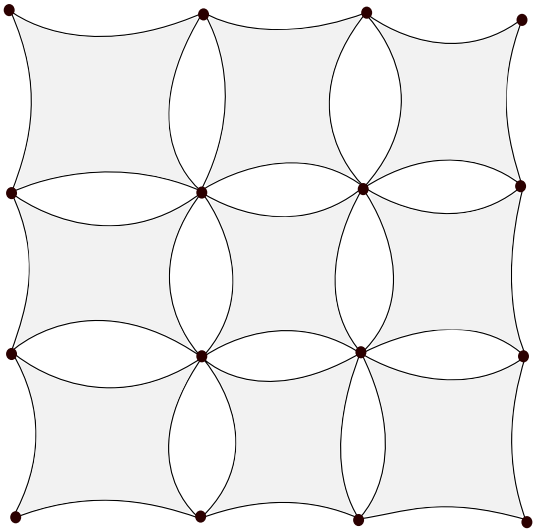

Figure 1.1: Substructures that are partially assembled in primal vertices.

Interconnecting (FETI-DP) method in two dimensions; see, e.g., [23, 24, 49, 46, 45] and [14, 13, 56, 54, 57] for the closely related BDDC algorithm described in the next section. For a more detailed introduction to FETI-DP, see, e.g., [49, 43, 82].

Let Ω be decomposed into N nonoverlapping subdomains Ω_i, $i = 1, \ldots, N$. Here, each Ω_i is the union of shape regular triangular elements of diameter $\mathcal{O}(h)$ with matching finite element nodes on neighboring subdomain boundaries across the interface

$$\Gamma := \overline{\bigcup_{i=1}^{N} \partial\Omega_i \setminus \partial\Omega}.$$

Let Ω be additionally the union of a uniformly bounded number of shape regular finite elements with a diameter of $\mathcal{O}(H)$. We note that this assumption is only needed for the analysis given in Chapter 4.

The interface in two dimensions is composed of subdomain edges and vertices. In the following, we will define those sets by equivalence classes. We define the sets of nodes on $\partial\Omega_N$, $\partial\Omega_i$, and Γ by $\Omega_{N,h}$, $\Omega_{i,h}$ and Γ_h, respectively. Following [49, 43], let for each interface node $x \in \Gamma_h$ the set

$N_x := \{j \in \{1,\dots,N\} : x \in \partial\Omega_{j,h}\}$ be the set containing the indices of subdomains which have x on their boundary. For a given node $x \in \Gamma_h$ we define $C_{\text{con}}(x)$ as the connected component of the nodal subgraph, defined by N_x, to which x belongs. For two interface points x, $y \in \Gamma_h$, we define an equivalence relation by

$$
\begin{aligned}
&x \sim y \Leftrightarrow N_x = N_y \text{ and } y \in C_{\text{con}}(x)\\
&x \in \mathcal{E} \Leftrightarrow |N_x| = 2 \text{ and } x \in \Gamma_h \setminus \partial\Omega_{N,h}\\
&x \in \mathcal{V} \Leftrightarrow |N_x| \geq 3 \text{ and } \nexists\, y \in \Gamma_h \text{ such that } x \sim y.
\end{aligned}
$$

We partition the set $\mathcal{E}$ by building connectivity components and denote the edge between two subdomains Ω_i and Ω_j by $\mathcal{E}_{ij}$ and the vertices of Ω_i by $\mathcal{V}^{ik}$. For the theoretical analysis of the coarse space in Chapter 4 we will also assume that all the edges of Ω_i are straight line segments.

In the following the standard piecewise linear finite element space on Ω_i is denoted by $W^h(\Omega_i)$. We assume that these finite element functions vanish on $\partial\Omega_D$ and that the triangulation on each subdomain is quasi-uniform. The diameter of a subdomain Ω_i is denoted by H_i or generically by H. For a part of the boundary $\Xi \subset \partial\Omega_i$ with positive measure, we denote by $W^h(\Xi)$ the corresponding finite element trace space.

For each subdomain, we introduce local finite element trace spaces $W_i := W^h(\partial\Omega_i \cap \Gamma)$, $i = 1,\dots,N$ and the product space $W := \Pi_{i=1}^N W_i$. Furthermore, we define by $\widehat{W}$ the space of functions in W which are continuous across the interface and introduce an intermediate space $\widetilde{W}$, $\widehat{W} \subset \widetilde{W} \subset W$, which consists of functions that are continuous in the primal variables, i.e., in all primal vertices and other primal constraints if a transformation of basis has been carried out; see Section 1.4. All these notations are standard; see, e.g., the monograph by Toselli and Widlund [82, Chapter 6] or Klawonn and Widlund [49, p. 1546].

For each subdomain Ω_i, $i = 1, \ldots, N$, we assemble a local stiffness matrix $K^{(i)}$ and a local right hand side $f^{(i)}$. We denote the unknowns in Ω_i by $u^{(i)}$ which we further partition into unknowns, $u_I^{(i)}$, in the interior part of the subdomain and unknowns, $u_\Gamma^{(i)}$, on the interface. We further partition the unknowns on the interface into primal unknowns, $u_\Pi^{(i)}$, and dual unknowns, $u_\Delta^{(i)}$. Continuity in the primal unknowns is enforced by global subassembly. For the dual unknowns, we introduce a jump operator and Lagrange multipliers to guarantee continuity at convergence of the iterative method. The local stiffness matrices $K^{(i)}$ and right hand sides $f^{(i)}$ are partitioned correspondingly to the unknowns $u^{(i)}$. Combining, for each subdomain, the nonprimal unknowns $u_I^{(i)}$ and $u_\Delta^{(i)}$ to a vector $u_B^{(i)}$ and partitioning the coefficients in the local stiffness matrices and right hand sides accordingly, we obtain

$$u_B^{(i)} = \begin{bmatrix} u_I^{(i)} \\ u_\Delta^{(i)} \end{bmatrix}, \quad f_B^{(i)} = \begin{bmatrix} f_I^{(i)} \\ f_\Delta^{(i)} \end{bmatrix} \quad \text{and} \quad K_{BB}^{(i)} = \begin{bmatrix} K_{II}^{(i)} & K_{\Delta I}^{(i)T} \\ K_{\Delta I}^{(i)} & K_{\Delta\Delta}^{(i)} \end{bmatrix}.$$

The local stiffness matrices and right hand sides are then of the form

$$K^{(i)} = \begin{bmatrix} K_{BB}^{(i)} & K_{\Pi B}^{(i)\,T} \\ K_{\Pi B}^{(i)} & K_{\Pi\Pi}^{(i)} \end{bmatrix}, \quad f^{(i)} = \begin{bmatrix} f_B^{(i)} \\ f_\Pi^{(i)} \end{bmatrix}. \tag{1.4}$$

We define

$$K = \operatorname{diag}_{i=1}^N(K^{(i)}),\ u = \left[u^{(1)T}, \ldots, u^{(N)T}\right]^T,\ f = \left[f^{(1)T}, \ldots, f^{(N)T}\right]^T,$$

and the global block matrices

$$\begin{aligned} &K_{II} = \operatorname{diag}_{i=1}^N(K_{II}^{(i)}),\ K_{\Delta I} = \operatorname{diag}_{i=1}^N(K_{\Delta I}^{(i)}),\ K_{\Delta\Delta} = \operatorname{diag}_{i=1}^N(K_{\Delta\Delta}^{(i)}), \\ &K_{\Pi I} = \operatorname{diag}_{i=1}^N(K_{\Pi I}^{(i)}),\ K_{\Pi\Delta} = \operatorname{diag}_{i=1}^N(K_{\Pi\Delta}^{(i)}),\ K_{\Pi\Pi} = \operatorname{diag}_{i=1}^N(K_{\Pi\Pi}^{(i)}), \\ &K_{BB} = \operatorname{diag}_{i=1}^N(K_{BB}^{(i)}),\ \text{and}\ \ K_{\Pi B} = \operatorname{diag}_{i=1}^N(K_{\Pi B}^{(i)}). \end{aligned} \tag{1.5}$$

The block diagonal matrix K will be partially assembled in the primal variables resulting in a matrix $\widetilde{K}$. Therefore, we define finite elements assembly operators mapping the local numbering to the global numbering. They consist of entries in $\{0, 1\}$ and are denoted by $R_\Pi^{(i)T}$. We also define the global

assembly operator

$$R_\Pi^T = [R_\Pi^{(1)T} \dots R_\Pi^{(N)T}]$$

and denote the global assembled primal degrees of freedom by

$$\widetilde{u}_\Pi = R_\Pi^T u_\Pi = \sum_{i=1}^{N} R_\Pi^{(i)T} u_\Pi^{(i)}.$$

The non primal variables are not assembled. The result is a partially assembled global stiffness matrix

$$\widetilde{K} = \begin{bmatrix} K_{BB} & \widetilde{K}_{\Pi B}^T \\ \widetilde{K}_{\Pi B} & \widetilde{K}_{\Pi\Pi} \end{bmatrix} = \begin{bmatrix} I_B & 0 \\ 0 & R_\Pi^T \end{bmatrix} \begin{bmatrix} K_{BB} & K_{\Pi B}^T \\ K_{\Pi B} & K_{\Pi\Pi} \end{bmatrix} \begin{bmatrix} I_B & 0 \\ 0 & R_\Pi \end{bmatrix}.$$

We obtain the corresponding right hand side

$$\widetilde{f} = \begin{bmatrix} f_B \\ \widetilde{f}_\Pi \end{bmatrix} = \begin{bmatrix} I_B & 0 \\ 0 & R_\Pi^T \end{bmatrix} \begin{bmatrix} f_B \\ f_\Pi \end{bmatrix}.$$

See Figure 1.1 for a graphical representation of partially assembled substructures. Thus, we have a global coupling in a few variables and keep the block diagonal structure of K_{BB}. With the local block matrices, we have

$$\widetilde{K} = \begin{bmatrix} K_{BB}^{(1)} & & & \widetilde{K}_{\Pi B}^{(1)T} \\ & \ddots & & \vdots \\ & & K_{BB}^{(N)} & \widetilde{K}_{\Pi B}^{(N)T} \\ \widetilde{K}_{\Pi B}^{(1)} & \dots & \widetilde{K}_{\Pi B}^{(N)} & \widetilde{K}_{\Pi\Pi} \end{bmatrix}, \quad \widetilde{f} = \begin{bmatrix} f_B^{(1)} \\ \vdots \\ f_B^{(N)} \\ \widetilde{f}_\Pi \end{bmatrix}.$$

The local problems are invertible and the variables $\widetilde{u}$ can be eliminated. The factorization of $\widetilde{K}$ involves a factorization of the Schur complement

$$\widetilde{S}_{\Pi\Pi} = \widetilde{K}_{\Pi\Pi} - \sum_{i=1}^{N} \widetilde{K}_{\Pi B}^{(i)} \left(K_{BB}^{(i)}\right)^{-1} \widetilde{K}_{\Pi B}^{(i)T}.$$

The coupling, and thus $\widetilde{S}_{\Pi\Pi}$, provides a coarse problem. If we choose a sufficient number of primal variables $u_\Pi^{(i)}$ the matrix $\widetilde{K}$ is symmetric positive definite for elliptic problems. Let $x \in (\partial\Omega_i \cap \partial\Omega_j) \subset \Gamma$ be a node on the dual part of the interface belonging to the two subdomains Ω_i and Ω_j. The

condition $u^{(j)}(x) - u^{(i)}(x) = 0$ needs to be satisfied for the continuity of the solution in that point. We enforce this using a jump operator

$$B_B = \begin{bmatrix} B_B^{(1)} & \dots & B_B^{(N)} \end{bmatrix}$$

together with Lagrange multipliers λ. The operator B_B consists of entries in $\{-1, 0, 1\}$ and enforces the continuity in the dual part by

$$B_B u_B = \sum_{i=1}^{N} B_B^{(i)} u_B^{(i)} = 0.$$

We obtain a saddle point problem of the form

$$\begin{bmatrix} K_{BB} & \widetilde{K}_{\Pi B}^T & B_B^T \\ \widetilde{K}_{\Pi B} & \widetilde{K}_{\Pi\Pi} & 0 \\ B_B & 0 & 0 \end{bmatrix} \begin{bmatrix} u_B \\ \widetilde{u}_\Pi \\ \lambda \end{bmatrix} = \begin{bmatrix} f_B \\ \widetilde{f}_\Pi \\ 0 \end{bmatrix} \tag{1.6}$$

or

$$\begin{bmatrix} \widetilde{K} & B^T \\ B & 0 \end{bmatrix} \begin{bmatrix} \widetilde{u} \\ \lambda \end{bmatrix} = \begin{bmatrix} \widetilde{f} \\ 0 \end{bmatrix},$$

where $B = [B_B \quad 0]$. By eliminating u_B in (1.6), we obtain

$$\begin{bmatrix} \widetilde{S}_{\Pi\Pi} & -\widetilde{K}_{\Pi B} K_{BB}^{-1} B_B^T \\ -B_B K_{BB}^{-1} \widetilde{K}_{\Pi B}^T & -B_B K_{BB}^{-1} B_B^T \end{bmatrix} \begin{bmatrix} \widetilde{u}_\Pi \\ \lambda \end{bmatrix} = \begin{bmatrix} \widetilde{f}_\Pi - \widetilde{K}_{\Pi B} K_{BB}^{-1} f_B \\ -B_B K_{BB}^{-1} f_B \end{bmatrix}.$$

We reduce the system of equations to an equation in λ. It remains to solve

$$F\lambda = d,$$

where

$$F = B_B K_{BB}^{-1} B_B^T + B_B K_{BB}^{-1} \widetilde{K}_{\Pi B}^T \widetilde{S}_{\Pi\Pi}^{-1} \widetilde{K}_{\Pi B} K_{BB}^{-1} B_B^T = B \widetilde{K}^{-1} B^T \quad \text{and}$$

$$d = B_B K_{BB}^{-1} f_B - B_B K_{BB}^{-1} \widetilde{K}_{\Pi B}^T \widetilde{S}_{\Pi\Pi}^{-1} (\widetilde{f}_\Pi - \widetilde{K}_{\Pi B} K_{BB}^{-1} f_B).$$

As a preconditioner for F, we use the standard Dirichlet preconditioner

$$M_D^{-1} := B_D R_\Gamma^T S R_\Gamma B_D^T.$$

Here, S is the Schur complement obtained by eliminating the interior variables in every subdomain, i.e.,

$$S = \begin{bmatrix} S^{(1)} & & \\ & \ddots & \\ & & S^{(N)} \end{bmatrix}$$

with

$$S^{(i)} = \begin{bmatrix} S^{(i)}_{\Delta\Delta} & S^{(i)T}_{\Pi\Delta} \\ S^{(i)}_{\Pi\Delta} & S^{(i)}_{\Pi\Pi} \end{bmatrix} = \begin{bmatrix} K^{(i)}_{\Delta\Delta} & K^{(i)T}_{\Pi\Delta} \\ K^{(i)}_{\Pi\Delta} & K^{(i)}_{\Pi\Pi} \end{bmatrix} - \begin{bmatrix} K^{(i)}_{\Delta I} \\ K^{(i)}_{\Pi I} \end{bmatrix} K^{(i)-1}_{II} \begin{bmatrix} K^{(i)T}_{\Delta I} K^{(i)T}_{\Pi I} \end{bmatrix}.$$

The restriction matrix R_Γ consists of zeros and ones and removes the interior variables when applied to a vector $\widetilde{u}$. The matrices B_D are scaled variants of the jump operator B. Various kinds of scalings can be introduced in the preconditioner. We define the multiplicity of a node as the number of subdomains containing the node. The simplest form of scaling is to scale each row by the inverse of the multiplicity $1/|N_x|$ of the corresponding node x. This is denoted as *multiplicity scaling* or *cardinality scaling* in the literature; see, e.g., [74]. In the following we will describe a scaling that only depends on the maximum of the coefficient function that is attained on each subdomain. For this, we define weighted counting functions on the interface by

$$\delta_j(x_k) := \left(\sum_{i \in N_{x_k}} \widehat{\rho}_i \right) / \widehat{\rho}_j, \tag{1.7}$$

where

$$\widehat{\rho}_j = \max_{x \in \Omega_{j,h}} \rho_j(x), \tag{1.8}$$

for $x_k \in \partial\Omega_{j,h} \cap \Gamma_h$, $j = 1, \ldots, N$. The pseudoinverses are defined by

$$\delta^\dagger_j(x_k) := \widehat{\rho}_j / \sum_{i \in N_{x_k}} \widehat{\rho}_i. \tag{1.9}$$

Each row of $B^{(i)}$ with a nonzero entry connects a point of $\Gamma^{(i)}_h$ with the corresponding point of a neighboring subdomain $x_k \in \Gamma^{(i)}_h \cap \Gamma^{(j)}_h$. Multiplying

each such row with $\delta_j(x_k)^\dagger$ for each $B^{(i)}$, $i = 1, \ldots, N$, results in the scaled operator B_D. Formally, we can write

$$B_D = [D^{(1)}B^{(1)}, \ldots, D^{(N)}B^{(N)}].$$

We will refer to this approach as *max-ρ-scaling*. Another possible variant is to define

$$\widehat{\rho}_j(x) = \max_{x \in \omega(x) \cap \Omega_{j,h}} \rho_j(x), \tag{1.10}$$

where $\omega(x)$ is the support of the finite element basis function associated with the node x. We will denote this approach by *patch-ρ-scaling*. In the case of coefficients that are constant on each subdomain both approaches reduce to the standard ρ-scaling; see, e.g., [50, 82, 49] for more details.

A more recently introduced kind of scaling uses scaling matrices which are obtained from local Schur complements; cf. Section 2.4.1, Definition 2.4.1. In the literature this approach is referred to as *deluxe scaling*; see, e.g., [17, 18, 16, 68]. Note that the resulting scaling matrices are not diagonal anymore. Thus, they do not define a scaling in the strict sense.

The standard FETI-DP algorithm is the preconditioned conjugate gradient method to solve $F\lambda = d$ with the preconditioner M_D^{-1}.

In our approach we choose every node with multiplicity of three or higher as primal. Later we also choose weighted edge averages as primal variables and will enforce additional constraints by subassembly or by a projection method as described in following sections.

1.3 The BDDC Algorithm

The BDDC algorithm has been introduced in [14]. Related algorithms were also proposed in [13] and [26]. It was shown in [57] and in [54] that FETI-DP and BDDC share essentially the same spectra with the exception of eigenvalues that are zero or one.

To describe the BDDC algorithm in 2D, we consider a domain Ω which is decomposed into N nonoverlapping subdomains

$$\Omega = \bigcup_{i=1}^{N} \Omega_i$$

with diameter H_i or generically $H := \max_i H_i$. As in the FETI-DP method, for each subdomain Ω_i, we assemble local stiffness matrices $K^{(i)}$ and load vectors $f^{(i)}$ and denote the unknowns on subdomain Ω_i as $u^{(i)}$. We partition the indices in our stiffness matrices, right hand sides, and unknowns into an interior part and an interface part

$$u^{(i)} = \begin{bmatrix} u_I^{(i)} \\ u_\Gamma^{(i)} \end{bmatrix}, \qquad K^{(i)} = \begin{bmatrix} K_{II}^{(i)} & K_{\Gamma I}^{(i)T} \\ K_{\Gamma I}^{(i)} & K_{\Gamma\Gamma}^{(i)} \end{bmatrix}, \quad \text{and} \quad f^{(i)} = \begin{bmatrix} f_I^{(i)} \\ f_\Gamma^{(i)} \end{bmatrix}.$$

For the definition of the BDDC-preconditioner we further partition the interface part of the subdomain stiffness matrices, right hand sides, and unknowns into a primal set, analogously to the FETI-DP algorithm, denoted by the index Π and a remaining dual set denoted by the index Δ. The primal variables consist of subdomain vertices and possibly - after a transformation of basis - certain weighted edge averages. The dual variables consist of the remaining unknowns. We define block matrices and right hand sides in the same way as for the FETI-DP algorithm; see (1.5). In the global block matrix

$$\begin{bmatrix} K_{II} & K_{\Delta I}^T & K_{\Pi I}^T \\ K_{\Delta I} & K_{\Delta\Delta} & K_{\Pi\Delta}^T \\ K_{\Pi I} & K_{\Pi\Delta} & K_{\Pi\Pi} \end{bmatrix}$$

we eliminate the interior unknowns and obtain the Schur complement

$$\begin{bmatrix} S_{\Delta\Delta} & S_{\Pi\Delta}^T \\ S_{\Pi\Delta} & S_{\Pi\Pi} \end{bmatrix} = \begin{bmatrix} K_{\Delta\Delta} & K_{\Pi\Delta}^T \\ K_{\Pi\Delta} & K_{\Pi\Pi} \end{bmatrix} - \begin{bmatrix} K_{\Delta I} \\ K_{\Pi I} \end{bmatrix} K_{II}^{-1} \begin{bmatrix} K_{\Delta I}^T K_{\Pi I}^T \end{bmatrix}$$

as well as right hand side

$$\begin{bmatrix} g_\Delta \\ g_\Pi \end{bmatrix} = \begin{bmatrix} f_\Delta - K_{\Delta I} K_{II}^{-1} f_I \\ f_\Pi - K_{\Pi I} K_{II}^{-1} f_I \end{bmatrix}.$$

Let R_Π^T be defined as in the previous section and let $R_\Delta^{(i)T}$ for $i = 1, \ldots, N$ be the operator that maps local dual degrees of freedom of subdomain Ω_i to global degrees of freedom. By

$$R_\Delta^T = [R_\Delta^{(1)T} \ldots R_\Delta^{(N)T}],$$

we denote the assembly operator that assembles dual degrees of freedom on the interface. By assembly we obtain the matrix

$$S_{\Gamma\Gamma} = \begin{bmatrix} R_\Delta^T & \\ & R_\Pi^T \end{bmatrix} \begin{bmatrix} S_{\Delta\Delta} & S_{\Pi\Delta}^T \\ S_{\Pi\Delta} & S_{\Pi\Pi} \end{bmatrix} \begin{bmatrix} R_\Delta & \\ & R_\Pi \end{bmatrix}$$

and the right hand side

$$g_\Gamma = \begin{bmatrix} R_\Delta^T & \\ & R_\Pi^T \end{bmatrix} \begin{bmatrix} g_\Delta \\ g_\Pi \end{bmatrix}.$$

Additionally, we need a scaled version of the operator R_Δ^T denoted by $R_{\Delta,D}^T$. The same scalings as in the FETI-DP algorithm can be used. Instead of scaling the jump operator associated with the dual degrees of freedom, here we scale the assembly operator which connects the dual degrees of freedom on opposing sides of the interface, e.g., for ρ-scaling an entry in a row of R_Δ^T associated with a node x in subdomain Ω_j will be scaled by $\delta_j^\dagger(x)$. Let $R_{\Delta B}$ be the operator restricting the remaining degrees of freedom u_B to dual degrees of freedom by $R_{\Delta B} u_B = u_\Delta$. The BDDC preconditioner is defined by

$$M_{\mathrm{BDDC}}^{-1} = \begin{bmatrix} R_{D,\Delta}^T R_{\Delta B} & 0 \\ 0 & I_\Pi \end{bmatrix} \begin{bmatrix} K_{BB} & \widetilde{K}_{\Pi B}^T \\ \widetilde{K}_{\Pi B} & \widetilde{K}_{\Pi\Pi} \end{bmatrix}^{-1} \begin{bmatrix} R_{\Delta B}^T R_{D,\Delta} & 0 \\ 0 & I_\Pi \end{bmatrix}.$$

The BDDC algorithm is the preconditioned conjugate gradient method to solve $S_{\Gamma\Gamma} u_\Gamma = g_\Gamma$ with the preconditioner M_{BDDC}^{-1}.

1.4 Transformation of Basis in the FETI-DP and BDDC Methods

In this section, we describe how to transform the basis such that weighted edge average constraints can be enforced by subassembly. The presentation in this chapter is based on the proceedings article [41]. Supposing that a set of primal constraints is given, e.g., weighted edge averages which are computed in a preprocessing step, we describe a way to enforce these constraints as primal variables. For a transformation of basis for standard edge averages or certain weighted averages, see, e.g., [43, 54, 33]. To implement these edge averages, we transform our local stiffness matrices $K^{(i)}$ and right hand sides $f^{(i)}$ with a transformation matrix $T^{(i)}$. Then, the resulting transformed stiffness matrices

$$\overline{K}^{(i)} = T^{(i)T} K^{(i)} T^{(i)}$$

and right hand sides

$$\overline{f}^{(i)} = T^{(i)T} f^{(i)}$$

will replace $K^{(i)}$ and $f^{(i)}$ in the FETI-DP or BDDC algorithm; see, e.g., [37] for more details. We construct the transformation matrices $T^{(i)}$ edge by edge. Let us consider an edge $\mathcal{E}$ of Ω_i and denote by T_E the restriction of $T^{(i)}$ to this edge. Suppose we have selected a set of weighted edge averages with weights described by orthonormal column vectors $\{v^{(i)}_{E,1}, \ldots, v^{(i)}_{E,m}\}$. Then, we augment this set to an orthonormal basis

$$\{v^{(i)}_{E,1}, \ldots, v^{(i)}_{E,m}, v^{(i)}_{E,m+1}, \ldots, v^{(i)}_{E,n_E}\} \tag{1.11}$$

of $\mathbb{R}^{n_E}$, where n_E denotes the number of degrees of freedom of the edge E. The transformation matrix T_E is defined by

$$T_E = [v^{(i)}_{E,1}, \ldots, v^{(i)}_{E,m}, v^{(i)}_{E,m+1}, \ldots, v^{(i)}_{E,n_E}]$$

and describes the change of basis from the new to the original nodal basis. The first m columns of T_E correspond to the new additional primal variables and the remaining columns correspond to the new dual unknowns. Denoting the edge unknowns in the new basis by $\widehat{u}_E$ and the unknowns in the original basis by u_E, we have $u_E = T_E \widehat{u}_E$. We denote by $T_E^{(i)}$ the transformation matrix which operates on all edges of $\partial\Omega_i$. The transformation matrix $T^{(i)}$ is then defined by

$$T^{(i)} = \begin{bmatrix} I_I & & \\ & I_V & \\ & & T_E^{(i)} \end{bmatrix},$$

where I_I and I_V denote the identities on interior variables and on vertex variables, respectively. The transformed stiffness matrices are of the form

$$T^{(i)T} K^{(i)} T^{(i)} = \begin{bmatrix} K_{II}^{(i)} & K_{IV}^{(i)} & K_{IE}^{(i)} T_E^{(i)} \\ K_{VI}^{(i)} & K_{VV}^{(i)} & K_{VE}^{(i)} T_E^{(i)} \\ T_E^{(i)T} K_{EI}^{(i)} & T_E^{(i)T} K_{EV}^{(i)} & T_E^{(i)T} K_{EE}^{(i)} T_E^{(i)} \end{bmatrix},$$

with right hand sides $T^{(i)T} f^{(i)} = [f_I^{(i)T} \quad f_V^{(i)T} \quad f_E^{(i)T} T_E^{(i)}]^T$. We can now perform our FETI-DP or BDDC algorithm on the transformed problem.

1.5 Projector Preconditioning and Balancing

An alternative is to enrich the coarse space of FETI-DP by additional constraints using projections; see, e.g., [47, 33]. This subsection is partly based on [42].

Here, we give a brief revision of the approach known as projector preconditioning or deflation; see [47] for more details. In the following we will recall the notation for projector preconditioning and deflation as in [47]. For projection methods in the context of Krylov subspace methods, see [20, 64, 63]. For a given rectangular matrix U containing the constraints as columns, the

constraint

$$U^T Bu = 0$$

is enforced in each iteration of the preconditioned conjugate gradient (PCG) method. We define the F-orthogonal projection P onto the range of U as

$$P = U(U^T FU)^{-1} U^T F$$

if F is symmetric positive definite or as

$$P = U(U^T FU)^{+} U^T F$$

with a pseudoinverse of $U^T FU$ if F is symmetric positive semidefinite and $U^T FU$ is singular. Then, we will solve the projected system

$$(I - P)^T F\lambda = (I - P)^T d.$$

Since Range (P) and Ker (P) are F-orthogonal the projection P is called an F-conjugate projection or conjugate projector. If $\lambda \in$ Range (U), we have

$$\begin{aligned}(I - P)^T F\lambda =& F\lambda - P^T F\lambda = FU\hat{\lambda} - P^T FU\hat{\lambda} \\ =& FU\hat{\lambda} - FU(U^T FU)^{+}(U^T FU)\hat{\lambda} = 0,\end{aligned}$$

which yields

$$U^T(I - P)^T F\lambda = 0$$

with $U\hat{\lambda} = \lambda$. Since U has full column rank, we have

$$\lambda \in \text{Ker}\,((I - P)^T F).$$

Let F be nonsingular and $\lambda \in$ Ker $((I - P)^T F)$. With

$$(I - P)^T F\lambda = (F - FU(U^T FU)^{-1} U^T F)\lambda = 0,$$

we obtain

$$\lambda = U(U^T FU)^{-1} U^T F\lambda$$

and see that $\lambda \in \text{Range}\,(U)$. It follows

$$\text{Ker}((I-P)^T F) = \text{Range}(U).$$

The matrix $(I-P)^T F$ is singular but the linear system is consistent and can be solved by CG. The preconditioned system is

$$M^{-1}(I-P)^T F\lambda = M^{-1}(I-P)^T d \tag{1.12}$$

with the Dirichlet preconditioner M^{-1}. Let λ^* be the solution of the original system $F\lambda = d$ and we define

$$\overline{\lambda} := PF^+ d$$

for any pseudoinverse F^+ or

$$\overline{\lambda} := PF^{-1} d$$

for invertible F, respectively. We denote the solution of (1.12) by λ. The solution of the original problem can then be written as

$$\lambda^* = \overline{\lambda} + (I-P)\lambda.$$

We will include the projection $(I-P)^T$ into the preconditioner and project the correction onto $\text{Range}\,(I-P)$ in each iteration. This yields the symmetric preconditioner

$$M_{PP}^{-1} = (I-P)M^{-1}(I-P)^T.$$

We then solve the original problem applying this preconditioner. This preconditioned system is singular but still consistent. The solution λ of this system is in the subspace $\text{Range}\,(I-P)$. The solution λ^* of the original problem is then computed by

$$\lambda^* = \overline{\lambda} + \lambda.$$

If we include the computation of $\overline{\lambda}$ into the iteration, we get the balancing preconditioner

$$M_{BP}^{-1} = (I - P)M^{-1}(I - P)^T + U(U^T F U)^{-1} U^T. \tag{1.13}$$

We use this preconditioner to solve $F\lambda = d$ by PCG and directly obtain the solution without an additional correction.

Let us briefly describe how the projection in the deflation approach can be built efficiently since the cost of a naive implementation is prohibitive. First

$$FU = B\widetilde{K}^{-1}B^T U$$

has to be computed. This is performed by exploiting neighborship information as in one and two-level FETI methods; see, e.g., [25]. Let us consider the standard block factorization

$$\begin{bmatrix} K_{BB} & \widetilde{K}_{\Pi B}^T \\ \widetilde{K}_{\Pi B} & \widetilde{K}_{\Pi\Pi} \end{bmatrix}^{-1} = \begin{bmatrix} I & -K_{BB}^{-1}\widetilde{K}_{\Pi B}^T \\ 0 & I \end{bmatrix} \begin{bmatrix} K_{BB}^{-1} & 0 \\ 0 & \widetilde{S}_{\Pi\Pi}^{-1} \end{bmatrix} \begin{bmatrix} I & 0 \\ -\widetilde{K}_{\Pi B}K_{BB}^{-1} & I \end{bmatrix}.$$

Applying K_{BB}^{-1}, only a small number of subdomains has to be considered, i.e., the computation involves only neighboring subdomains. For edges in 2D, for each column of U, only two subdomain solves are necessary. A coarse solve follows for every column of U. Finally, the matrix $U^T(FU)$ has to be assembled, again exploiting neighborship information.

Let us note that our strategy is to start with a small and cheap coarse space which is large enough to ensure invertibility of $\widetilde{K}$. Then, in order to accelerate the convergence, the coarse space is enriched using additional constraints. In the approaches presented here, these are built using certain eigenvectors; see Chapters 2, 3, and 4, for details. The new, larger coarse space can be implemented in many different ways, including transformation of basis, local saddle point problems, or deflation. From the discussion above, for the deflation approach, we see that the number of applications of $\widetilde{S}_{\Pi\Pi}^{-1}$ is

reduced, compared to the small first coarse problem, if an additional constraint (eigenvector) reduces the number of iterations by one. Note that a similar decomposition of the coarse problem into two stages is also used in the two level FETI method; see [25] and [81], where in the latter the second level is also based on certain eigenvectors. The implementation of the second level in two-level FETI methods is the same as in projector preconditioning.

The following lemma is an alternative to the proof for the condition number bound provided in [47] using projector preconditioning or deflation applied to FETI-DP methods. It directly applies to a larger class of scalings.

Lemma 1.5.1. *Let $P_D = B_D^T B$. Assuming that $||P_D w||_{\widetilde{S}}^2 \leq C||w||_{\widetilde{S}}^2$ for all $w \in \{w \in \widetilde{W} \,|\, U^T B w = 0\}$ with a constant $C > 0$, we have*

$$\kappa\,(M_{PP}^{-1} F) \leq C.$$

Here, the constant C can depend on H/h or η/h (cf. Definition 2.6.1), and possibly on a prescribed tolerance from local generalized eigenvalue problems.

Proof. Similar to [49, p. 1553] by using $(I-P)^T F = F(I-P)$ and the standard Dirichlet preconditioner M^{-1} and observing that

$$\widetilde{S}^{-1} B^T (I-P)\lambda \in \widetilde{W} \quad \text{and}$$
$$(I-P)U = 0 \Rightarrow U^T B(\widetilde{S}^{-1} B^T (I-P)\lambda) = U^T (I-P)^T B \widetilde{S}^{-1} B^T \lambda = 0$$

we obtain for the upper bound

$$\begin{aligned}
\left\langle M_{PP}^{-1} F\lambda, \lambda \right\rangle_F &= \left\langle (I-P)M^{-1}(I-P)^T F\lambda, F\lambda \right\rangle \\
&= \left\langle M^{-1}F(I-P)\lambda, F(I-P)\lambda \right\rangle \\
&= \left\langle B_D^T B \widetilde{S}^{-1} B^T (I-P)\lambda, B_D^T B \widetilde{S}^{-1} B^T (I-P)\lambda \right\rangle_{\widetilde{S}} \\
&= |P_D(\widetilde{S}^{-1} B^T (I-P)\lambda)|_{\widetilde{S}}^2 \\
&= |P_D w|_{\widetilde{S}}^2 \leq C|w|_{\widetilde{S}}^2 \\
&= C|\widetilde{S}^{-1} B^T (I-P)\lambda|_{\widetilde{S}}^2 \\
&= C \left\langle \widetilde{S}^{-1} B^T (I-P)\lambda, \widetilde{S}^{-1} B^T (I-P)\lambda \right\rangle_{\widetilde{S}} \\
&= C \left\langle (I-P)\lambda, (I-P)\lambda \right\rangle_F .
\end{aligned}$$

Since $\lambda \in \text{range}\,(I-P)$, we have $\lambda = (I-P)\lambda$. Hence, we have

$$\lambda_{\max}(M_{PP}^{-1} F) \leq C.$$

We will now derive an estimate for the lower bound. With

$$E_D w(x) := \sum_{j \in N_x} D^{(j)} w_j(x),$$

we see that $P_D w = B_D^T B w = (I - E_D)w$, and, since $E_D w$ is continuous across the interface, P_D preserves the jump of any function $w \in \widetilde{W}$ in the sense that $Bw = Bw - 0 = B(I - E_D)w = BP_D w$. We obtain for the lower bound,

analogously to [49, p. 1552]

$$\begin{aligned}
\langle \lambda, \lambda \rangle_F^2 &= \left\langle \lambda, B\widetilde{S}^{-1}B^T\lambda \right\rangle^2 \\
&= \left\langle \lambda, B\widetilde{S}^{-1}P_D^T B^T\lambda \right\rangle^2 \\
&= \left\langle \lambda, B\widetilde{S}^{-1}B^T B_D B^T\lambda \right\rangle^2 \\
&= \left\langle \lambda, B_D B^T\lambda \right\rangle_F^2 \\
&= \left\langle F\lambda, B_D\widetilde{S}^{1/2}\widetilde{S}^{-1/2}B^T\lambda \right\rangle^2 \\
&\leq \left\langle \widetilde{S}^{1/2}B_D^T F\lambda, \widetilde{S}^{1/2}B_D^T F\lambda \right\rangle \left\langle \widetilde{S}^{-1/2}B^T\lambda, \widetilde{S}^{-1/2}B^T\lambda \right\rangle \\
&= \left\langle M^{-1}F\lambda, F\lambda \right\rangle \langle F\lambda, \lambda \rangle \\
&= \left\langle M^{-1}F(I-P)\lambda, F(I-P)\lambda \right\rangle \langle F\lambda, \lambda \rangle \\
&= \left\langle M_{PP}^{-1}F\lambda, \lambda \right\rangle_F \langle F\lambda, \lambda \rangle .
\end{aligned}$$

Hence, we have $\lambda_{\min}(M_{PP}^{-1}F) \geq 1$. □

Remark 1.5.2. *In [47], it was shown that eigenvalues of $M_{PP}^{-1}F$ and $M_{BP}^{-1}F$ which are nonzero and not one are the same. Thus Lemma 1.5.1 also holds for $M_{BP}^{-1}F$. If all primal constraints are implemented using a transformation of basis instead of projector preconditioning, we can use Lemma 1.5.1 with $P = \mathbf{0}$ to obtain the estimate for the Dirichlet preconditioner given in [49, p.1553].*

1.6 Some Spectral Estimates

We repeat some properties of projections on eigenspaces of generalized eigenvalue problems. The following two lemmas can also be found in [38]. The next lemma is a standard argument from linear algebra.

Lemma 1.6.1. *Let $A \in \mathbb{R}^{n\times n}$ be symmetric positive semidefinite and $B \in \mathbb{R}^{n\times n}$ be symmetric positive definite. Consider the generalized eigenvalue*

problem

$$Ax_k = \lambda_k B x_k \qquad \text{for } k = 1, \ldots, n. \tag{1.14}$$

Then, the eigenvectors can be chosen to be B-orthogonal and such that $x_k^T B x_k = 1$. All eigenvalues are positive or zero.

Proof. Set $y_k = B^{1/2} x_k$. Then we have

$$Ax_k = \lambda_k B x_k \Leftrightarrow AB^{-1/2} y_k = \lambda_k B^{1/2} y_k \Leftrightarrow B^{-1/2} A B^{-1/2} y_k = \lambda_k y_k.$$

All eigenvalues are positive or zero and the eigenvectors y_k are orthogonal since $B^{-1/2} A B^{-1/2}$ is symmetric positive semidefinite and the $x_k = B^{-1/2} y_k$ are B-orthogonal. If we choose $\hat{x}_k = (x_k^T B x_k)^{-1/2} x_k$, then $\hat{x}_k$ are eigenvectors of (1.14) and $\hat{x}_k^T B \hat{x}_k = 1$. □

The proof of the next lemma is based on arguments from classical spectral theory. For completeness, we provide the arguments in detail. A related abstract lemma, also based on classical spectral theory, can be found in [80, Lemma 2.11].

Lemma 1.6.2. *Let A, B be as in Lemma 1.6.1 and define $\Pi_m^B := \sum_{i=1}^m x_i x_i^T B$. Let the eigenvalues be sorted in an increasing order $0 = \lambda_1 \leq \ldots \leq \lambda_m < \lambda_{m+1} \leq \ldots \leq \lambda_n$. Then, $x = \Pi_n^B x$ and*

$$|x - \Pi_m^B x|_B^2 = (x - \Pi_m^B x)^T B (x - \Pi_m^B x) \quad \leq \quad \lambda_{m+1}^{-1} x^T A x = \lambda_{m+1}^{-1} |x|_A^2.$$

Additionally, we have the stability of Π_m^B in the B-norm

$$|x - \Pi_m^B x|_B^2 \leq |x|_B^2.$$

Proof. Since $\{x_1, \ldots, x_n\}$ forms a B-orthonormal basis of $\mathbb{R}^n$, we can write $x = \sum_{i=1}^n \alpha_i x_i$ with scalars $\alpha_1, \ldots, \alpha_n \in \mathbb{R}$. From the B-orthogonality of the x_k and $x_k^T B x_k = 1$ we obtain

$$x^T B x_i = \alpha_i x_i^T B x_i = \alpha_i \quad \Rightarrow \quad x = \sum_{i=1}^n x^T B x_i x_i = \Pi_n^B x.$$

Since $x - \Pi_m^B x = \sum_{i=m+1}^n (x_i^T B x) x_i$, we obtain with Lemma 1.6.1

$$\begin{aligned}
(x - \Pi_m^B x)^T B (x - \Pi_m^B x) &= \left(\sum_{i=m+1}^n (x_i^T B x) x_i \right)^T B \left(\sum_{j=m+1}^n (x_j^T B x) x_j \right) \\
&= \sum_{i=m+1}^n \sum_{j=m+1}^n x_i^T B x \, x_j^T B x \, x_i^T B x_j \\
&= \sum_{i=m+1}^n (x_i^T B x)^2 \\
&= \sum_{i=m+1}^n (\lambda_i)^{-1} x^T B x_i \, x^T A x_i \\
&\leq (\lambda_{m+1})^{-1} \sum_{i=m+1}^n \lambda_i (x^T B x_i)^2 \\
&= (\lambda_{m+1})^{-1} \sum_{i=m+1}^n x_i^T A x_i (x^T B x_i)^2 \\
&= (\lambda_{m+1})^{-1} \sum_{i=m+1}^n \sum_{j=m+1}^n (x_i^T B x)(x_i^T A x_j)(x_j^T B x) \\
&\leq (\lambda_{m+1})^{-1} \sum_{i=1}^n \sum_{j=1}^n (x_i^T B x)(x_i^T A x_j)(x_j^T B x) \\
&= (\lambda_{m+1})^{-1} x^T A x.
\end{aligned}$$

The second assertion follows by

$$\begin{aligned}
(x - \Pi_m^B x)^T B (x - \Pi_m^B x) = \sum_{i=m+1}^n (x_i^T B x)^2 &\leq \sum_{i=1}^m (x_i^T B x)^2 \\
&= \sum_{i=1}^m \sum_{j=1}^m (x_i^T B x) x_i^T B x_j (x_j^T B x) = x^T B x.
\end{aligned}$$

□

2 Equivalence Class Coarse Space Based on the Operator P_D

In this chapter, we consider two approaches where general eigenvalue problems are solved which are based on a localization of the P_D-estimate $|P_D w|^2_{\widetilde{S}} \leq C|w|^2_{\widetilde{S}}$; see Lemma 1.5.1. By solving these eigenvalue problems, adaptive constraints will be computed to guarantee a bound on the condition number. This chapter is based on [38] and organized as follows. In Section 2.1, we introduce the relevant notation and in Section 2.2 we show how the energy of the P_D operator can be bounded by local estimates. We collect some known information on the parallel sum of matrices and show some related spectral estimates in Section 2.3. We introduce two approaches to enhance the coarse space with adaptively computed constraints in Sections 2.4 and 2.5. In both approaches, the constraints are computed with local generalized eigenvalue problems. This first approach has been proposed in [68] and relies on deluxe scaling. In the second approach, first proposed in [39], any kind of scaling is possible as long as it satisfies the partition-of-unity property (2.2). For the special case of deluxe scaling, the second approach is the same as the first. In Section 2.6, we consider an economic variant solving eigenvalue problems on slabs that we introduced in [38]. We conclude this chapter by proving a condition number bound for the FETI-DP algorithm with adaptive constraints as described in Sections 2.4.2, 2.5.1, or 2.6.2. For the corresponding numerical results see Section 5.2.

2.1 Notation

We define the energy minimal extension of v from the local interface to the interior of the subdomain Ω_l as

$$\mathcal{H}^{(l)}v := \arg \min_{u \in V^h(\Omega_l)} \left\{ a_l(u,u) : u_{|\partial\Omega_l} = v \right\} \qquad \text{for } l = i, j.$$

Let $\theta_{E_{ij}}$ be the standard finite element cutoff function, which equals 1 at the nodes on the edge $\mathcal{E}_{ij}$ and is zero on $\partial\Omega_i \backslash \mathcal{E}_{ij}$. With I^h we denote the standard finite element interpolation operator. We will make use of the seminorm

$$|v|^2_{E_l} := a_l(v,v), \tag{2.1}$$

and of an energy minimal extension from an edge $\mathcal{E}_{ij}$ to the interface $\Gamma^{(l)}$, $l = i, j$.

Definition 2.1.1. *Let $\mathcal{E} \subset \Gamma^{(i)} := \partial\Omega_i$ be an edge and $\mathcal{E}^c \subset \Gamma^{(i)}$ be the complement of $\mathcal{E}$ with respect to $\Gamma^{(i)}$ and let $S^{(i)}$ be partitioned as follows*

$$S^{(i)} = \begin{bmatrix} S^{(i)}_{\mathcal{E}\mathcal{E}} & S^{(i)T}_{\mathcal{E}^c\mathcal{E}} \\ S^{(i)}_{\mathcal{E}^c\mathcal{E}} & S^{(i)}_{\mathcal{E}^c\mathcal{E}^c} \end{bmatrix}.$$

We define the extension operator $\mathcal{H}^{(i)}_{\mathcal{E}} v := \begin{bmatrix} v_{|\mathcal{E}} \\ -S^{-1}_{\mathcal{E}^c\mathcal{E}^c} S_{\mathcal{E}^c\mathcal{E}} v_{|\mathcal{E}} \end{bmatrix}$ and the matrices $S^{(l)}_{E_{ij},0} := S^{(l)}_{\mathcal{E}_{ij}\mathcal{E}_{ij}}$ and $S^{(l)}_{E_{ij}} := S^{(l)}_{\mathcal{E}_{ij}\mathcal{E}_{ij}} - S^{(l)T}_{\mathcal{E}^c_{ij}\mathcal{E}_{ij}} S^{(l)-1}_{\mathcal{E}^c_{ij}\mathcal{E}^c_{ij}} S^{(l)}_{\mathcal{E}^c_{ij}\mathcal{E}_{ij}}$.

The proof of the next lemma follows from a standard variational argument.

Lemma 2.1.2. *Using the same notation as in Definition 2.1.1, for all $w_i \in V^h(\Gamma^{(i)})$ with $w_{i|\mathcal{E}} = v_{\mathcal{E}}$, we have $|\mathcal{H}^{(i)}_{\mathcal{E}} v_{\mathcal{E}}|^2_{S^{(i)}} \leq |w_i|^2_{S^{(i)}}$.*

Proof. Define

$$F(x) = \begin{bmatrix} v_{\mathcal{E}} \\ x \end{bmatrix}^T \begin{bmatrix} S_{\mathcal{E}\mathcal{E}} & S^T_{\mathcal{E}^c\mathcal{E}} \\ S_{\mathcal{E}^c\mathcal{E}} & S_{\mathcal{E}^c\mathcal{E}^c} \end{bmatrix} \begin{bmatrix} v_{\mathcal{E}} \\ x \end{bmatrix}.$$

With

$$\begin{aligned}\frac{\partial F(x)}{\partial x} &= \frac{\partial \left(v_{\mathcal{E}}^T S_{\mathcal{E}\mathcal{E}} v_{\mathcal{E}} + 2v_{\mathcal{E}}^T S_{\mathcal{E}^c\mathcal{E}}^T x + x^T S_{\mathcal{E}^c\mathcal{E}^c} x\right)}{\partial x} \\ &= 2v_{\mathcal{E}}^T S_{\mathcal{E}^c\mathcal{E}}^T + 2x^T S_{\mathcal{E}^c\mathcal{E}^c}\end{aligned}$$

we obtain

$$\frac{\partial F(x)}{\partial x} = 0 \Leftrightarrow x = -S_{\mathcal{E}^c\mathcal{E}^c}^{-1} S_{\mathcal{E}^c\mathcal{E}} v_{\mathcal{E}}.$$

□

With Definition 2.1.1, we have the following correspondences between (semi)norms and the matrices given in Definition 2.1.1:

$$\begin{aligned}|\mathcal{H}^{(l)} I^h(\theta_{E_{ij}} v)|_{E_l}^2 &= v_{|\mathcal{E}_{ij}}^T S_{E_{ij},0}^{(l)} v_{|\mathcal{E}_{ij}} \quad l = i, j \\ |\mathcal{H}^{(l)} \mathcal{H}_{\mathcal{E}_{ij}}^{(l)} v|_{E_l}^2 &= v_{|\mathcal{E}_{ij}}^T S_{E_{ij}}^{(l)} v_{|\mathcal{E}_{ij}}.\end{aligned}$$

Let $D^{(l)}$, $l = i, j$, be scaling matrices, such that

$$D^{(i)} + D^{(j)} = I, \tag{2.2}$$

where I is the identity matrix; this is a partition-of-unity.

2.2 Splitting the P_D-Operator into Local Contributions

In the following, we will assume that vectors are restricted to the edge $\mathcal{E}_{ij}$ if they are multiplied by a matrix with the index E_{ij} or $E_{ij,0}$ to avoid excessive use of restriction operators. As a classical result in the analysis of iterative substructuring, see, e.g., [49, 82], we have

$$|P_D w|_{\widetilde{S}}^2 = |R P_D w|_S^2 = \sum_{i=1}^{N} |R^{(i)} P_D w|_{S_i}^2.$$

Let $N_{\mathcal{E}}$ denote the maximum number of edges of a subdomain. For $w \in \widetilde{W}$, we define $w_i = R^{(i)} w$ and $w_j = R^{(j)} w$. In the following, in order to avoid the

introduction of additional extension and restriction operators, whenever the difference $w_i - w_j$ is used, we assume that w_i and w_j are first restricted to the edge $\mathcal{E}_{ij}$ and that the difference is then extended by zero to the rest of the interface Γ. Under the assumption that all vertices are primal, we obtain

$$|R^{(i)}P_D w|^2_{S_i} \leq N_{\mathcal{E}} \sum_{j\in N_i} |\mathcal{H}^{(i)} I^h(\theta_{E_{ij}} D^{(i)}(w_i - w_j))|^2_{E_i},$$

where N_i denotes the set of indices of the subdomains that share an edge with Ω_i. Hence, we are interested in obtaining bounds for the local contributions on the edges $\mathcal{E}_{ij}$ of the form:

$$\begin{aligned}&|\mathcal{H}^{(i)} I^h(\theta_{E_{ij}} D^{(i)}(w_i - w_j))|^2_{E_i} + |\mathcal{H}^{(j)} I^h(\theta_{E_{ij}} D^{(j)}(w_j - w_i))|^2_{E_j}\\ \leq & C\left(|\mathcal{H}^{(i)}\mathcal{H}^{(i)}_{\mathcal{E}_{ij}} w_i|^2_{E_i} + |\mathcal{H}^{(j)}\mathcal{H}^{(j)}_{\mathcal{E}_{ij}} w_j|^2_{E_j}\right) \leq C\left(|w_i|^2_{E_i} + |w_j|^2_{E_j}\right).\end{aligned}$$

Using Definition 2.1.1, this is equivalent to

$$\begin{aligned}&(w_i - w_j)^T D^{(j)T}_{E_{ij}} S^{(i)}_{E_{ij},0} D^{(j)}_{E_{ij}}(w_i - w_j) + (w_j - w_i)^T D^{(i)T}_{E_{ij}} S^{(j)}_{E_{ij},0} D^{(i)}_{E_{ij}}(w_j - w_i)\\ \leq & C\left(w_i^T S^{(i)}_{E_{ij}} w_i + w_j^T S^{(j)}_{E_{ij}} w_j\right).\end{aligned}$$

Note that C depends on the chosen primal space.

2.3 Parallel Sum of Matrices and Spectral Estimates

The next lemma introduces the notion of the parallel sum of matrices of two symmetric positive semidefinite matrices and properties of that operation. The definition of a parallel sum of matrices was first given in [1] and used for the first time in our context in [68]. The first two properties of Lemma 2.3.2 are given and proven in [1]. The third property is given, without a proof, in [68].

Remark 2.3.1. *Using that*

$$\text{Ker}\,(A+B) \subset \text{Ker}\,(A) \text{ and } \text{Ker}\,(A+B) \subset \text{Ker}\,(B)$$

for symmetric positive semidefinite matrices A and B and that $U \subset V$ implies $V^\perp \subset U^\perp$ we obtain

$$\text{Range}\,(A) \subset \text{Range}\,(A+B) \;\text{ and }\; \text{Range}\,(B) \subset \text{Range}\,(A+B).$$

In [62, Theorem 2.1] it was shown for matrices C, D which satisfy

$$\begin{aligned}\text{Range}\,(C) &\subset \text{Range}\,(C+D) \;\; \textit{and}\\ \text{Range}\,(C^H) &\subset \text{Range}\,\left((C+D)^H\right)\end{aligned}$$

or equivalently

$$\begin{aligned}\text{Range}\,(D) &\subset \text{Range}\,(C+D) \;\; \textit{and}\\ \text{Range}\,(D^H) &\subset \text{Range}\,\left((C+D)^H\right)\end{aligned}$$

that $C : D := C(C+D)^+D$ is invariant under the choice of the pseudoinverse $(C+D)^+$. With the symmetry of A and B we conclude that this holds true for $A : B$.

Lemma 2.3.2 (Parallel sum of matrices)**.** *Let A, B be symmetric positive semidefinite and define*

$$A : B = A(A+B)^+B$$

as in Remark 2.3.1 where $(A+B)^+$ denotes a pseudoinverse with

$$\begin{aligned}(A+B)(A+B)^+(A+B) &= (A+B)\\ \textit{and }\; (A+B)^+(A+B)(A+B)^+ &= (A+B)^+.\end{aligned}$$

Then, we have

1. *the spectral estimate*

$$A : B \leq A \qquad \textit{and} \qquad A : B \leq B. \tag{2.3}$$

2. *$A : B$ is symmetric positive semidefinite.*

3. *With $D_A := (A+B)^+A$ and $D_B := (A+B)^+B$, we have additionally:*

$$D_A^T B D_A \leq A : B \qquad \text{and} \qquad D_B^T A D_B \leq A : B. \tag{2.4}$$

Proof. For the proof of 1. and 2., see [1]. Next, we provide a proof of 3. Since A and B are symmetric positive semidefinite (s.p.s.d.), $D_B^T A D_B$ and $D_A^T B D_A$ are also s.p.s.d., and we obtain

$$D_A^T B D_A + D_B^T A D_B = (A : B) D_A + (A : B) D_B = (A : B)(A+B)^+(A+B).$$

Since A and B are s.p.s.d., $x^T(A+B)x = 0$ implies $x^T A x = -x^T B x = 0$. Thus, we have

$$\operatorname{Ker}(A+B) = \operatorname{Ker}(A) \cap \operatorname{Ker}(B).$$

For any x we can write $x = x_R + x_K$ with

$$x_R \in \operatorname{Range}(A+B)^+$$
$$\text{and } x_K \in \operatorname{Ker}(A+B) = \operatorname{Ker}(A) \cap \operatorname{Ker}(B).$$

Using that $(A+B)^+(A+B)$ is a projection onto $\operatorname{Range}(A+B)^+$, we obtain

$$\begin{aligned} x^T D_A^T B D_A x + x^T D_B^T A D_B x &= x^T (A : B)(A+B)^+(A+B)x \\ &= x^T (A : B) x_R \\ &= x^T (A : B) x. \end{aligned}$$

□

2.4 First Approach

In this section, we discuss a first adaptive coarse space which is computed using local eigenvalue problems. The construction of these eigenvalue problems relies on the notion of the parallel sum of matrices introduced in Lemma 2.3.2. This approach was first proposed in [68].

2.4.1 Notation

In the following, we define a scaling for the FETI-DP and BDDC method, denoted as deluxe scaling, which was first introduced in [17]; for further applications, see [2, 51, 65, 9, 12, 41]. Note that this is not a scaling in the common sense since more than just a multiplication with a diagonal matrix is involved.

Definition 2.4.1 (Deluxe scaling)**.** *Let $\mathcal{E}_{ij} \subset \Gamma^{(i)}$ be an edge and let the Schur complements $S^{(i)}_{E_{ij},0}$, $S^{(j)}_{E_{ij},0}$ be as defined in Definition 2.1.1. We define the following scaling matrices*

$$D^{(l)}_{E_{ij}} = \left(S^{(i)}_{E_{ij},0} + S^{(j)}_{E_{ij},0}\right)^{-1} S^{(l)}_{E_{ij},0}, \quad l = i, j.$$

Let $R^{(l)}_{E_{ij}}$ be the restriction operator restricting the degrees of freedom of Lagrange multipliers on Γ to the degrees of freedom of Lagrange multipliers on the open edge $\mathcal{E}_{ij}$. Then, we define the subdomain (deluxe) scaling matrices by

$$D^{(i)} = \sum_{\mathcal{E}_{ij} \subset \Gamma^{(i)}} R^{(i)T}_{E_{ij}} D^{(j)}_{E_{ij}} R^{(i)}_{E_{ij}}.$$

Each pair of scaling matrices $D^{(i)}$, $D^{(j)}$ and $D^{(i)}_{E_{ij}}$, $D^{(j)}_{E_{ij}}$ satisfies the partition-of-unity property (2.2). The scaled jump operator B_D in the FETI-DP algorithm is then given by

$$B_D := [D^{(1)T} B^{(1)}, \ldots, D^{(N)T} B^{(N)}].$$

The transpose is necessary since the $D^{(i)}$ are not symmetric. Using Lemma 2.3.2, we obtain

$$D^{(j)T}_{E_{ij}} S^{(i)}_{E_{ij},0} D^{(j)}_{E_{ij}} \leq S^{(i)}_{E_{ij},0} : S^{(j)}_{E_{ij},0} \quad \text{and} \quad D^{(i)T}_{E_{ij}} S^{(j)}_{E_{ij},0} D^{(i)}_{E_{ij}} \leq S^{(i)}_{E_{ij},0} : S^{(j)}_{E_{ij},0}.$$

2.4.2 Generalized Eigenvalue Problem (First Approach)

We solve the eigenvalue problem

$$S^{(i)}_{E_{ij}} : S^{(j)}_{E_{ij}} x_k = \mu_k \, S^{(i)}_{E_{ij},0} : S^{(j)}_{E_{ij},0} x_k, \tag{2.5}$$

where $\mu_k \leq \text{TOL}$ for a chosen tolerance TOL and enforce the constraints

$$x_k^T (S_{E_{ij},0}^{(i)} : S_{E_{ij},0}^{(j)})(w_i - w_j) = 0,$$

e.g., as described in Section 1.5.

Lemma 2.4.2. *Let*

$$\Pi_k := \sum_{m=1}^{k} x_m x_m^T S_{E_{ij},0}^{(i)} : S_{E_{ij},0}^{(j)}$$

using the eigenvectors x_m of the generalized eigenvalue problem (2.5). Then, we have $\Pi_k(w_i - w_j) = 0$ and the following inequality holds:

$$\begin{aligned}
&(w_i - w_j)^T \left(D_{E_{ij}}^{(j)T} S_{E_{ij},0}^{(i)} D_{E_{ij}}^{(j)} + D_{E_{ij}}^{(i)T} S_{E_{ij},0}^{(j)} D_{E_{ij}}^{(i)} \right) (w_i - w_j) \\
\leq\, & C(\mu_{k+1})^{-1} \left(w_i^T S_{E_{ij}}^{(i)} w_i + w_j^T S_{E_{ij}}^{(j)} w_j \right).
\end{aligned}$$

Proof. The property $\Pi_k(w_i - w_j) = 0$ follows directly. We have

$$\begin{aligned}
&(w_i - w_j)^T D_{E_{ij}}^{(j)T} S_{E_{ij},0}^{(i)} D_{E_{ij}}^{(j)} (w_i - w_j) + (w_j - w_i)^T D_{E_{ij}}^{(i)T} S_{E_{ij},0}^{(j)} D_{E_{ij}}^{(i)} (w_j - w_i) \\
=\, & (w_i - w_j)^T S_{E_{ij},0}^{(j)} (S_{E_{ij},0}^{(i)} + S_{E_{ij},0}^{(j)})^{-1} S_{E_{ij},0}^{(i)} D_{E_{ij}}^{(j)} (w_i - w_j) \\
& + (w_i - w_j)^T S_{E_{ij},0}^{(i)} (S_{E_{ij},0}^{(i)} + S_{E_{ij},0}^{(j)})^{-1} S_{E_{ij},0}^{(j)} D_{E_{ij}}^{(i)} (w_i - w_j) \\
=\, & (w_i - w_j)^T ((S_{E_{ij},0}^{(i)} : S_{E_{ij},0}^{(j)}) D_{E_{ij}}^{(j)} + (S_{E_{ij},0}^{(i)} : S_{E_{ij},0}^{(j)}) D_{E_{ij}}^{(i)})(w_i - w_j) \\
=\, & (w_i - w_j)^T (S_{E_{ij},0}^{(i)} : S_{E_{ij},0}^{(j)})(w_i - w_j) \qquad (2.6) \\
\leq\, & 2(\mu_{k+1})^{-1} \left(w_i^T S_{E_{ij}}^{(i)} : S_{E_{ij}}^{(j)} w_i + w_j^T S_{E_{ij}}^{(i)} : S_{E_{ij}}^{(j)} w_j \right) \\
\leq\, & 2(\mu_{k+1})^{-1} \left(w_i^T S_{E_{ij}}^{(i)} w_i + w_j^T S_{E_{ij}}^{(j)} w_j \right).
\end{aligned}$$

For the last two estimates notice that

$$w_i - w_j = w_i - \Pi_k w_i - (w_j - \Pi_k w_j)$$

and apply Lemma 1.6.2 with $A = S_{E_{ij}}^{(i)} : S_{E_{ij}}^{(j)}$ and $B = S_{E_{ij},0}^{(i)} : S_{E_{ij},0}^{(j)}$. Using the first property of Lemma 2.3.2, we obtain the desired bound. □

Remark 2.4.3. *Up to equation (2.6) no generalized eigenvalue problem is used but only deluxe scaling. Since the term in (2.6) is bounded by*

$$2\left(w_i^T S_{E_{ij},0}^{(i)} w_i + w_j^T S_{E_{ij},0}^{(j)} w_j\right)$$

the inequality

$$\begin{aligned}&(w_i - w_j)^T D_{E_{ij}}^{(j)T} S_{E_{ij},0}^{(i)} D_{E_{ij}}^{(j)} (w_i - w_j) + (w_j - w_i)^T D_{E_{ij}}^{(i)T} S_{E_{ij},0}^{(j)} D_{E_{ij}}^{(i)} (w_j - w_i)\\ \leq\, &2\left(w_i^T S_{E_{ij},0}^{(i)} w_i + w_j^T S_{E_{ij},0}^{(j)} w_j\right)\end{aligned}$$

replaces a classical extension theorem. In [48], the analysis of FETI-DP methods in two dimensions has been extended to uniform domains which are a subset of John domains. Since all tools were provided for John domains with the exception of the extension theorem which requires uniform domains, by using deluxe scaling, the analysis carries over to the broader class of John domains.

2.5 Second Approach

In this section, we describe a variant of the first approach that allows different types of scalings. In the case of standard deluxe scaling, this algorithm is the same as the algorithm introduced in [68]; cf., Section 2.4. A short description of this variant has already been presented in the proceedings article [39]. In this section, we use the same notation as in Section 2.1.

2.5.1 Generalized Eigenvalue Problem (Second Approach)

We solve the eigenvalue problem

$$S_{E_{ij}}^{(i)} : S_{E_{ij}}^{(j)} x_k = \mu_k \left(D_{E_{ij}}^{(j)T} S_{E_{ij},0}^{(i)} D_{E_{ij}}^{(j)} + D_{E_{ij}}^{(i)T} S_{E_{ij},0}^{(j)} D_{E_{ij}}^{(i)}\right) x_k. \tag{2.7}$$

We select the x_k for which $\mu_k \leq \text{TOL}$ and enforce the constraints

$$x_k^T \left(D_{E_{ij}}^{(j)T} S_{E_{ij},0}^{(i)} D_{E_{ij}}^{(j)} + D_{E_{ij}}^{(i)T} S_{E_{ij},0}^{(j)} D_{E_{ij}}^{(i)}\right) (w_i - w_j) = 0,$$

e.g., as described in Section 1.5. Note that (2.5) and (2.7) are the same in the case of deluxe scaling. Analogously to Lemma 2.4.2, we obtain the following bound.

Lemma 2.5.1. *Let*

$$\Pi_k := \sum_{m=1}^{k} x_m x_m^T (D_{E_{ij}}^{(j)T} S_{E_{ij},0}^{(i)} D_{E_{ij}}^{(j)} + D_{E_{ij}}^{(i)T} S_{E_{ij},0}^{(j)} D_{E_{ij}}^{(i)})$$

using the eigenvectors x_m of the generalized eigenvalue problem (2.7). Then, we have

$$\Pi_k(w_i - w_j) = 0$$

and the following inequality holds:

$$\begin{aligned}&(w_i - w_j)^T \left(D_{E_{ij}}^{(j)T} S_{E_{ij},0}^{(i)} D_{E_{ij}}^{(j)} + D_{E_{ij}}^{(i)T} S_{E_{ij},0}^{(j)} D_{E_{ij}}^{(i)} \right) (w_i - w_j) \\ \leq\, & 2(\mu_{k+1})^{-1} w_i^T \left(S_{E_{ij}}^{(i)} w_i + w_j^T S_{E_{ij}}^{(j)} w_j \right)\end{aligned}$$

where $D_{E_{ij}}^{(l)}$, $l = i, j$ are arbitrary scaling matrices that provide a partition-of-unity, i.e., satisfy (2.2).

Proof. Notice that

$$w_i - w_j = w_i - \Pi_k w_i - (w_j - \Pi_k w_j)$$

and apply Lemma 1.6.2 with

$$A = S_{E_{ij}}^{(i)} : S_{E_{ij}}^{(j)} \text{ and } B = D_{E_{ij}}^{(j)T} S_{E_{ij},0}^{(i)} D_{E_{ij}}^{(j)} + D_{E_{ij}}^{(i)T} S_{E_{ij},0}^{(j)} D_{E_{ij}}^{(i)}.$$

With (2.4), we obtain the desired bound. □

2.6 Economic Variant of the Algorithm

In this section, we introduce a new, more economic variant, solving eigenvalue problems on slabs, see Definition 2.6.2. Using such a variant for deluxe scaling but without such eigenvectors in the coarse space was first introduced and numerically tested in [18]; see Remark 2.6.4. Let us note that with respect to the eigenvalue problems on slabs, this variant was first proposed in [38].

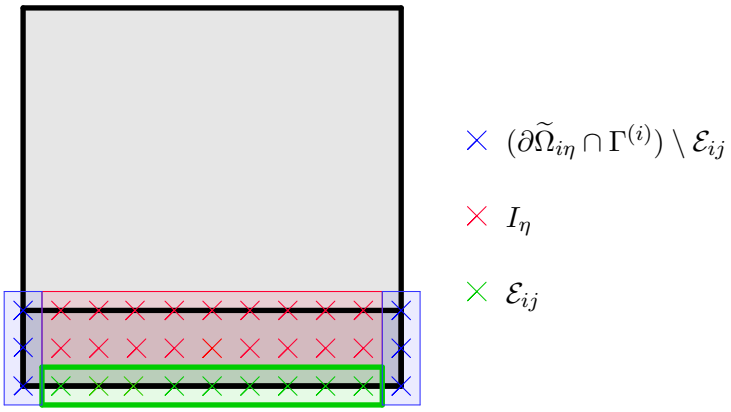

Figure 2.1: Illustration of the sets of indices for the slab variant.

2.6.1 Notation

We first give the definition of an η-patch; see, e.g., also [82, Lemma 3.10], [42, Def. 6.1] and [71, Def. 2.5 and 2.6].

Definition 2.6.1. *An η-patch $\omega \subset \Omega$ denotes an open set which can be represented as a union of shape regular finite elements of diameter $\mathcal{O}(h)$ and which has $diam(\omega) = \mathcal{O}(\eta)$ and a measure of $\mathcal{O}(\eta^2)$.*

The definition of a slab in three dimensions was introduced in [29]; see also [42, 36].

Definition 2.6.2. *Let $\mathcal{E}_{ij} \subset \partial\Omega_i$ be an edge. Then, a slab $\widetilde{\Omega}_{i\eta}$ is a subset of Ω_i of width η with $\mathcal{E}_{ij} \subset \partial\widetilde{\Omega}_{i\eta}$ which can be represented as the union of η-patches ω_{ik}, $k = 1, \ldots, n$, such that $(\partial\omega_{ik} \cap \mathcal{E}_{ij})^\circ \neq \emptyset$, $k = 1, \ldots, n$.*

In addition to $|v|_{E_l}$, c.f. (2.1), we define $|v|^2_{E_{l,\eta}} := a_{l,\eta}(v, v)$, where $a_{l,\eta}(v, v)$ is the same bilinear form as $a_l(v, v)$ but only integrating over the slab $\widetilde{\Omega}_{l,\eta}$, e.g., for scalar diffusion we have

$$a_{l,\eta}(u, v) := \int_{\widetilde{\Omega}_{l,\eta}} \rho_l \nabla u \nabla v \, dx.$$

Let $K_\eta^{\mathcal{E},(l)}$ be the corresponding locally assembled stiffness matrix of the slab of width η corresponding to an edge $\mathcal{E}$ of subdomain Ω_l. Here, we use homogeneous Neumann boundary conditions on the part of the boundary of the slab which intersects the interior of Ω_l.

Definition 2.6.3. *Let $\mathcal{E} \subset \Gamma^{(l)} \cap \partial\widetilde{\Omega}_{l,\eta}$ be an edge and $\mathcal{E}^c \subset \Gamma^{(l)} \cap \partial\widetilde{\Omega}_{l,\eta}$ be the complement of $\mathcal{E}$ with respect to $\Gamma^{(l)} \cap \partial\widetilde{\Omega}_{l,\eta}$. Let $K_\eta^{\mathcal{E},(l)}$ be partitioned as follows*

$$K_\eta^{\mathcal{E},(l)} = \begin{bmatrix} K_{\eta,II}^{\mathcal{E},(l)} & K_{\eta,\Gamma I}^{\mathcal{E},(l)T} \\ K_{\eta,\Gamma I}^{\mathcal{E},(l)} & K_{\eta,\Gamma\Gamma}^{\mathcal{E},(l)} \end{bmatrix}$$

where the index Γ corresponds to degrees of freedom on $\Gamma^{(l)} \cap \partial\widetilde{\Omega}_{l,\eta}$ and the index I corresponds to the remaining degrees of freedom in $\overline{\widetilde{\Omega}}_{l,\eta}$. Define the extension operator

$$\mathcal{H}_\eta^{(l)} v = \begin{bmatrix} v_{|\Gamma^{(l)}\cap\partial\widetilde{\Omega}_{l,\eta}} \\ -K_{\eta,II}^{\mathcal{E},(l)-1} K_{\eta,\Gamma I}^{\mathcal{E},(l)T} v_{|\Gamma^{(l)}\cap\partial\widetilde{\Omega}_{l,\eta}} \end{bmatrix}.$$

Let

$$S_\eta^{\mathcal{E},(l)} = \begin{pmatrix} S_{\mathcal{E}\mathcal{E},\eta}^{\mathcal{E},(l)} & S_{\mathcal{E}^c\mathcal{E},\eta}^{\mathcal{E},(l)T} \\ S_{\mathcal{E}^c\mathcal{E},\eta}^{\mathcal{E},(l)} & S_{\mathcal{E}^c\mathcal{E}^c,\eta}^{\mathcal{E},(l)} \end{pmatrix}$$

be the Schur complement of $K_\eta^{\mathcal{E},(l)}$ after elimination of the interior degrees of freedom. Eliminating further all degrees of freedom except those on the edge we obtain the Schur complement

$$S_{E,\eta}^{(l)} = S_{\mathcal{E}\mathcal{E},\eta}^{\mathcal{E},(l)} - S_{\mathcal{E}^c\mathcal{E},\eta}^{\mathcal{E},(l)T} S_{\mathcal{E}^c\mathcal{E}^c,\eta}^{\mathcal{E},(l)-1} S_{\mathcal{E}^c\mathcal{E},\eta}^{\mathcal{E},(l)}.$$

With the discrete energy minimal extension operator $\mathcal{H}_\eta^{(l)}$ from $\Gamma^{(l)} \cap \partial\widetilde{\Omega}_{l,\eta}$ to the interior, we have

$$|\mathcal{H}_\eta^{(l)} \mathcal{H}_{\mathcal{E}}^{(l)} v_E|_{E_{l,\eta}}^2 \geq v_E^T S_{E,\eta}^{(l)} v_E.$$

Let the local finite element space be partitioned into variables on the edge $\mathcal{E}$ and the remaining variables $\mathcal{E}^c$. Then the local stiffness matrices $K^{(l)}$ can be partitioned accordingly and we obtain

$$K^{(l)} = \begin{pmatrix} K^{(l)}_{\mathcal{E}\mathcal{E}} & K^{(l)T}_{\mathcal{E}^c\mathcal{E}} \\ K^{(l)}_{\mathcal{E}^c\mathcal{E}} & K^{(l)}_{\mathcal{E}^c\mathcal{E}^c} \end{pmatrix}.$$

Thus, by removing all columns and rows related to the degrees of freedom outside the closure of the slab and those on $(\partial\widetilde{\Omega}_{l\eta} \cap \Gamma^{(l)}) \setminus \mathcal{E}$, we obtain a matrix of the form

$$\begin{pmatrix} K^{(l)}_{\mathcal{E}\mathcal{E}} & K^{(l)T}_{I_\eta\mathcal{E}} \\ K^{(l)}_{I_\eta\mathcal{E}} & K^{(l)}_{I_\eta I_\eta} \end{pmatrix}.$$

Here, the index I_η relates to the degrees of freedom on the closure of the slab except those on $\partial\widetilde{\Omega}_{l\eta} \cap \Gamma^{(l)}$; see Figure 2.1 for an illustration. We define another Schur complement by

$$S^{(l)}_{E,0,\eta} = K^{(l)}_{\mathcal{E}\mathcal{E}} - K^{(l)T}_{I_\eta\mathcal{E}} K^{(l)-1}_{I_\eta I_\eta} K^{(l)}_{I_\eta\mathcal{E}}.$$

We define an extension operator $\mathcal{H}^{(l)}_{\eta,0}$ from the local interface $\partial\widetilde{\Omega}_{l,\eta} \cap \Gamma^{(l)}$ of a subdomain Ω_l to the interior by

$$\mathcal{H}^{(l)}_{\eta,0} v = \begin{cases} v, & \text{on } \partial\Omega_l \cap \partial\widetilde{\Omega}_{l,\eta}, \\ \text{minimal energy extension}, & \text{in } \overline{\widetilde{\Omega}}_{l,\eta} \cap \Omega_l, \\ 0, & \text{elsewhere.} \end{cases}$$

Then, we have $v^T S^{(l)}_{E,0,\eta} v = |\mathcal{H}^{(l)}_{\eta,0} I^h(\theta_{\mathcal{E}} v)|^2_{E_l}$.

Remark 2.6.4 (economic deluxe scaling)**.** *In [18], the authors proposed an economic variant of deluxe scaling by replacing the Schur complements $S^{(l)}_{E,0}$, $l = i, j$ by $S^{(l)}_{E,0,\eta}$ with $\eta = h$. As in [18] we will denote this variant by e-deluxe scaling.*

2.6.2 Generalized Eigenvalue Problem (Economic Version)

We solve the eigenvalue problem

$$S^{(i)}_{E_{ij},\eta} : S^{(j)}_{E_{ij},\eta} x_k = \mu_k \left(D^{(j)T}_{E_{ij}} S^{(i)}_{E_{ij},0,\eta} D^{(j)}_{E_{ij}} + D^{(i)T}_{E_{ij}} S^{(j)}_{E_{ij},0,\eta} D^{(i)}_{E_{ij}} \right) x_k, \qquad (2.8)$$

where $\mu_k \leq \text{TOL}$ and

$$D^{(l)}_{E_{ij}} = \left(S^{(i)}_{E_{ij},0,\eta} + S^{(j)}_{E_{ij},0,\eta} \right)^{-1} S^{(l)}_{E_{ij},0,\eta} \text{ for } l = i, j.$$

We then enforce the constraints

$$x_k^T \left(D^{(j)T}_{E_{ij}} S^{(i)}_{E_{ij},0,\eta} D^{(j)}_{E_{ij}} + D^{(i)T}_{E_{ij}} S^{(j)}_{E_{ij},0,\eta} D^{(i)}_{E_{ij}} \right) (w_i - w_j) = 0,$$

as in Section 1.5.

Lemma 2.6.5. *We define*

$$\Pi_k := \sum_{m=1}^{k} x_k x_k^T \left(D^{(j)T}_{E_{ij}} S^{(i)}_{E_{ij},0,\eta} D^{(j)}_{E_{ij}} + D^{(i)T}_{E_{ij}} S^{(j)}_{E_{ij},0,\eta} D^{(i)}_{E_{ij}} \right)$$

using the eigenvectors x_m of the generalized eigenvalue problem (2.8). Then $\Pi_k(w_i - w_j) = 0$ and the following inequality holds:

$$\begin{aligned} &(w_i - w_j)^T \left(D^{(j)T}_{E_{ij}} S^{(i)}_{E_{ij},0} D^{(j)}_{E_{ij}} + D^{(i)T}_{E_{ij}} S^{(j)}_{E_{ij},0} D^{(i)}_{E_{ij}} \right) (w_i - w_j) \\ \leq &2(\mu_{k+1})^{-1} w_i^T S^{(i)}_{E_{ij}} w_i + w_j^T S^{(j)}_{E_{ij}} w_j. \end{aligned}$$

Proof. Since the discrete harmonic extension $|\mathcal{H}^{(l)} I^h(\theta_{E_{ij}} v)|^2_{E_l} = v^T S^{(l)}_{E_{ij},0} v$

has the smallest energy, we obtain

$$
\begin{aligned}
&(w_i - w_j)^T \left(D_{E_{ij}}^{(j)T} S_{E_{ij},0}^{(i)} D_{E_{ij}}^{(j)} + D_{E_{ij}}^{(i)T} S_{E_{ij},0}^{(j)} D_{E_{ij}}^{(i)} \right) (w_i - w_j) \\
\leq &(w_i - w_j)^T \left(D_{E_{ij}}^{(j)T} S_{E_{ij},0,\eta}^{(i)} D_{E_{ij}}^{(j)} + D_{E_{ij}}^{(i)T} S_{E_{ij},0,\eta}^{(j)} D_{E_{ij}}^{(i)} \right) (w_i - w_j) \\
\leq &(\mu_{k+1})^{-1} (w_i - w_j)^T S_{E_{ij},\eta}^{(i)} : S_{E_{ij},\eta}^{(j)} (w_i - w_j) \\
\leq &2(\mu_{k+1})^{-1} \left(|w_i|^2_{S_{E_{ij},\eta}^{(i)}} + |w_j|^2_{S_{E_{ij},\eta}^{(j)}} \right) \\
\leq &2\,(\mu_{k+1})^{-1} \left(|\mathcal{H}_\eta^{(i)} \mathcal{H}_{\mathcal{E}_{ij}}^{(i)} w_i|^2_{E_{i,\eta}} + |\mathcal{H}_\eta^{(j)} \mathcal{H}_{\mathcal{E}_{ij}}^{(j)} w_j|^2_{E_{j,\eta}} \right) \\
\leq &2\,(\mu_{k+1})^{-1} \left(|\mathcal{H}^{(i)} \mathcal{H}_{\mathcal{E}_{ij}}^{(i)} w_i|^2_{E_{i,\eta}} + |\mathcal{H}^{(j)} \mathcal{H}_{\mathcal{E}_{ij}}^{(j)} w_j|^2_{E_{j,\eta}} \right) \\
\leq &2\,(\mu_{k+1})^{-1} \left(|\mathcal{H}^{(i)} \mathcal{H}_{\mathcal{E}_{ij}}^{(i)} w_i|^2_{E_i} + |\mathcal{H}^{(j)} \mathcal{H}_{\mathcal{E}_{ij}}^{(j)} w_j|^2_{E_j} \right) \\
= &2\,(\mu_{k+1})^{-1} \left(w_i^T S_{E_{ij}}^{(i)} w_i + w_j^T S_{E_{ij}}^{(j)} w_j \right).
\end{aligned}
$$

□

2.7 Condition Number Bound

Based on the estimates for P_D for the first coarse space, given in Sections 2.4.2, 2.5.1, and 2.6.2, we now present our condition number estimate.

Lemma 2.7.1. *Let $N_{\mathcal{E}}$ be the maximum number of edges of a subdomain. The condition number $\kappa(\widehat{M}^{-1}F)$ of the FETI-DP algorithm with adaptive constraints defined as in Sections 2.4.2, 2.5.1, or 2.6.2 either enforced by the projector preconditioner $\widehat{M}^{-1} = M_{PP}^{-1}$ or the balancing preconditioner $\widehat{M}^{-1} = M_{BP}^{-1}$ satisfies*

$$\kappa(\widehat{M}^{-1}F) \leq 2N_{\mathcal{E}}^2 \, TOL^{-1}.$$

Proof. For $w \in \widetilde{W}$ we have the estimate

$$\begin{aligned}
|P_D w|_{\widetilde{S}}^2 &= \sum_{i=1}^{N} |R^{(i)} P_D w|_{S_i}^2 \\
&\leq N_{\mathcal{E}} \sum_{i=1}^{N} \sum_{j \in N_i} |I^h(\theta_{\mathcal{E}_{ij}} D^{(i)}(w_i - w_j))|_{S_i}^2 \\
&\leq N_{\mathcal{E}} \sum_{\mathcal{E}_{ij} \subset \Gamma} (w_i - w_j)^T \left(D_{E_{ij}}^{(j)T} S_{E_{ij},0}^{(i)} D_{E_{ij}}^{(j)} + D_{E_{ij}}^{(i)T} S_{E_{ij},0}^{(j)} D_{E_{ij}}^{(i)} \right) (w_i - w_j).
\end{aligned}$$

Using Lemma 2.4.2 for the coarse space in Section 2.4.2, Lemma 2.5.1 for the coarse space in Section 2.5.1, and Lemma 2.6.5 for the coarse space in Section 2.6.2 and using that $\mu_{k+1} \geq \text{TOL}$ we obtain the estimate

$$\begin{aligned}
|P_D w|_{\widetilde{S}}^2 &\leq 2N_{\mathcal{E}} \sum_{\mathcal{E}_{ij} \subset \Gamma} \text{TOL}^{-1} \left(w_i^T S_{E_{ij}}^{(i)} w_i + w_j^T S_{E_{ij}}^{(j)} w_j \right) \\
&\leq 2N_{\mathcal{E}} \sum_{\mathcal{E}_{ij} \subset \Gamma} \text{TOL}^{-1} \left(w_i^T S_i w_i + w_j^T S_j w_j \right) \\
&\leq 2N_{\mathcal{E}}^2 \, \text{TOL}^{-1} \sum_{i=1}^{N} |R^{(i)} w|_{S_i}^2 \\
&\leq 2N_{\mathcal{E}}^2 \, \text{TOL}^{-1} \, |w|_{\widetilde{S}}^2.
\end{aligned}$$

□

3 Coarse Space Based on a Local Jump Operator

We will now discuss an approach which has been successfully used in FETI-DP and BDDC for some time [59]. Let us note that this approach is also based on eigenvalue estimates related to the P_D-operator. In the following, we give a brief description of the algorithm in [59] for the convenience of the reader. The chapter is based on [38]. In Section 3.1, we introduce the relevant notation and in Section 3.2 the specific eigenvalue problem. In Section 3.3, we also give an estimate of the condition number in the case of a two-dimensional problem where all vertices are primal in the initial coarse space. We proved this result in [38]. In Section 3.4, we will give some numerical results for perfect elastoplasticity from [40]. For numerical results comparing this coarse space to various other adaptive coarse spaces, see Section 5.2.

3.1 Notation

For an edge $\mathcal{E}_{ij}$ let $B_{E_{ij}} = \begin{bmatrix} B_{E_{ij}}^{(i)} & B_{E_{ij}}^{(j)} \end{bmatrix}$ be the submatrix of $\begin{bmatrix} B^{(i)} & B^{(j)} \end{bmatrix}$ with the rows that consist of exactly one 1 and one -1 and are zero otherwise. Let $B_{D,E_{ij}} = \begin{bmatrix} B_{D,E_{ij}}^{(i)} & B_{D,E_{ij}}^{(j)} \end{bmatrix}$ be obtained by keeping the same rows of $\begin{bmatrix} B_D^{(i)} & B_D^{(j)} \end{bmatrix}$. Let

$$S_{ij} = \begin{bmatrix} S_i & 0 \\ 0 & S_j \end{bmatrix}$$

and a local version of the P_D-operator $P_{D_{ij}} = B^T_{D,E_{ij}} B_{E_{ij}}$. By $\widetilde{W}_{ij}$ we denote the space of functions in $W_i \times W_j$ which are continuous in those primal variables that the subdomains Ω_i and Ω_j have in common. We define by Π_{ij} the l_2-orthogonal projection from $W_i \times W_j$ onto $\widetilde{W}_{ij}$. Another orthogonal projection $\overline{\Pi}_{ij}$ maps from $W_i \times W_j$ to Range $(\Pi_{ij} S_{ij} \Pi_{ij} + \sigma(I - \Pi_{ij}))$, where σ is a positive constant, e.g., the maximum of the entries of the diagonal of S_{ij}.

Let us briefly describe how the projections Π_{ij} and $\overline{\Pi}_{ij}$ can be obtained. Let $R^{(l)T}_{ij}$ be the assembly operators which assemble the primal variables on $\partial\Omega_i \cap \partial\Omega_j$ and are the identity on the remaining variables of $\Gamma^{(i)} \times \Gamma^{(j)}$. We define an operator R_{ij} by

$$R_{ij} = \begin{bmatrix} R^{(i)}_{ij} \\ R^{(j)}_{ij} \end{bmatrix}.$$

Then, we obtain the l_2-orthogonal projection onto $\widetilde{W}_{ij}$ by

$$\Pi_{ij} = R_{ij} (R^T_{ij} R_{ij})^{-1} R^T_{ij}.$$

For the construction of $\overline{\Pi}_{ij}$ let

$$\{v_1, \ldots, v_l\} \tag{3.1}$$

be an l_2-orthonormal basis of Ker $(\Pi_{ij} S_{ij} \Pi_{ij} + \sigma(I - \Pi_{ij}))$. In the case of linear elasticity, we take the approximations of the rigid body modes restricted to $\Gamma^{(i)} \times \Gamma^{(j)}$ that move both structures Ω_i and Ω_j simultaneously and orthonormalize them with the modified Gram-Schmidt algorithm. In case of a diffusion problem (3.1) consists of a constant vector. Then, we have $(I - \overline{\Pi}_{ij}) = \sum_{r=1}^{l} v_r v_r^T$ and thus $\overline{\Pi}_{ij} = I - \sum_{r=1}^{l} v_r v_r^T$. For the case that Ker $(\Pi_{ij} S_{ij} \Pi_{ij} + \sigma(I - \Pi_{ij}))$ is unknown, we note that we could also use the matrices $\Psi^{(i)}$ and $\Psi^{(j)}$ containing the coarse basis functions of $\Gamma^{(i)}$ and $\Gamma^{(j)}$ to compute (3.1). The matrix $\Psi^{(i)}$ is obtained by extending the columns of $R^{(i)}_{\Pi}$ to the substructure Ω_i discrete harmonically and restricting them to the

interface $\Gamma^{(i)}$. For details on computing (3.1), see [59]. For the computation of the functions $\Psi^{(i)}$, cf. [59, 54].

Note that $\Pi_{ij}(I-\overline{\Pi}_{ij})w_{ij} = (I-\overline{\Pi}_{ij})w_{ij}$ since $(I-\overline{\Pi}_{ij})$ is an orthogonal projection onto the space of rigid body modes that are continuous on $W_i \times W_j$. Hence, $P_{D_{ij}}\Pi_{ij}(I-\overline{\Pi}_{ij})w_{ij} = 0$ and thus

$$P_{D_{ij}}\Pi_{ij}\overline{\Pi}_{ij}w_{ij} = P_{D_{ij}}\Pi_{ij}w_{ij}. \tag{3.2}$$

3.2 Generalized Eigenvalue Problem

We solve the eigenvalue problem

$$\overline{\Pi}_{ij}\Pi_{ij}P_{D_{ij}}^T S_{ij} P_{D_{ij}}\Pi_{ij}\overline{\Pi}_{ij}w_{ij}^k = \mu_{ij}^k(\overline{\Pi}_{ij}\overline{S}_{ij}\overline{\Pi}_{ij} + \sigma(I-\overline{\Pi}_{ij}))w_{ij}^k, \tag{3.3}$$

where $\mu_{ij}^k \geq$TOL and

$$\overline{S}_{ij} = \Pi_{ij}S_{ij}\Pi_{ij} + \sigma(I-\Pi_{ij}).$$

We then enforce the constraints ${w_{ij}^k}^T P_{D_{ij}}^T S_{ij} P_{D_{ij}} w_{ij} = 0$. From (3.3), we obtain by using (3.2)

$$\Pi_{ij}P_{D_{ij}}^T S_{ij} P_{D_{ij}}\Pi_{ij}w_{ij}^k = \mu_{ij}^k(\overline{\Pi}_{ij}(\Pi_{ij}S_{ij}\Pi_{ij} + \sigma(I-\Pi_{ij}))\overline{\Pi}_{ij} + \sigma(I-\overline{\Pi}_{ij}))w_{ij}^k. \tag{3.4}$$

From (3.4) using [59, Theorem 9] and [59, Theorem 11], we obtain the estimate

$$w_{ij}^T\Pi_{ij}P_{D_{ij}}^T S_{ij} P_{D_{ij}}\Pi_{ij}w_{ij} \leq \mu_{ij}^{k-1} w_{ij}^T\Pi_{ij}S_{ij}\Pi_{ij}w_{ij} \tag{3.5}$$

for all w_{ij} in $W_i \times W_j$ with ${w_{ij}^k}^T P_{D_{ij}}^T S_{ij} P_{D_{ij}} w_{ij} = 0$, $\mu_{ij}^k \geq$ TOL.

3.3 Condition Number Estimate of the Coarse Space in 2D

To the best of our knowledge, the following estimate for the classic approach [59] was first proposed in [38].

Theorem 3.3.1. *Let $N_{\mathcal{E}}$ be the maximum number of edges of a subdomain. The condition number $\kappa(\widehat{M}^{-1}F)$ of the FETI-DP algorithm with adaptive constraints defined in Section 3.2 either enforced by the projector preconditioner $\widehat{M}^{-1} = M_{PP}^{-1}$ or by the balancing preconditioner $\widehat{M}^{-1} = M_{BP}^{-1}$ satisfies*

$$\kappa(\widehat{M}^{-1}F) \leq N_{\mathcal{E}}^2 \, TOL.$$

Proof. The local jump operator in the eigenvalue problems is

$$P_{D_{ij}} = \begin{bmatrix} B_{D,E_{ij}}^{(i)T} B_{E_{ij}}^{(i)} & B_{D,E_{ij}}^{(i)T} B_{E_{ij}}^{(j)} \\ B_{D,E_{ij}}^{(j)T} B_{E_{ij}}^{(i)} & B_{D,E_{ij}}^{(j)T} B_{E_{ij}}^{(j)} \end{bmatrix}.$$

Application to a vector yields

$$P_{D_{ij}} \begin{bmatrix} R^{(i)}w \\ R^{(j)}w \end{bmatrix} = \begin{bmatrix} I^h(\theta_{E_{ij}} D^{(i)}(w_i - w_j)) \\ I^h(\theta_{E_{ij}} D^{(j)}(w_j - w_i)) \end{bmatrix}.$$

For $w \in \widetilde{W}$ we have $\begin{bmatrix} R^{(i)}w \\ R^{(j)}w \end{bmatrix} \in \widetilde{W}_{ij}$, and therefore $\Pi_{ij} \begin{bmatrix} R^{(i)}w \\ R^{(j)}w \end{bmatrix} = \begin{bmatrix} R^{(i)}w \\ R^{(j)}w \end{bmatrix}$.

All vertices are assumed to be primal. Thus, for $w \in \widetilde{W}$, we obtain

$$\begin{aligned}
|P_D w|_{\widetilde{S}}^2 &= \sum_{i=1}^{N} |R^{(i)} P_D w|_{S_i}^2 \\
&\leq N_{\mathcal{E}} \sum_{i=1}^{N} \sum_{j \in N_i} |I^h(\theta_{\mathcal{E}_{ij}} D^{(i)}(w_i - w_j))|_{S_i}^2 \\
&= N_{\mathcal{E}} \sum_{\mathcal{E}_{ij} \subset \Gamma} |I^h(\theta_{\mathcal{E}_{ij}} D^{(i)}(w_i - w_j))|_{S_i}^2 + |I^h(\theta_{\mathcal{E}_{ij}} D^{(j)}(w_j - w_i))|_{S_j}^2 \\
&= N_{\mathcal{E}} \sum_{\mathcal{E}_{ij} \subset \Gamma} \begin{bmatrix} w_i \\ w_j \end{bmatrix}^T \Pi_{ij} P_{D_{ij}}^T \begin{bmatrix} S_i & \\ & S_j \end{bmatrix} P_{D_{ij}} \Pi_{ij} \begin{bmatrix} w_i \\ w_j \end{bmatrix} \\
&\overset{(3.5)}{\leq} N_{\mathcal{E}} \sum_{\mathcal{E}_{ij} \subset \Gamma} \mu_{ij}^{k-1} \begin{bmatrix} w_i \\ w_j \end{bmatrix}^T \Pi_{ij} \begin{bmatrix} S_i & \\ & S_j \end{bmatrix} \Pi_{ij} \begin{bmatrix} w_i \\ w_j \end{bmatrix} \\
&\leq N_{\mathcal{E}} \, TOL \sum_{\mathcal{E}_{ij} \subset \Gamma} |w_i|_{S_i}^2 + |w_j|_{S_j}^2
\end{aligned}$$

$$\leq N_{\mathcal{E}}^2 \, TOL \, \sum_{i=1}^{N} |R^{(i)} w|_{S_i}^2$$

$$= N_{\mathcal{E}}^2 \, \text{TOL} \, |w|_{\widetilde{S}}^2. \qquad \square$$

3.4 Nonlinear Numerical Example for Perfect Elastoplasticity

In the following, we will present numerical examples for the case of perfect elastoplasticity. Note that these can also be found in [40]. Consider a square domain $\Omega = (0,1)^2$ with zero Dirichlet boundary conditions imposed on the lower edge $\{(x,y) \in \partial\Omega \,|\, y = 0\}$ which is exposed to a surface force $g(x,y,t) = (150t, 0)^T$ if $(x,y) \in \{(x,y) \in \partial\Omega \,|\, y = 1\}$ and $g(x,y,t) = 0$ elsewhere. The material has a Young modulus of $E = 206900$, a Poisson ratio of $\nu = 0.29$ and $\sigma_y = 200$. We compute the solution in the time interval $T = [0, 0.45]$ in nine time steps of step length $\Delta t = 0.05$. In all our examples in this section the space is discretized with $\mathbb{P}2$ finite elements. In the first set of numerical experiments, we consider a classical coarse space with vertex and edge average constraints using different partitions into elements and subdomains. The classical coarse space is sufficient if the plastically activated zone

$n = H/h$	$N = 1/H$	max. cond	max. CG-It.	Newton its per timestep
20	2	**4.06**	**13**	1/1/1/4/4/6/7/9/11
30	2	**4.53**	**14**	1/1/3/5/5/7/8/10/11
40	2	**4.87**	**14**	1/1/3/4/5/7/9/13/13

Table 3.1: FETI-DP maximal condition numbers and iteration counts in Newton's scheme with a coarse space consisting of vertices and edge averages. We use $\mathbb{P}2$ finite elements; published in [40].

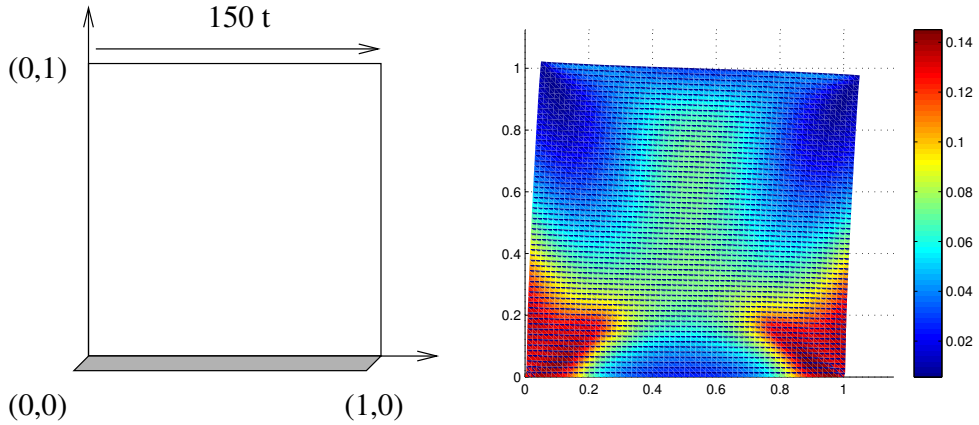

Figure 3.1: Unit square with zero Dirichlet boundary conditions at the lower edge $y = 0$ exposed to a surface force $g(t) = (150t, 0)^T$ at the upper edge $y = 1$ (left). Displacement magnified by factor 20 and shear energy density in the last timestep (right). Material parameters $E = 206900$, $\nu = 0.29$ and $\sigma_y = 200$; published in [40].

$n = H/h$	$N = 1/H$	max. cond	max. CG-It.
4	15	**900837**	**371**
6	15	$> \mathbf{10^6}$	$> \mathbf{1000}$
8	15	$> \mathbf{10^6}$	$> \mathbf{1000}$

Table 3.2: Problems with the Classical Coarse Space. FETI-DP maximal condition numbers and iteration counts. We use $\mathbb{P}2$ finite elements; published in [40].

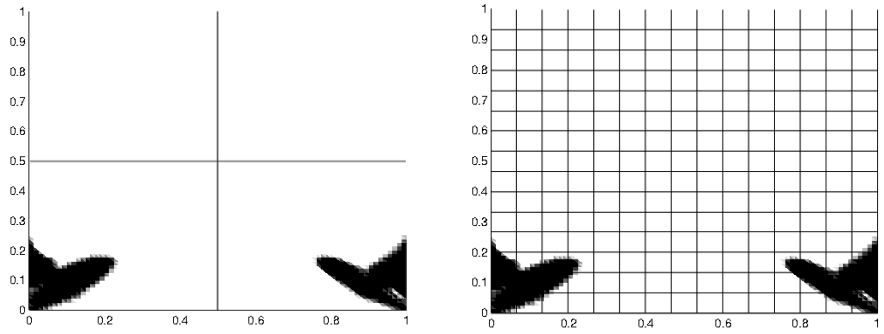

Figure 3.2: Plastically activated zone in the last timestep. Decomposition into 2×2 subdomains. The plastically activated zones stay completely inside of subdomains (left). Decomposition into 15×15 subdomains. The plastically activated zones intersect the interface (right); published in [40].

does not intersect the interface; see Table 3.1 for a decomposition in 2×2 subdomains. In this case each linearized system can be analyzed as in [29] using a slab technique. However, if the plastically activated zone intersects the interface, the condition numbers and iteration counts increase considerably; see Table 3.2 for the results with a decomposition into 15×15 subdomains. If H/h exceeds six, the method does not converge in 1000 iterations. For the results with the adaptive coarse space described in Section 3.2, see Table 3.3. The eigenpairs were computed using the MATLAB built-in function 'eig'. The complexity thus is cubic with respect to the number of nodes on the subdomain edges. For constant H/h the number of nodes on the subdomain edges is constant. Moreover, the global number of subdomain edges, and thus also the number of eigenvalue problems, grows linearly with the number of subdomains. The solution of the eigenvalue problems can be performed in parallel. The condition numbers and iteration counts in Table 3.3 compared to the classical coarse space decrease significantly compared to Table 3.2 for the cost of a few more primal constraints in the last time steps. The tolerance is currently determined heuristically; see Table 3.3. For more numerical

results with the adaptive approach introduced in this chapter, see Chapter 5.

$n = H/h$	$N = 1/H$	TOL	max cond	max it	elas. it	constraints/ timestep	global dofs	#EV/ #dofs
4	15	6.0	**5.84**	**25**	25	0/0/0/0/0/ 0/20/46/121	8316	1.5%
6	15	7.0	**7.06**	**28**	27	0/0/0/0/0/ 0/30/71/180	11676	1.5%
8	15	8.0	**8.01**	**30**	29	0/0/0/0/0/ 0/37/82/225	15036	1.5%
4	15	5.9	**5.84**	**25**	25	0/0/0/0/0/ 0/20/46/124	8316	1.5%
6	15	7.1	**7.06**	**28**	27	0/0/0/0/0/ 0/30/71/180	11676	1.5%

Table 3.3: For each subdomain in each spatial direction, there are n finite elements and in each spatial direction there are N subdomains. 'TOL' denotes the prescribed tolerance for the condition number, 'max cond' the maximal condition number in the Newton iterations, 'max it' the maximal number of preconditioned conjugate gradient iterations, and 'constraints/timestep' the amount of constraints in each timestep. The tolerances 'TOL' were chosen from considering the condition numbers of corresponding linear elastic problems. The number in the 'elas. it' column refers to the iteration counts of these corresponding elasticity problems. We can also use the condition number of the first few time steps, where the material still behaves elastically, as a reference. It can be seen that the results are not very sensitive to small changes in the tolerance; published in [40].

4 Coarse Space Related to Weighted Poincaré Inequalities

The following approach is aimed at replacing different technical tools that may no longer be available in a general context, in particular a weighted Poincaré inequality and an extension theorem. This is the case, e.g., if the coefficient in the diffusion equation has many jumps across and along the interface of the partition into subdomains. The presentation here is based on [42] and [38]; see also the proceedings articles [41, 36].

In some special cases of varying coefficients, robustness of FETI-DP and BDDC methods can be obtained at no or almost no additional computational cost. If the coefficient of the partial differential equation is constant or only slightly varying on every subdomain but possibly has arbitrarily large jumps across the interface, a robust coarse space can be constructed using only vertices as primal variables in combination with a proper scaling in the preconditioner; see, e.g., [73, 48]. Other simple configurations where the coefficient jump is not across the interface can be treated by weighted constraints [45]. Some configurations do not need any modification of the algorithm [70, 29].

In this section, we present coarse spaces which are tailored for more general coefficient distributions. Of course, we obtain the robustness at additional computational cost, i.e., we have to solve local eigenvalue problems and we have to accept a slightly larger coarse space.

Let $\mathcal{E}_{ij}$ be an edge shared by the subdomains Ω_i and Ω_j and let $S^{(i)}_{\mathcal{E}_{ij},c,\rho}$ be the Schur complement that is obtained from $K^{(i)}$ after eliminating all

variables except of the degrees of freedom on the closure of the edge. Let

$$s^{(i)}_{\mathcal{E}_{ij},c,\rho}(u,v) := u^T S^{(i)}_{\mathcal{E}_{ij},c,\rho} v$$

be the corresponding bilinear form. In addition, we define the weighted $L^2(\mathcal{E}_{ij})$-inner product

$$m^{(l)}_{\mathcal{E}_{ij},\rho}(u,v) := \int_{\mathcal{E}_{ij}} \rho_l \, u \cdot v \, ds, \quad \text{for } l = i, j.$$

For $\rho_{|\mathcal{E}_{ij}} = 1$ we have the Poincaré inequality on an edge $\mathcal{E}_{ij}$

$$\begin{aligned} ||v^{(i)} - \overline{v^{(i)}}||^2_{L^2(\mathcal{E}_{ij})} &= m_{\mathcal{E}_{ij},1}(v^{(i)} - \overline{v^{(i)}}, v^{(i)} - \overline{v^{(i)}}) \\ &\leq C H_i |v^{(i)}|^2_{H^1(\Omega_i)} \quad \forall\, v^{(i)} \in H^1(\Omega_i), \end{aligned}$$

where

$$\overline{v^{(i)}} = \frac{1}{|\mathcal{E}_{ij}|} \int_{\mathcal{E}_{ij}} v^{(i)} ds$$

is the edge average of $v^{(i)}$. However, if the coefficient on a subdomain has a large variation, the constant in the Poincaré inequality may depend on the ratio of the largest and the smallest value of the coefficient, and the higher the contrast the larger the Poincaré constant becomes; see, e.g., [72, Theorem 2.9, Proposition 3.7].

Definition 4.0.1 ([72])**.** *Let the weight function $\rho \in L^\infty_+(\Omega)$ be piecewise constant with respect to a nonoverlapping partitioning of Ω into open, connected Lipschitz polygons (polyhedra) $\mathcal{Y} := \{Y^{(l)} : l = 1, \ldots, n\}$, i.e.,*

$$\overline{\Omega} = \cup_{l=1}^n \overline{Y}^{(l)} \quad \textit{and} \quad \rho_{|Y^{(l)}} \equiv \rho^{(l)}$$

for some constants $\rho^{(l)}$ and let l^* be such that $\rho^{(l^*)} = \max\{\rho^{(l)}\}_{l=1}^n$.

1. *We call the region*

$$P^{(l_1,l_s)} := \left(\overline{Y}^{(l_1)} \cup \overline{Y}^{(l_2)} \cup \cdots \overline{Y}^{(l_s)}\right)^\circ, 1 \leq l_1, \ldots, l_s \leq n$$

a quasimonotone path from $Y^{(l_1)}$ to $Y^{(l_s)}$ (with respect to ρ), if the following two conditions are satisfied:

a) for each $i = 1, \ldots, s-1$, *the regions* $\overline{Y}^{(l_i)}$ *and* $\overline{Y}^{(l_{i+1})}$ *share a common* $(d-1)$*-dimensional manifold* X_i,

b) $\rho^{(l_1)} \leq \rho^{(l_2)} \leq \cdots \leq \rho^{(l_s)}$.

2. *We say* ρ *is quasimonotone on* Ω, *if for any* $k = 1, \ldots, n$ *there exists a quasimonotone path* $P^{(k,l^*)}$ *from* $Y^{(k)}$ *to* $Y^{(l^*)}$.

Note that Definition 4.0.1 is a generalization of quasimonotone coefficients as introduced in [21]. In case of a quasimonotone coefficient it is possible to show the independence of the constant on the contrast by introducing weighted Poincaré inequalities and weighted edge averages. If the coefficient is not quasimonotone, this approach is not successful. For a coefficient that is quasimonotone on the subdomains, see Figure 4.4 (right); for counterexamples, see, e.g., Figure 4.5. In the following, we will use a different approach to obtain a constant independent of the jump of the coefficients which are not quasimonotone by solving local eigenvalue problems and enriching the coarse space with certain eigenvectors. Similar approaches have been used for overlapping Schwarz methods in [28, 27, 19, 80, 22]. To obtain a similar estimate for coefficients which are not quasimonotone, we need to replace the Poincaré inequality by a more general estimate since the Poincaré constant is contrast dependent in this case. However, we need to enforce more constraints on the function to get a contrast independent estimate. In general, the Poincaré constant can also depend on the geometric scale; for a more detailed discussion of quasimonotone coefficients and generalized Poincaré inequalities, see [72, 67, 69].

4.1 First Eigenvalue Problem and a Spectral Estimate

Let $\mathcal{E}_{ij}$ be an edge. We solve the following generalized eigenvalue problem on $\mathcal{E}_{ij}$.

Eigenvalue Problem 1. *Find* $(u_k^{(i)}, \mu_k^{(i)}) \in W^h(\mathcal{E}_{ij}) \times \mathbb{R}$ *such that*

$$s^{(i)}_{\mathcal{E}_{ij},c,\rho}(u_k^{(i)}, v) = \mu_k^{(i)} m^{(i)}_{\mathcal{E}_{ij},\rho}(u_k^{(i)}, v) \; \forall v \in W^h(\mathcal{E}_{ij}),\; k = 1, \ldots, n_{\mathcal{E}_{ij}}. \quad (4.1)$$

We do not need to solve this problem for all but only for a number of small eigenvalues and their corresponding eigenvectors. Let the eigenvalues

$$0 = \mu_1^{(i)} \leq \ldots \leq \mu^{(i)}_{n_{\mathcal{E}_{ij}}}$$

be sorted in an increasing order. For a given natural number $L \leq n_{\mathcal{E}_{ij}}$ and for every subdomain, we define the projection

$$I_L^{\mathcal{E}_{ij},(l)} v := \sum_{k=1}^{L} m^{(l)}_{\mathcal{E}_{ij},\rho}(u_k^{(l)}, v) u_k^{(l)}, \quad l = i, j,$$

where $u_k^{(l)}$ are the eigenvectors of (4.1) corresponding to the eigenvalues $\mu_k^{(l)}$. Note that the eigenvectors $u_k^{(l)}$ can be chosen orthonormal with respect to $m^{(l)}_{\mathcal{E}_{ij},\rho}(\cdot,\cdot)$. For our analysis, we will use the seminorm

$$|v|^2_{H^1_{\rho_l}(\Omega_l)} := \int_{\Omega_l} \rho_l (\nabla v)^2 dx$$

and the norms

$$||v||^2_{L^2_{\rho_l}(\mathcal{E}_{ij})} := \int_{\mathcal{E}_{ij}} \rho_l v^2 ds, \quad ||v||^2_{L^2_{\rho_l}(\Omega_l)} := \int_{\Omega_l} \rho_l v^2 dx.$$

Furthermore, we define the ρ_l-harmonic extension of v as

$$\mathcal{H}^{(l)}_{\rho_l} v := \arg \min_{u \in H^1(\Omega_l)} \left\{ \int_{\Omega_l} \rho_l (\nabla u)^2 dx : u_{|\partial\Omega_l} = v \right\}.$$

By standard variational arguments we obtain the following lemma.

Lemma 4.1.1. *Let* $\mathcal{E} \subset \Gamma^{(i)} := \partial\Omega_i$ *be an edge,* E *its closure, and* $E^c \subset \Gamma^{(i)}$ *be the complement of* E *with respect to* $\Gamma^{(i)}$*. Define an extension from the edge* $\mathcal{E} \subset \Gamma^{(i)}$ *to* $\Gamma^{(i)}$ *by*

$$v^{(i)} = \begin{bmatrix} v_E^{(i)} \\ -S^{(i)-1}_{E^cE^c} S^{(i)}_{E^cE} v_E^{(i)}. \end{bmatrix}, \text{ where } S^{(i)} = \begin{bmatrix} S^{(i)}_{EE} & S^{(i)T}_{E^cE} \\ S^{(i)}_{E^cE} & S^{(i)}_{E^cE^c} \end{bmatrix}.$$

For $w^{(i)} \in W^h(\Gamma^{(i)})$ we denote by $v_E^{(i)}$ the nodal vector of $w^{(i)}_{|\mathcal{E}}$. Then, for all $w^{(i)} \in W^h(\Gamma^{(i)})$, we have $|v^{(i)}|^2_{S^{(i)}} \leq |w^{(i)}|^2_{S^{(i)}}$.

Proof. The proof is analogous to Lemma 2.1.2. □

Remark 4.1.2. *Note that in contrary to Lemma 2.1.2 in Section 2.1 the extension established in Lemma 4.1.1 is constructed using the boundary data on the closed edge.*

Remark 4.1.3. *Using the extension operator*

$$\mathcal{H}_{\mathcal{E}\to\Gamma^{(i)}} v_{\mathcal{E}}^{(i)} := \begin{bmatrix} v_E^{(i)} \\ -S^{-1}_{E^cE^c} S_{E^cE} v_E^{(i)} \end{bmatrix} \tag{4.2}$$

constructed in Lemma 4.1.1, we have

$$|\mathcal{H}^{(i)}_{\rho_i} \mathcal{H}_{\mathcal{E}\to\Gamma^{(i)}} v_{\mathcal{E}}^{(i)}|^2_{H^1_{\rho_i}(\Omega_i)} = s^{(i)}_{\mathcal{E},c,\rho_i}(v_E^{(i)}, v_E^{(i)}) \quad \forall v_{\mathcal{E}}^{(i)} \in W^h(\mathcal{E}). \tag{4.3}$$

Here, $v_E^{(i)}$ denotes the nodal vector of $v_{\mathcal{E}}^{(i)}$.

Lemma 4.1.4. *For $v \in W^h(\mathcal{E}_{ij})$ and $w := \left(v - I_L^{\mathcal{E}_{ij},(l)} v\right) \in W^h(\mathcal{E}_{ij})$, we have*

$$\begin{aligned} ||v - I_L^{\mathcal{E}_{ij},(l)} v||^2_{L^2_{\rho_l}(\mathcal{E}_{ij})} = m^{(l)}_{\mathcal{E}_{ij},\rho}(w,w) \leq & \frac{1}{\mu^{(l)}_{L+1}} s^{(l)}_{\mathcal{E}_{ij},c,\rho}(v,v) \\ = & \frac{1}{\mu^{(l)}_{L+1}} |\mathcal{H}^{(l)}_{\rho_i} \mathcal{H}_{\mathcal{E}_{ij}\to\Gamma^{(l)}} v|^2_{H^1_{\rho_l}(\Omega_l)} \end{aligned} \tag{4.4}$$

and

$$s^{(l)}_{\mathcal{E}_{ij},c,\rho}(w,w) \leq s^{(l)}_{\mathcal{E}_{ij},c,\rho}(v,v). \tag{4.5}$$

Proof. We first prove (4.5). Since $u_k^{(l)T} S^{(l)}_{\mathcal{E}_{ij},\rho} u_m^{(l)} = 0$ for eigenvectors $u_k^{(l)}$ and $u_m^{(l)}$ with $k \neq m$, we have

$$s_{\mathcal{E}_{ij},\rho}(I_L^{\mathcal{E}_{ij},(l)} v, w) = s_{\mathcal{E}_{ij},\rho}(I_L^{\mathcal{E}_{ij},(l)} v, v - I_L^{\mathcal{E}_{ij},(l)} v) = 0. \tag{4.6}$$

We obtain

$$\begin{aligned} s^{(l)}_{\mathcal{E}_{ij},c,\rho}(w,w) &= s^{(l)}_{\mathcal{E}_{ij},c,\rho}(v - I_L^{\mathcal{E}_{ij},(l)} v, v - I_L^{\mathcal{E}_{ij},(l)} v) \\ &= s^{(l)}_{\mathcal{E}_{ij},c,\rho}\left(\sum_{i=L+1}^{n_{\mathcal{E}_{ij}}} m^{(l)}_{\mathcal{E}_{ij},\rho}(v, u_i^{(l)}) u_i^{(l)}, \sum_{j=L+1}^{n_{\mathcal{E}_{ij}}} m^{(l)}_{\mathcal{E}_{ij},\rho}(v, u_j^{(l)}) u_j^{(l)} \right) \\ &= \sum_{i=L+1}^{n_{\mathcal{E}_{ij}}} m^{(l)}_{\mathcal{E}_{ij},\rho}(v, u_i^{(l)})^2 \, s^{(l)}_{\mathcal{E}_{ij},c,\rho}\left(u_i^{(l)}, u_i^{(l)}\right) \end{aligned} \tag{4.7}$$

and analogously

$$s^{(l)}_{\mathcal{E}_{ij},c,\rho}(v,v) = \sum_{i=1}^{n_{\mathcal{E}_{ij}}} m^{(l)}_{\mathcal{E}_{ij},\rho}(v, u_i^{(l)})^2 \, s^{(l)}_{\mathcal{E}_{ij},c,\rho}\left(u_i^{(l)}, u_i^{(l)}\right). \tag{4.8}$$

The inequality (4.5) follows by noting that the terms of the sums in (4.7) and (4.8) are all positive or zero. Let $S^{(l)}_{\mathcal{E}_{ij},c,\rho}$ be the matrix associated with the bilinear form $s^{(l)}_{\mathcal{E}_{ij},c,\rho}$ in the sense that

$$s^{(l)}_{\mathcal{E}_{ij},c,\rho}(v,v) = v^T S^{(l)}_{\mathcal{E}_{ij},c,\rho} v \text{ for all } v \in W^h(\mathcal{E}_{ij})$$

and let $M^{(l)}_{\mathcal{E}_{ij}}$ be the corresponding matrix associated with $m^{(l)}_{\mathcal{E}_{ij},\rho}(\cdot,\cdot)$. Now we apply Lemma 1.6.2 with

$$A = S^{(l)}_{\mathcal{E}_{ij},c,\rho}, \quad B = M^{(l)}_{\mathcal{E}_{ij}}, \quad m = L, \text{ and } \Pi^B_m = I_L^{\mathcal{E}_{ij},(l)}$$

and obtain (4.4). □

A similar inequality for the whole domain Ω_i instead of just the edge $\mathcal{E}_{ij}$ is given in [28] and [27, (3.10)]. In [19] an analogous inequality has been shown for $\partial\Omega_i$ instead of $\mathcal{E}_{ij}$. Let us note that all these inequalities are also related to different eigenvalue problems. The eigenvalue problem considered here, cf. (4.1), is more local than those in [28, 27] and [19]. To take advantage of inequality (4.4) in our FETI-DP algorithm using projector preconditioning or our BDDC algorithm using a transformation of basis, we need to enforce the projected jumps across the interface to be zero to obtain

$$I_L^{\mathcal{E}_{ij},(i)} v^{(i)} = I_L^{\mathcal{E}_{ij},(i)} v^{(j)} \text{ and } I_L^{\mathcal{E}_{ij},(j)} v^{(i)} = I_L^{\mathcal{E}_{ij},(j)} v^{(j)}.$$

Let $v^{(l)}_{\mathcal{E}_{ij}}$ be the restriction of $v^{(l)}$ to the edge $\mathcal{E}_{ij}$. To guarantee this equality, we enforce the constraint

$$m^{(l)}_{\mathcal{E}_{ij},\rho}(u^{(l)}_k, v^{(i)}_{\mathcal{E}_{ij}} - v^{(j)}_{\mathcal{E}_{ij}}) = 0, \text{ for } k = 1, .., L.$$

To enrich the coarse space, we first multiply the eigenvectors by the mass matrix corresponding to $m^{(l)}_{\mathcal{E}_{ij},\rho}(\cdot,\cdot))$, then discard the entries associated with primal vertices, and finally extend these vectors by zero on the remaining part of the interface. Note that discarding these values at the primal vertices has no effect because the jump $w_i - w_j$ is zero there. Therefore, the original constraint holds. Then, these vectors define the corresponding columns of U from Section 1.5 or the transformation matrices $T^{(i)}_E$ and $T^{(j)}_E$ from Section 1.4, respectively. We carry out this process for each edge of each subdomain and for each eigenvector of the generalized eigenvalue problem (4.1) for which the corresponding eigenvalue is smaller than or equal to a chosen tolerance TOL_μ, i.e.,

$$\mu_L \leq \text{TOL}_\mu. \tag{4.9}$$

Let us note that linearly dependent eigenvectors are removed by using a singular value decomposition as described later in this chapter. Only this reduced set of eigenvectors is used to define the columns of U in the deflation approach or the columns of the transformation matrices $T^{(i)}_E$ and $T^{(j)}_E$ in case of a transformation of basis.

4.2 Technical Tools

In this section, we provide a few technical tools, together with their proofs, which are needed for the proof of our condition number estimate. We will show a weighted edge lemma, a weighted Friedrichs inequality and an extension theorem for the case that the coefficient functions on the subdomain satisfy certain conditions.

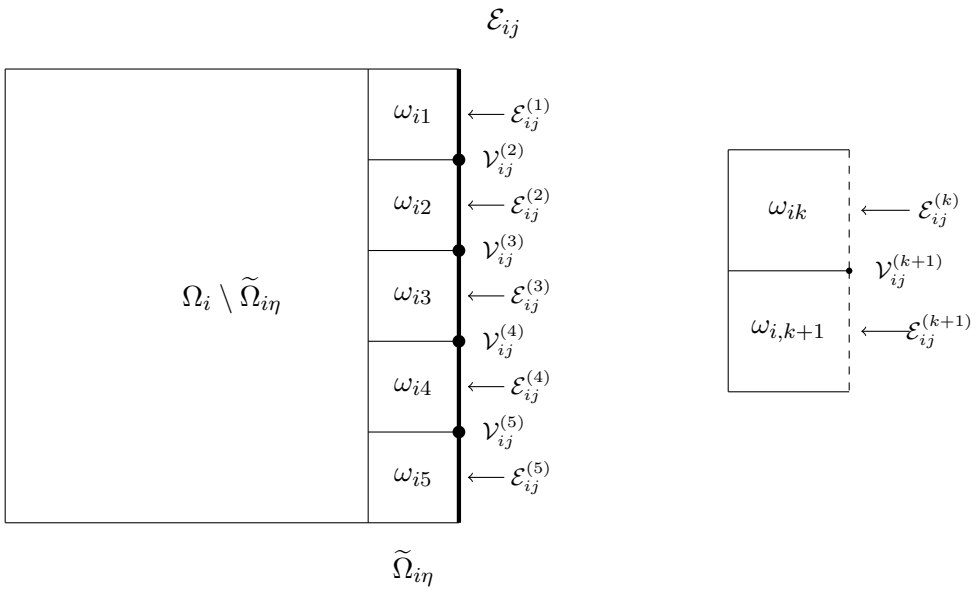

Figure 4.1: Example for the notation in Lemma 4.2.2.

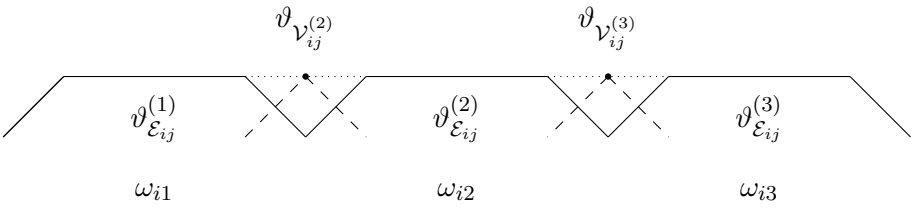

Figure 4.2: Decomposition of the edge cutoff function $\vartheta_{\mathcal{E}_{ij}}$ in Lemma 4.2.2.

For convenience of the reader we recall Definition 2.6.2 from Chapter 2.

Definition 4.2.1. *Let $\mathcal{E}_{ij} \subset \partial\Omega_i$ be an edge. Then, a slab $\widetilde{\Omega}_{i\eta}$ is a subset of Ω_i of width η with $\mathcal{E}_{ij} \subset \partial\widetilde{\Omega}_{i\eta}$ which can be represented as the union of η-patches ω_{ik}, $k = 1, \ldots, n$, such that*

$$\mathcal{E}_{ij}^{(k)} := (\partial\omega_{ik} \cap \mathcal{E}_{ij})^\circ \neq \emptyset, \qquad k = 1, \ldots, n.$$

Next, we formulate and prove an edge lemma.

Lemma 4.2.2. *Let $\widetilde{\Omega}_{i\eta} \subset \Omega_i$ be a slab of width η, such that $\mathcal{E}_{ij} \subset \partial\widetilde{\Omega}_{i\eta}$. Let $\omega_{ik} \subset \widetilde{\Omega}_{i\eta}$, $k = 1, \ldots, n$, be η-patches, such that*

$$\widetilde{\Omega}_{i\eta} = \bigcup_{k=1}^{n} \omega_{ik},$$

and the coefficient function $\rho_{i|\omega_{ik}} = \rho_{ik}$ is constant on each ω_{ik}. Let

$$\omega_{ik} \cap \omega_{il} = \emptyset, \quad k \neq l,$$

$\theta_{\mathcal{E}_{ij}}$ be the standard finite element cutoff function which equals 1 at the nodes on the edge $\mathcal{E}_{ij}$ and is zero on $\partial\widetilde{\Omega}_{i\eta} \setminus \mathcal{E}_{ij}$, and let $\mathcal{H}^{(i)}_{\rho_i}$ be the ρ_i-harmonic extension. Then, there exists a finite element function $\vartheta_{\mathcal{E}_{ij}}$, which equals $\theta_{\mathcal{E}_{ij}}$ on $\partial\widetilde{\Omega}_{i\eta}$, such that for $u \in W^h(\Omega_i)$

$$\begin{aligned} |\mathcal{H}^{(i)}_{\rho_i} I^h(\theta_{\mathcal{E}_{ij}} u)|^2_{H^1_{\rho_i}(\Omega_i)} &\leq |I^h(\vartheta_{\mathcal{E}_{ij}} u)|^2_{H^1_{\rho_i}(\widetilde{\Omega}_{i\eta})} \\ &\leq C\left(1 + \log\left(\frac{\eta}{h}\right)\right)^2 \left(|u|^2_{H^1_{\rho_i}(\widetilde{\Omega}_{i\eta})} + \frac{1}{\eta^2}||u||^2_{L^2_{\rho_i}(\widetilde{\Omega}_{i\eta})}\right), \end{aligned}$$

where $C > 0$ is a constant independent of H, h, η, and the contrast of ρ_i.

Proof. We define

$$\mathcal{E}^{(k)}_{ij} := (\partial\omega_{ik} \cap \mathcal{E}_{ij})^\circ,$$

where M° is the interior of the set M, i.e., $\mathcal{E}^{(k)}_{ij}$ is an open edge without its endpoints, and

$$\mathcal{V}^{(k+1)}_{ij} := \overline{\mathcal{E}^{(k)}_{ij}} \cap \overline{\mathcal{E}^{(k+1)}_{ij}}$$

is an endpoint of that edge. For each patch ω_{ik} and its local edge $\mathcal{E}^{(k)}_{ij}$, there exists a finite element function $\vartheta^{(k)}_{\mathcal{E}_{ij}}$ which equals one on $\mathcal{E}^{(k)}_{ij}$ and zero in all other nodes on the boundary of ω_{ik}. In the interior of the patch ω_{ik}, the function $\vartheta^{(k)}_{\mathcal{E}_{ij}}$ can be defined such that

$$|I^h(\vartheta^{(k)}_{\mathcal{E}_{ij}} u)|^2_{H^1(\omega_{ik})} \leq C(1 + \log\left(\frac{\eta}{h}\right))^2 \left(|u|^2_{H^1(\omega_{ik})} + \frac{1}{\eta^2}||u||^2_{L^2(\omega_{ik})}\right); \quad (4.10)$$

see, e.g., [48, proof of Lemma 4.4] or [82, Lemma 4.24], which is a three-dimensional analogon. For the endpoints $\mathcal{V}_{ij}^{(k)}$ and $\mathcal{V}_{ij}^{(k+1)}$ of $\mathcal{E}_{ij}^{(k)}$, we denote by $\vartheta_{\mathcal{V}_{ij}}^{(k)}$ and $\vartheta_{\mathcal{V}_{ij}}^{(k+1)}$, respectively, the corresponding nodal finite element basis function. Next, we define the finite element function

$$\vartheta_{\mathcal{E}_{ij}} := \sum_{k=1}^{n} \vartheta_{\mathcal{E}_{ij}}^{(k)} + \sum_{k=2}^{n} \vartheta_{\mathcal{V}_{ij}}^{(k)}.$$

Note that $\vartheta_{\mathcal{E}_{ij}}$ equals 1 in all nodes on $\mathcal{E}_{ij}$ and 0 in all nodes on $\partial\widetilde{\Omega}_{i\eta} \setminus \mathcal{E}_{ij}$, the boundary of the slab without the edge. Since the discrete ρ_i-harmonic extension has the smallest energy, we have

$$|\mathcal{H}_{\rho_i}^{(i)} I^h(\theta_{\mathcal{E}_{ij}} u)|^2_{H^1_{\rho_i}(\Omega_i)} \leq |I^h(\vartheta_{\mathcal{E}_{ij}} u)|^2_{H^1_{\rho_i}(\widetilde{\Omega}_{i\eta})}.$$

For the function $\vartheta_{\mathcal{V}^{ij}}^{(l)}$, $l = k, k+1$, we have

$$\begin{aligned} |I^h(\vartheta_{\mathcal{V}_{ij}}^{(l)} u)|^2_{H^1(\omega_{ik})} =& |\vartheta_{\mathcal{V}_{ij}}^{(l)} u(\mathcal{V}_{ij}^{(l)})|^2_{H^1(\omega_{ik})} \\ \leq& C\left(1 + \log\left(\frac{\eta}{h}\right)\right)\left(|u|^2_{H^1(\omega_{ik})} + \frac{1}{\eta^2}||u||^2_{L^2(\omega_{ik})}\right), \end{aligned} \tag{4.11}$$

which follows from an inverse inequality, see, e.g., [6] or [82, Lemma B.5], and a Sobolev inequality for finite element functions; see, e.g., [15, Lemma 3.2] or [6]. From (4.10), (4.11), and a triangle inequality, we obtain

$$\begin{aligned} |I^h(\vartheta_{\mathcal{E}_{ij}} u)|^2_{H^1_{\rho_i}(\widetilde{\Omega}_{i\eta})} =& \sum_{k=1}^{n} |I^h(\vartheta_{\mathcal{E}_{ij}} u)|^2_{H^1_{\rho_i}(\omega_{ik})} \\ \leq& 3\sum_{k=1}^{n} |I^h(\vartheta_{\mathcal{E}_{ij}}^{(k)} u)|^2_{H^1_{\rho_i}(\omega_{ik})} + 3\sum_{k=1}^{n-1} |I^h(\vartheta_{\mathcal{V}_{ij}^{(k+1)}} u)|^2_{H^1_{\rho_i}(\omega_{ik})} \\ &+ 3\sum_{k=2}^{n} |I^h(\vartheta_{\mathcal{V}_{ij}^{(k)}} u)|^2_{H^1_{\rho_i}(\omega_{i,k})} \\ \leq& C\left(1 + \log\left(\frac{\eta}{h}\right)\right)^2 \left(|u|^2_{H^1_{\rho_i}(\widetilde{\Omega}_{i\eta})} + \frac{1}{\eta^2}||u||^2_{L^2_{\rho_i}(\widetilde{\Omega}_{i\eta})}\right). \end{aligned} \tag{4.12}$$

Here, we have used that ρ_i is constant on each patch ω_{ik}, $k = 1, \ldots, n$. □

For a graphical illustration of the notation in Lemma 4.2.2, see Figures 4.1 and 4.2. Let us note that similar techniques using patches for heterogeneous

coefficients have been also used in [71]. For inequalities related to the next lemma, see [19, Lemma 2.4] and [82, proof of Lemma 3.10].

Lemma 4.2.3 (Weighted Friedrichs inequality)**.** *For $u \in H^1(\widetilde{\Omega}_{i\eta})$, we have*

$$||u||^2_{L^2_{\rho_i}(\widetilde{\Omega}_{i\eta})} \leq C \left(\eta^2 |u|^2_{H^1_{\rho_i}(\widetilde{\Omega}_{i\eta})} + \eta ||u||^2_{L^2_{\rho_i}(\mathcal{E}_{ij})} \right).$$

Proof. Let $\omega_{ik} \subset \widetilde{\Omega}_{i\eta}$, $k = 1, \ldots, n$ be η-patches, such that $\widetilde{\Omega}_{i\eta} = \cup_{k=1}^{n} \omega_{ik}$, and let the coefficient function $\rho_{i|\omega_{ik}} = \rho_{ik}$ be constant on each ω_{ik}. Furthermore, let

$$\overline{u}^{\mathcal{E}_{ij}^{(k)}} := \frac{1}{|\mathcal{E}_{ij}^{(k)}|} \int_{\mathcal{E}_{ij}^{(k)}} u \, dx$$

be the standard edge average. Then, we obtain by using a standard Poincaré inequality

$$\begin{aligned} ||u||^2_{L^2_{\rho_i}(\omega_{ik})} = \rho_{ik} ||u||^2_{L^2(\omega_{ik})} &\leq 2\rho_{ik} \left\| u - \overline{u}^{\mathcal{E}_{ij}^{(k)}} \right\|^2_{L^2(\omega_{ik})} + 2\rho_{ik} \left\| \overline{u}^{\mathcal{E}_{ij}^{(k)}} \right\|^2_{L^2(\omega_{ik})} \\ &\leq 2\rho_{ik} C_k \eta^2 |u|^2_{H^1(\omega_{ik})} + 2\rho_{ik} \eta^2 \left(\overline{u}^{\mathcal{E}_{ij}^{(k)}} \right)^2 \\ &\leq 2 \max\{C_k, 1\} \left(\eta^2 |u|^2_{H^1_{\rho_{ik}}(\omega_{ik})} + \eta ||u||^2_{L^2_{\rho_{ik}}(\mathcal{E}_{ij}^{(k)})} \right). \end{aligned}$$

In the last step, we applied a Cauchy-Schwarz inequality. Summing over k completes the proof. □

In order to obtain a condition number estimate independent of the contrast of the coefficient function, it is sufficient to have an extension operator from a slab to a neighboring slab across the shared edge, which is uniformly bounded with respect to the contrast.

Assumption 4.2.4 (special case)**.** *We assume that there exists an extension operator*

$$E_{ji} : W^h(\Omega_j) \to W^h(\Omega_i)$$

with

$$|E_{ji} u|^2_{H^1_{\rho_i}(\Omega_i)} \leq C |u|^2_{H^1_{\rho_j}(\Omega_j)},$$

$Y_1^{(i)}$	$Y_1^{(j)}$
$Y_2^{(i)}$	$Y_2^{(j)}$
$Y_3^{(i)}$	$Y_3^{(j)}$
$Y_4^{(i)}$	$Y_4^{(j)}$
$Y_5^{(i)}$	$Y_5^{(j)}$
$Y_6^{(i)}$	$Y_6^{(j)}$
$Y_7^{(i)}$	$Y_7^{(j)}$

Figure 4.3: Example of the polygons in Lemma 4.2.5.

where $C > 0$ is a constant independent of H, h, and the contrast of ρ.

The following Lemma shows that Assumption 4.2.4 is satisfied for some special coefficient distributions; see, e.g., Section 4.6, Figures 4.4, and 4.5.

In these cases, the coefficient distributions are symmetric with respect to the interface and E_{ji} can be obtained by reflecting the function across the edge and using the standard nodal finite element interpolation operator. This interpolation operator restricted to finite element spaces is stable between non-nested spaces; see, e.g., [8, Lemma 2.1], [82, Lemma 3.8], or [11, Lemma 1]. Here, we restrict ourselves to straight edges $\mathcal{E}_{ij}$. Thus, without loss of generality, let $\mathcal{E}_{ij} \subset \{0\} \times \mathbb{R}$. Let T be the transformation with

$$T : (x, y) \to (-x, y).$$

Let

$$\rho_i(x, y) = \rho_j(-x, y), \quad (x, y) \in \Omega_i,$$
$$\rho_j(x, y) = \rho_i(-x, y), \quad (x, y) \in \Omega_j.$$

Using the transformation formula for integrals, we obtain the next lemma.

Lemma 4.2.5. *Let $u \in W^h(\Omega_j)$. With the extension operator*

$$E_{ji} : W^h(\Omega_j) \to W^h(\Omega_i)$$
$$E_{ji}\,(u(x,y)) = I^h(u \circ T)(x,y) = I^h u(-x,y),$$

we have

$$|E_{ji}u|^2_{H^1_{\rho_i}(\Omega_i)} \leq C|u|^2_{H^1_{\rho_j}(\Omega_j)}.$$

Proof. As in Definition 4.0.1, we partition the subdomains Ω_i and Ω_j into open, connected Lipschitz polygons $\mathcal{Y}_k := \{Y_k^{(l)} : l = 1, \ldots, n\}$, $k = i, j$, such that $\overline{\Omega}_k = \bigcup_{l=1}^n \overline{Y}_k^{(l)}$ and define $\rho^{(l)} := \rho_{|Y_k^{(l)}}$. Note that $\rho_{|Y_j^{(l)}} = \rho_{|Y_i^{(l)}}$ and $T^{-1}(Y_i^{(l)}) = Y_j^{(l)}$. For each $Y_i^{(l)}$, we have $|I^h u|^2_{H^1(Y_i^{(l)})} \leq C_l |u|^2_{H^1(Y_i^{(l)})}$; see, e.g., [8, Lemma 2.1], [82, Lemma 3.8], or [11, Lemma 1]. With $C := \max_l C_l$, we obtain

$$\begin{aligned}
|E_{ji}u|^2_{H^1_{\rho_i}(\Omega_i)} =& \sum_{l=1}^n \rho^{(l)} \int_{Y_i^{(l)}} |\nabla(E_{ji}(u(x,y))|^2 \, dx\, dy \\
\leq& C \sum_{l=1}^n \rho^{(l)} \int_{Y_i^{(l)}} |\nabla(u \circ T)|^2 \, dx\, dy \\
=& C \sum_{l=1}^n \rho^{(l)} \int_{T^{-1}(Y_i^{(l)})} (\nabla u)^2 |\det(DT^{-1})| \, d\hat{x}\, d\hat{y} \\
=& C \sum_{l=1}^n \rho^{(l)} \int_{Y_j^{(l)}} (\nabla u)^2 \, d\hat{x}\, d\hat{y} \\
=& C|u|^2_{H^1_{\rho_j}(\Omega_j)}.
\end{aligned}$$

□

Remark 4.2.6. *Note that it is also possible to prove*

$$|E_{ji}\,u|^2_{H^1_{\rho_i}(\widetilde{\Omega}_{i\eta})} \leq C|u|^2_{H^1_{\rho_j}(\widetilde{\Omega}_{j\eta})}$$

for an extension operator $E_{ji} : W^h(\widetilde{\Omega}_{j\eta}) \to W^h(\widetilde{\Omega}_{i\eta})$ *if the coefficient function satisfies*

$$\rho_i(x,y) = \rho_j(-x,y),\ (x,y) \in \widetilde{\Omega}_{i\eta},$$
$$\rho_j(x,y) = \rho_i(-x,y),\ (x,y) \in \widetilde{\Omega}_{j\eta}.$$

In the proof, the Lipschitz polygons $Y_k^{(l)}$ *can then be replaced by the patches* ω_{lk}, $l = i, j$, *in Definitions 2.6.1 and 4.2.1.*

Remark 4.2.7. *For terms with the energy minimal extension operators* $\mathcal{H}^{(l)}_{\rho_l}$ *and* $\mathcal{H}^{(l)}_{\mathcal{E}_{ij}\to\Gamma^{(l)}}$, $l = i, j$, *we obtain*

$$\begin{aligned}|\mathcal{H}^{(j)}_{\rho_j}\mathcal{H}_{\mathcal{E}_{ij}\to\Gamma^{(j)}}u|^2_{H^1_{\rho_j}(\Omega_j)} &\leq |E_{ji}\mathcal{H}^{(i)}_{\rho_i}\mathcal{H}_{\mathcal{E}_{ij}\to\Gamma^{(i)}}u|_{H^1_{\rho_j}(\Omega_j)}\\ &\leq C|\mathcal{H}^{(i)}_{\rho_i}\mathcal{H}_{\mathcal{E}_{ij}\to\Gamma^{(i)}}u|^2_{H^1_{\rho_i}(\Omega_i)}.\end{aligned}$$

4.3 Second Eigenvalue Problem - Bounds on Extensions

Assumption 4.2.4 can only be used for special coefficient distributions. To be able to treat more general cases, we now consider a second set of primal constraints to bound the terms

$$|\mathcal{H}^{(i)}_{\rho_i}\mathcal{H}_{\mathcal{E}_{ij}\to\Gamma^{(i)}}\hat{w}^{(j)}|^2_{H^1_{\rho_i}(\Omega_i)} \leq C|\mathcal{H}^{(j)}_{\rho_j}\mathcal{H}_{\mathcal{E}_{ij}\to\Gamma^{(j)}}w^{(j)}|^2_{H^1_{\rho_j}(\Omega_j)}.$$

Here $\hat{w}^{(j)}$ is a projection of $w^{(j)}$ on a subspace; see the discussion below. To compute these additional primal constraints, we consider the following second generalized eigenvalue problem.

Eigenvalue Problem 2.

$$s^{(j)}_{\mathcal{E}_{ij},c,\rho_j}(v,w_\kappa) = \nu^{(i)}_\kappa \frac{\widehat{\rho}_j}{\widehat{\rho}_i} s^{(i)}_{\mathcal{E}_{ij},c,\rho_i}(v,w_\kappa)\ \forall v \in W^h(\mathcal{E}_{ij}),\ \kappa = 1,\dots,n_{\mathcal{E}_{ij}}. \tag{4.13}$$

We note that the bilinear forms in the generalized eigenvalue problem (4.13) may have nontrivial nullspaces. However, we can solve the problem on

$$\left(\text{Ker}\,\left(S^{(i)}_{\mathcal{E}_{ij},c,\rho_i}\right)\cap\text{Ker}\,\left(S^{(j)}_{\mathcal{E}_{ij},c,\rho_j}\right)\right)^{\perp}.$$

Let $w^{(j)}=w^{(j)}_K+w^{(j)}_R$ with

$$w^{(j)}_K\in\text{Ker}\,\left(S^{(i)}_{\mathcal{E}_{ij},c,\rho_i}\right)\cap\text{Ker}\,\left(S^{(j)}_{\mathcal{E}_{ij},c,\rho_j}\right)$$
$$\text{and } w^{(j)}_R\in\left(\text{Ker}\,\left(S^{(i)}_{\mathcal{E}_{ij},c,\rho_i}\right)\cap\text{Ker}\,\left(S^{(j)}_{\mathcal{E}_{ij},c,\rho_j}\right)\right)^{\perp}.$$

We consider the l_2-orthogonal projection $\overline{\Pi}$ onto

$$\left(\text{Ker}\,\left(S^{(i)}_{\mathcal{E}_{ij},c,\rho_i}\right)\cap\text{Ker}\,\left(S^{(j)}_{\mathcal{E}_{ij},c,\rho_j}\right)\right)^{\perp}$$

and the positive semidefinite bilinear forms

$$\overline{s}^{(j)}_{\mathcal{E}_{ij},c,\rho_j}(v,w):=s^{(j)}_{\mathcal{E}_{ij},c,\rho_j}(\overline{\Pi}v,\overline{\Pi}w)$$
$$\overline{s}^{(i)}_{\mathcal{E}_{ij},c,\rho_i}(v,w):=s^{(i)}_{\mathcal{E}_{ij},c,\rho_i}(\overline{\Pi}v,\overline{\Pi}w).$$

The orthogonal projection $\overline{\Pi}$ can be obtained by $\overline{\Pi}=I-(I-\overline{\Pi})$ with

$$I-\overline{\Pi}=\sum_{r=1}^{p}v_rv_r^T,$$

where $\{v_1,\ldots,v_p\}$ is an orthonormal basis of

$$\text{Ker}\,\left(S^{(i)}_{\mathcal{E}_{ij},c,\rho_i}\right)\cap\text{Ker}\,\left(S^{(j)}_{\mathcal{E}_{ij},c,\rho_j}\right).$$

In exact arithmetic, we have $\overline{s}^{(l)}_{\mathcal{E}_{ij},c,\rho_j}=s^{(l)}_{\mathcal{E}_{ij},c,\rho_j}$, $l=i,j$, but we use the projection $\overline{\Pi}$ for stability in our computations. We can formulate a modified problem on $\left(\text{Ker}\,\left(S^{(i)}_{\mathcal{E}_{ij},c,\rho_i}\right)\cap\text{Ker}\,\left(S^{(j)}_{\mathcal{E}_{ij},c,\rho_j}\right)\right)^{\perp}$ by

$$\overline{s}^{(j)}_{\mathcal{E}_{ij},c,\rho_j}(v,\overline{w}_\kappa)=\overline{\nu}^{(i)}_\kappa\frac{\widehat{\rho}_j}{\widehat{\rho}_i}\overline{s}^{(i)}_{\mathcal{E}_{ij},c,\rho_i}(v,\overline{w}_\kappa),$$
$$\forall v\in\left(\text{Ker}\,\left(S^{(i)}_{\mathcal{E}_{ij},c,\rho_i}\right)\cap\text{Ker}\,\left(S^{(j)}_{\mathcal{E}_{ij},c,\rho_j}\right)\right)^{\perp},\quad\kappa=1,\ldots,n_{\mathcal{E}_{ij}},\tag{4.14}$$

where $\widehat{\rho}_l$, $l = i, j$, is defined by (1.8). The eigenpairs $(\overline{\nu}_\kappa^{(i)}, \overline{w}_\kappa^{(i)})$ are also eigenpairs of the original problem (4.13). Let $K \in \{1, \ldots, n_{\mathcal{E}_{ij}}\}$ and the corresponding eigenvalues

$$\overline{\nu}_1^{(i)} \leq \ldots \leq \overline{\nu}_K^{(i)} \leq \ldots \leq \overline{\nu}_{n_{\mathcal{E}_{ij}}}^{(i)}$$

be sorted in an increasing order. We define the projection

$$\Pi_K^{(i)} v := \sum_{\kappa=1}^{K} \frac{\widehat{\rho}_j}{\widehat{\rho}_i} \overline{s}_{\mathcal{E}_{ij},c,\rho_i}^{(i)}(v, \overline{w}_\kappa)\overline{w}_\kappa$$

and obtain the following lemma.

Lemma 4.3.1. *We have for all* $w^{(j)} \in W^h(\mathcal{E}_{ij})$

$$s_{\mathcal{E}_{ij},c,\rho_i}^{(i)}\left(w^{(j)} - \Pi_K^{(i)} w^{(j)}, w^{(j)} - \Pi_K^{(i)} w^{(j)}\right) \leq \frac{1}{\nu_{K+1}^{(i)}} \frac{\widehat{\rho}_i}{\widehat{\rho}_j} s_{\mathcal{E}_{ij},c,\rho_j}^{(j)}\left(w^{(j)}, w^{(j)}\right) \tag{4.15}$$

which is equivalent to

$$|\mathcal{H}_{\rho_i}^{(i)} \mathcal{H}_{\mathcal{E}_{ij}\to\Gamma^{(i)}}\left(w^{(j)} - \Pi_K^{(i)} w^{(j)}\right)|_{H^1_{\rho_i}(\Omega_i)}^2 \leq \frac{1}{\nu_{K+1}^{(i)}} \frac{\widehat{\rho}_i}{\widehat{\rho}_j} |\mathcal{H}_{\rho_j}^{(j)} \mathcal{H}_{\mathcal{E}_{ij}\to\Gamma^{(j)}} w^{(j)}|_{H^1_{\rho_j}(\Omega_j)}^2.$$

Additionally, we have

$$s_{\mathcal{E}_{ij},c,\rho_i}^{(i)}\left(w^{(i)} - \Pi_K^{(i)} w^{(i)}, w^{(i)} - \Pi_K^{(i)} w^{(i)}\right) \leq s_{\mathcal{E}_{ij},c,\rho_i}^{(i)}\left(w^{(i)}, w^{(i)}\right). \tag{4.16}$$

Proof. Using the additive decomposition $w^{(j)} = w_K^{(j)} + w_R^{(j)}$ with

$$w_K^{(j)} \in \left(\mathrm{Ker}\left(S_{\mathcal{E}_{ij},c,\rho_i}^{(i)}\right) \cap \mathrm{Ker}\left(S_{\mathcal{E}_{ij},c,\rho_j}^{(j)}\right)\right),$$

$$w_R^{(j)} \in \left(\mathrm{Ker}\left(S_{\mathcal{E}_{ij},c,\rho_i}^{(i)}\right) \cap \mathrm{Ker}\left(S_{\mathcal{E}_{ij},c,\rho_j}^{(j)}\right)\right)^{\perp},$$

we have

$$\Pi_K^{(i)} w_K^{(j)} = \sum_{\kappa=1}^{K} \frac{\widehat{\rho}_j}{\widehat{\rho}_i} \overline{s}_{\mathcal{E}_{ij},c,\rho_i}^{(i)}(w_K^{(j)}, \overline{w}_\kappa)\overline{w}_\kappa = \sum_{\kappa=1}^{K} \frac{\widehat{\rho}_j}{\widehat{\rho}_i} s_{\mathcal{E}_{ij},c,\rho_i}^{(i)}(\overline{\Pi} w_K^{(j)}, \overline{w}_\kappa)\overline{w}_\kappa = 0.$$

The proof can be completed using that $s_{\mathcal{E}_{ij},c,\rho_i}^{(i)}(\overline{w}_\kappa, \overline{w}_\kappa) = 0$ for $\overline{w}_\kappa \in \mathrm{Ker}\left(S_{\mathcal{E}_{ij},c,\rho_i}^{(i)}\right)$ and $s_{\mathcal{E}_{ij},c,\rho_i}^{(i)}(\overline{w}_\kappa, \overline{w}_l) = \delta_{\kappa l}$ else, for the eigenvectors $\overline{w}_\kappa$ and $\overline{w}_l$. As usual δ_{kl} is the Kronecker symbol. Using Lemma 1.6.2 we conclude the proof. □

The additional primal constraints which we enforce for each edge $\mathcal{E}_{ij}$ are of the form

$$\Pi_K^{(i)} w^{(i)} = \Pi_K^{(i)} w^{(j)} \text{ and } \Pi_K^{(j)} w^{(i)} = \Pi_K^{(j)} w^{(j)}.$$

The following remark is motivated by [59].

Remark 4.3.2. *We are only interested in eigenvectors in* $\left(\text{Ker}\left(S^{(i)}_{\mathcal{E}_{ij},c,\rho_i}\right) \cap \text{Ker}\left(S^{(j)}_{\mathcal{E}_{ij},c,\rho_j}\right)\right)^{\perp}$ *of (4.14). Instead of solving this problem on* $\left(\text{Ker}\left(S^{(i)}_{\mathcal{E}_{ij},c,\rho_i}\right) \cap \text{Ker}\left(S^{(j)}_{\mathcal{E}_{ij},c,\rho_j}\right)\right)^{\perp}$*, we can consider instead*

$$\overline{S}^{(j)}_{\mathcal{E}_{ij},c,\rho_j} \overline{w} = \nu \left(\overline{S}^{(i)}_{\mathcal{E}_{ij},c,\rho_i} + \sigma \left(I - \overline{\Pi}\right)\right) \overline{w}, \tag{4.17}$$

where $\overline{S}^{(k)}_{\mathcal{E}_{ij},c,\rho_k}$, $k = i, j$, *is the matrix associated with the bilinear form* $\overline{s}^{(k)}_{\mathcal{E}_{ij},c,\rho_k}$ *and* σ *is any positive constant. In our computations we have chosen* σ *as the maximum diagonal entry of* $\overline{S}^{(i)}_{\mathcal{E}_{ij},c,\rho_i}$*; see also [59]. The projection ensures that there are no arbitrary eigenvalues in (4.17) in the sense that every vector in* $\text{Ker}\,(S^{(i)}_{\mathcal{E}_{ij},c,\rho_i}) \cap \text{Ker}\,(S^{(j)}_{\mathcal{E}_{ij},c,\rho_j})$ *satisfies (4.13) for all* $\nu \in \mathbb{C}$.

To enhance our coarse problem, we consider for a given tolerance TOL_ν the eigenpairs $(\overline{w}_k, \nu_k)$, where $k \leq K$ and

$$\nu_K \leq \text{TOL}_\nu. \tag{4.18}$$

For these eigenvectors, we first build $\left(\overline{S}^{(i)}_{\mathcal{E}_{ij},c,\rho_i} + \sigma \left(I - \overline{\Pi}\right)\right) \overline{w}_k$, discard the entries related to primal vertices, and finally extend them by zero on the remaining interface. We add these vectors to the constraints obtained from the eigenvalue problem (4.1). Let us now consider the set of all constraints obtained from Eigenvalue Problems 1 and 2. We need to remove linearly dependent vectors from this set. In our experiments we orthonormalize all these vectors and remove linearly dependent vectors. The resulting vectors are added as columns to the matrix U from Section 1.5 or the matrices $T_E^{(i)}$ and $T_E^{(j)}$ from Section 1.4. In our FETI-DP method we use a singular value decomposition with a drop tolerance of $1e-6$. In our BDDC method we

use a modified Gram-Schmidt algorithm with a drop tolerance of $1e-12$. The orthogonal basis in (1.11) is computed using a QR decomposition with Householder reflections.

4.4 Condition Number Estimate

We can now prove our condition number estimate. For simplicity we will restrict ourselves to the case of second order scalar elliptic equations.

Theorem 4.4.1. *The condition number for the FETI-DP method with a ρ-scaling, as defined in (1.9), and using adaptive constraints computed from eigenvalue problems (4.1) and (4.13) satisfies*

$$\kappa(\hat{M}^{-1}F) \leq C\left(1+\log\left(\frac{\eta}{h}\right)\right)^2 \frac{1}{\nu_{K+1}}\left(1+\frac{1}{\eta\mu_{L+1}}\right),$$

where $\hat{M}^{-1} = M_{PP}^{-1}$ or $\hat{M}^{-1} = M_{BP}^{-1}$, or alternatively $\hat{M}^{-1} = M^{-1}$ if all constraints have been enforced by a transformation of basis. Here, $C > 0$ is a constant independent of H, h, and η and

$$\frac{1}{\mu_{L+1}} = \max_{k=1,\ldots,N}\left\{\frac{1}{\mu^{(k)}_{L_k+1}}\right\}, \quad \frac{1}{\nu_{K+1}} = \max\left\{1, \max_{k=1,\ldots,N}\frac{1}{\nu^{(k)}_{K+1}}\right\}.$$

Remark 4.4.2.

1. *Note that in the case of a coefficient distribution where Assumption 4.2.4 is satisfied, we have an estimate of the form*

$$\kappa(\hat{M}^{-1}F) \leq C\left(1+\log\left(\frac{\eta}{h}\right)\right)^2 \left(1+\frac{1}{\eta\mu_{L+1}}\right).$$

   In general, such an estimate holds for coefficient distributions where an extension operator exists with an upper bound independent of the values of the coefficients.

2. *A similar result can be obtained for linear elasticity, e.g., by using the tools provided in [49].*

3. *An algorithm for the related BDDC method using a transformation of basis can be found in [41]; see also the numerical results with this algorithm in Section 4.6.2.*

4. *The constant in the condition number estimate for the third coarse space (cf. Theorem 4.4.1) depends on $N_{\mathcal{E}}^2$ in the same way as the condition number estimate for the first coarse space in Lemma 2.7.1 and as for the second coarse space in Lemma 3.3.1. Additionally, the constant depends on the constants in the weighted edge lemma (Lemma 4.2.2) and in the weighted Friedrichs inequality (Lemma 4.2.3); see also Remark 4.5.4.*

Proof of Theorem 4.4.1. We can either directly use Lemma 1.5.1 or observe that FETI-DP with projector preconditioning and FETI-DP using a transformation of basis have the same spectra if the same constraints are enforced; see [47, Theorem 6.9]. Therefore, it makes no difference if we assume for the proof that a transformation of basis has been carried out to enforce the eigenvector constraints. Then the proof of the condition number estimate can be modeled on the corresponding proof of Lemma 8.5 in Klawonn and Widlund [49]. As usual, we always assume functions from these trace spaces to be ρ-harmonically extended to the interior of the subdomains.

We consider an arbitrary $\widetilde{w} \in \widetilde{W}$. Let $R^{(i)T}$ be the local operator assembling in the primal variables and $R^T = \left[R^{(1)\,T}, \ldots, R^{(N)\,T}\right]$; see, e.g., [49, p. 1533]. In the following, we will use the notation $w^{(i)} := R^{(i)}\widetilde{w} \in W_i$ and $w^{(j)} := R^{(j)}\widetilde{w} \in W_j$. With $v^{(i)} := R^{(i)}P_D\widetilde{w}$ and $\tilde{S}_\rho = R^T S_\rho R$, we obtain

$$|P_D\widetilde{w}|^2_{\widetilde{S}_\rho} = |RP_D\widetilde{w}|^2_{S_\rho} = \sum_{i=1}^{n} |R^{(i)}P_D\widetilde{w}|^2_{S^{(i)}_{\rho_i}} = \sum_{i=1}^{n} |v^{(i)}|^2_{S^{(i)}_{\rho_i}}.$$

If all vertices are chosen to be primal, we can write $v^{(i)} = \sum_{\mathcal{E}_{ij}} I^h(\theta_{\mathcal{E}_{ij}} v^{(i)})$. Here, we sum over all edges $\mathcal{E}_{ij} \subset \Gamma^{(i)}$. In the following, we will develop bounds for the edge contributions

$$|\mathcal{H}^{(i)}_{\rho_i} I^h(\theta_{\mathcal{E}_{ij}} v^{(i)})|^2_{H^1_{\rho_i}(\Omega_i)}.$$

Obviously, we have $v^{(i)}_{|\mathcal{E}_{ij}} = (\delta_j^\dagger(w^{(i)} - w^{(j)}))_{|\mathcal{E}_{ij}}$. We use *max-$\rho$-scaling* (cf. (1.8)) in this approach and thus $\delta_j^\dagger$ is given by (1.9) with $\widehat{\rho}_l$ defined in (1.8). We choose L such that $\mu^{(l)}_{L+1}$ is independent of the contrast in the coefficient ρ.

To avoid excessive use of extension operators we define $\mathcal{H}^{(i)}_{\mathcal{E}_{ij}} = \mathcal{H}^{(i)}_{\rho_i}\mathcal{H}^{(i)}_{\mathcal{E}_{ij}\to\Gamma^{(i)}}$. Moreover we enforce the equalities

$$I_L^{\mathcal{E}_{ij},(i)} w^{(i)} = I_L^{\mathcal{E}_{ij},(i)} w^{(j)}, \quad I_L^{\mathcal{E}_{ij},(j)} w^{(i)} = I_L^{\mathcal{E}_{ij},(j)} w^{(j)},$$
$$\Pi_K^{(i)} w^{(i)} = \Pi_K^{(i)} w^{(j)}, \text{ and } \Pi_K^{(j)} w^{(i)} = \Pi_K^{(j)} w^{(j)},$$

either with projector preconditioning or a transformation of basis. Further, we define $\hat{w}^{(l)} := w^{(l)} - \Pi_K^{(i)} w^{(l)}$ and $\overline{w}^{(l)} = \hat{w}^{(l)} - I_L^{\mathcal{E}_{ij},(i)}\hat{w}^{(l)}$ for $l = i, j$. Then, using Lemma 4.2.2, we have

$$\begin{aligned}
|\mathcal{H}^{(i)}_{\rho_i} I^h(\theta_{\mathcal{E}_{ij}} v^{(i)})|^2_{H^1_{\rho_i}(\Omega_i)} &= |\mathcal{H}^{(i)}_{\rho_i} I^h(\theta_{\mathcal{E}_{ij}} \mathcal{H}_{\mathcal{E}_{ij}\to\Gamma^{(i)}} \delta_j^\dagger(w^{(i)} - w^{(j)}))|^2_{H^1_{\rho_i}(\Omega_i)} \\
&= |\mathcal{H}^{(i)}_{\rho_i} I^h(\theta_{\mathcal{E}_{ij}} \mathcal{H}_{\mathcal{E}_{ij}\to\Gamma^{(i)}} \delta_j^\dagger(\hat{w}^{(i)} - \hat{w}^{(j)}))|^2_{H^1_{\rho_i}(\Omega_i)} \\
&= |\mathcal{H}^{(i)}_{\rho_i} I^h(\theta_{\mathcal{E}_{ij}} \mathcal{H}_{\mathcal{E}_{ij}\to\Gamma^{(i)}} \delta_j^\dagger(\overline{w}^{(i)} - \overline{w}^{(j)}))|^2_{H^1_{\rho_i}(\Omega_i)} \\
&\leq 2(\delta_j^\dagger)^2 |\mathcal{H}^{(i)}_{\rho_i} I^h(\theta_{\mathcal{E}_{ij}} \mathcal{H}_{\mathcal{E}_{ij}\to\Gamma^{(i)}} \overline{w}^{(i)})|^2_{H^1_{\rho_i}(\Omega_i)} \\
&\quad + 2(\delta_j^\dagger)^2 |\mathcal{H}^{(i)}_{\rho_i} I^h(\theta_{\mathcal{E}_{ij}} \mathcal{H}_{\mathcal{E}_{ij}\to\Gamma^{(i)}} \overline{w}^{(j)})|^2_{H^1_{\rho_i}(\Omega_i)} \\
\leq C\left(1 + \log\left(\frac{\eta}{h}\right)\right)^2 (\delta_j^\dagger)^2 &\left(|\mathcal{H}^{(i)}_{\mathcal{E}_{ij}} \overline{w}^{(i)}|^2_{H^1_{\rho_i}(\widetilde{\Omega}_{i\eta})} + \frac{1}{\eta^2} ||\mathcal{H}^{(i)}_{\mathcal{E}_{ij}} \overline{w}^{(i)}||^2_{L^2_{\rho_i}(\widetilde{\Omega}_{i\eta})} \right. \\
&\left. + |\mathcal{H}^{(i)}_{\mathcal{E}_{ij}} \overline{w}^{(j)}|^2_{H^1_{\rho_i}(\widetilde{\Omega}_{i\eta})} + \frac{1}{\eta^2} ||\mathcal{H}^{(i)}_{\mathcal{E}_{ij}} \overline{w}^{(j)}||^2_{L^2_{\rho_i}(\widetilde{\Omega}_{i\eta})} \right).
\end{aligned}$$

Now, Lemma 4.2.3 yields with the stability of the projections $I_L^{\mathcal{E}_{ij},(i)}$ and $\Pi_K^{(i)}$

$$\begin{aligned}
\frac{1}{\eta^2} ||\mathcal{H}^{(i)}_{\mathcal{E}_{ij}} \overline{w}^{(i)}||^2_{L^2_{\rho_i}(\widetilde{\Omega}_{i\eta})} &\leq C\left(|\mathcal{H}^{(i)}_{\mathcal{E}_{ij}} \overline{w}^{(i)}|^2_{H^1_{\rho_i}(\widetilde{\Omega}_{i\eta})} + \frac{1}{\eta} ||\overline{w}^{(i)}||^2_{L^2_{\rho_i}(\mathcal{E}_{ij})} \right) \qquad (4.19) \\
&\leq C\left(|\mathcal{H}^{(i)}_{\mathcal{E}_{ij}} \overline{w}^{(i)}|^2_{H^1_{\rho_i}(\widetilde{\Omega}_{i\eta})} + \frac{1}{\eta\mu^{(i)}_{L+1}} |\mathcal{H}^{(i)}_{\mathcal{E}_{ij}} \hat{w}^{(i)}|^2_{H^1_{\rho_i}(\Omega_i)} \right) \\
&\leq C\left(1 + \frac{1}{\eta\mu^{(i)}_{L+1}}\right) |w^{(i)}|^2_{H^1_{\rho_i}(\Omega_i)}.
\end{aligned}$$

In the penultimate step, we have applied (4.4). In the last step, we have used

Remark 4.1.3, (4.5), and (4.16). Finally, we obtain

$$\begin{aligned}&(\delta_j^\dagger)^2|\mathcal{H}^{(i)}_{\mathcal{E}_{ij}}\overline{w}^{(i)}|^2_{H^1_{\rho_i}(\widetilde{\Omega}_{i\eta})}+\frac{1}{\eta^2}(\delta_j^\dagger)^2||\mathcal{H}^{(i)}_{\mathcal{E}_{ij}}\overline{w}^{(i)}||^2_{L^2_{\rho_i}(\widetilde{\Omega}_{i\eta})}\\ \leq& C\left(1+\frac{1}{\eta\mu^{(i)}_{L+1}}\right)|w^{(i)}|^2_{H^1_{\rho_i}(\Omega_i)}.\end{aligned}$$

We can estimate the term $(\delta_j^\dagger)^2||\mathcal{H}^{(i)}_{\mathcal{E}_{ij}}\overline{w}^{(j)}||^2_{H^1_{\rho_i}(\widetilde{\Omega}_{i\eta})}$ analogously and obtain

$$(\delta_j^\dagger)^2||\mathcal{H}^{(i)}_{\mathcal{E}_{ij}}\overline{w}^{(j)}||^2_{H^1_{\rho_i}(\widetilde{\Omega}_{i\eta})}\leq C\left(1+\frac{1}{\eta\mu^{(i)}_{L+1}}\right)(\delta_j^\dagger)^2|\mathcal{H}^{(i)}_{\mathcal{E}_{ij}}\hat{w}^{(j)}|^2_{H^1_{\rho_i}(\Omega_i)}.$$

Application of Lemma 4.3.1 yields

$$\begin{aligned}(\delta_j^\dagger)^2|\mathcal{H}^{(i)}_{\mathcal{E}_{ij}}\left(w^{(j)}-\Pi^{(i)}_K w^{(j)}\right)|^2_{H^1_{\rho_i}(\Omega_i)}&\leq\frac{1}{\nu^{(i)}_{K+1}}(\delta_j^\dagger)^2\frac{\hat{\rho}_i}{\hat{\rho}_j}|\mathcal{H}^{(j)}_{\mathcal{E}_{ij}}w^{(j)}|^2_{H^1_{\rho_j}(\Omega_j)}\\ &\leq\frac{1}{\nu^{(i)}_{K+1}}|w^{(j)}|^2_{H^1_{\rho_j}(\Omega_j)}\end{aligned}$$

and we obtain the estimate

$$\begin{aligned}&|\mathcal{H}^{(i)}_{\rho_i}I^h(\theta_{\mathcal{E}_{ij}}v^{(i)})|^2_{H^1_{\rho_i}(\Omega_i)}\\ \leq&\hat{C}\left(1+\log\left(\frac{\eta}{h}\right)\right)^2\left(1+\frac{1}{\eta\mu^{(i)}_{L+1}}\right)\left(|w^{(i)}|^2_{H^1_{\rho_i}(\Omega_i)}+|w^{(j)}|^2_{H^1_{\rho_i}(\Omega_i)}\right)\end{aligned}$$

with $\hat{C}=C\max\left\{1,\frac{1}{\nu^{(i)}_{K+1}}\right\}$. □

Remark 4.4.3. *In our final estimate we see that there is no dependence on* $\left(\frac{H}{\eta}\right)^2$ *for the upper bound. The reason for this is the eigenvalue estimate. Consider a problem where the smallest non-zero eigenvalue* μ_2 *does not depend on the contrast in the coefficient* ρ*, e.g., the case where the coefficient is constant on each subdomain. In that case, we can estimate the* L^2*-term in* (4.19) *with the trace theorem and a Poincaré inequality. To get an explicit dependence of the trace theorem constant on* H/η *we transform the integral on the edge to unit length and transform integrals over* $\widetilde{\Omega}_{i\eta}$ *to the unit square* $\hat{\Omega}$*. Without loss of generality, let* $\widetilde{\Omega}_{i\eta}=[0,\eta]\times[0,H]$ *and* $u\in H^1(\widetilde{\Omega}_{i\eta})$*. Let*

$$\Phi(\hat{x}_1,\hat{x}_2)=(\eta\hat{x}_1,H\hat{x}_2)=:(x_1,x_2)$$

be the linear transformation from the unit square $\hat{\Omega}$ *to the slab* $\widetilde{\Omega}_{i\eta}$ *and*

$$\phi(1, \hat{x}_2) = (\eta, H\hat{x}_2) = (\eta, x_2)$$

be the transformation from an edge of unit length to the edge $\{\eta\} \times [0, H]$. *Further let* $\hat{u} := u \circ \Phi$. *We then have* $\hat{u}_{|\hat{\mathcal{E}}} = (u \circ \Phi)_{|\hat{\mathcal{E}}} = u_{|\mathcal{E}} \circ \phi$. *Applying the trace theorem on the edge of unit length for the trace* γu *yields*

$$\begin{aligned}
\frac{1}{\eta}||\gamma u||^2_{L^2(\mathcal{E})} =& \frac{1}{\eta}\int_{\mathcal{E}} (\gamma u)^2 d\sigma \\
=& \int_{\hat{\mathcal{E}}} (\gamma u \circ \phi)^2 \sqrt{(D\phi)^T (D\phi)} d\sigma \\
=& \frac{1}{\eta}\int_{\hat{\mathcal{E}}} (\gamma u \circ \phi)^2 H d\sigma \\
=& \frac{H}{\eta}||\gamma u \circ \phi||^2_{L^2(\hat{\mathcal{E}})} \\
\leq& \frac{H}{\eta}||\gamma u \circ \phi||^2_{L^2(\partial\hat{\Omega})} \\
\leq& C(\hat{\Omega})\frac{H}{\eta}\left(||u \circ \Phi||^2_{L^2(\hat{\Omega})} + |u \circ \Phi|^2_{H^1(\hat{\Omega})}\right),
\end{aligned}$$

where $C(\hat{\Omega})$ *depends on the shape and on the diameter of* $\hat{\Omega}$. *By transformation to the slab with* Φ^{-1} *we obtain*

$$\begin{aligned}
\frac{1}{\eta}||u||^2_{L^2(\mathcal{E})} &\leq C(\hat{\Omega})\frac{H}{\eta}\left(\frac{1}{H\eta}||u||^2_{L^2(\widetilde{\Omega}_{i\eta})} + \left(\frac{H}{\eta}\right)|u|^2_{H^1(\widetilde{\Omega}_{i\eta})}\right) \\
&= C(\hat{\Omega})\left(\frac{1}{\eta^2}||u||^2_{L^2(\widetilde{\Omega}_{i\eta})} + \left(\frac{H}{\eta}\right)^2|u|^2_{H^1(\widetilde{\Omega}_{i\eta})}\right).
\end{aligned}$$

Using this estimate for $w^{(i)} - c$ *and applying a Poincaré inequality, we have*

$$\begin{aligned}
\frac{1}{\eta}||w^{(i)} - c||^2_{L^2(\mathcal{E}_{ij})} &\leq C(\hat{\Omega})\left(\frac{1}{\eta^2}||w^{(i)} - c||^2_{L^2(\widetilde{\Omega}_{i\eta})} + \left(\frac{H}{\eta}\right)^2|w^{(i)}|^2_{H^1(\widetilde{\Omega}_{i\eta})}\right) \\
&\leq C(\hat{\Omega})\left(\frac{H}{\eta}\right)^2|w^{(i)}|^2_{H^1(\widetilde{\Omega}_{i\eta})}.
\end{aligned}$$

For similar scaling arguments regarding slabs, see also [29, 70].

4.5 Extension by Scaling

In the following, we construct a scaling for the extension which can be used as an alternative to (4.13), i.e., the Eigenvalue Problem 2.

Definition 4.5.1 (Extension scaling)**.** *For a pair of subdomains Ω_i and Ω_j sharing an edge $\mathcal{E}_{ij}$, let $D^{(i)}_{E_{ij},c}$ and $D^{(j)}_{E_{ij},c}$ be defined by*

$$D^{(i)}_{E_{ij},c} = (S^{(i)}_{\mathcal{E}_{ij},c,\rho_i} + S^{(j)}_{\mathcal{E}_{ij},c,\rho_j})^+ S^{(i)}_{\mathcal{E}_{ij},c,\rho_i} + A_{ij},$$

$$D^{(j)}_{E_{ij},c} = (S^{(i)}_{\mathcal{E}_{ij},c,\rho_i} + S^{(j)}_{\mathcal{E}_{ij},c,\rho_j})^+ S^{(j)}_{\mathcal{E}_{ij},c,\rho_j} + A_{ij},$$

where A_{ij} is defined by

$$A_{ij} = \frac{1}{2}\left(I - (S^{(i)}_{\mathcal{E}_{ij},c,\rho_i} + S^{(j)}_{\mathcal{E}_{ij},c,\rho_j})^+ (S^{(i)}_{\mathcal{E}_{ij},c,\rho_i} + S^{(j)}_{\mathcal{E}_{ij},c,\rho_j})\right).$$

By removing those columns and rows associated with the primal vertices at the endpoints of $\mathcal{E}_{ij}$, from the matrices $D^{(l)}_{E_{ij},c}$, $l = i, j$, we obtain the matrices $D^{(l)}_{E_{ij}}$. We define subdomain scaling matrices by

$$D^{(i)} = \sum_{\mathcal{E}_{ij} \subset \Gamma^{(i)}} R^{(i)T}_{E_{ij}} D^{(j)}_{E_{ij}} R^{(i)}_{E_{ij}}.$$

The scaled jump operator B_D in the FETI-DP algorithm is consequently given by $B_D := [D^{(1)T}B^{(1)}, \ldots, D^{(N)T}B^{(N)}]$ where the transpose is necessary since the $D^{(i)}$ are not symmetric.

When using the scaling in Definition 4.5.1, we build the vectors $D^{(j)T}_{E_{ij},c} M^{(i)}_{E_{ij}} x^{(i)}_k$ and $D^{(i)T}_{E_{ij},c} M^{(j)}_{E_{ij}} x^{(j)}_k$ instead of $M^{(l)}_{E_{ij}} x^{(l)}_k$, $l = i, j$, where $x^{(l)}_k$ are the eigenvectors computed from (4.1) and $M^{(l)}_{E_{ij}}$ is the mass matrix corresponding to the bilinear form $m^{(l)}_{\mathcal{E}_{ij},\rho}(\cdot,\cdot)$. We then discard the entries which are not associated with dual variables to obtain our constraints $u^{(l)}_k$.

Lemma 4.5.2. *For an edge $\mathcal{E}_{ij}$, let $I^{\mathcal{E}_{ij},(l)}_{L_l}$ for $l = i, j$ be defined by*

$$I^{\mathcal{E}_{ij},(l)}_{L_l} = \sum_{k=1}^{L_l} x^{(l)}_k x^{(l)T}_k M^{(l)}_{E_{ij}}$$

where $x_k^{(l)}$ are the eigenvectors from (4.1). Let $D_{E_{ij},c}^{(l)}$ be the scaling matrices in Definition 4.5.1. With the choice of the constraints $u_k^{(l)T}(w_i - w_j) = 0$, $l = i, j$ where $u_k^{(i)}$ and $u_k^{(j)}$ are obtained by discarding the entries not associated with dual variables in the vectors $D_{E_{ij},c}^{(j)T} M_{E_{ij}}^{(i)} x_k^{(i)}$ and $D_{E_{ij},c}^{(i)T} M_{E_{ij}}^{(j)} x_k^{(j)}$ with $\mu_k^{(l)} \leq TOL$ for $k = 1, \ldots, L_l$ we have

$$I_{L_i}^{\mathcal{E}_{ij},(i)} D_{E_{ij},c}^{(j)}(w_i - w_j) = 0 \quad \textit{and} \quad I_{L_j}^{\mathcal{E}_{ij},(j)} D_{E_{ij},c}^{(i)}(w_j - w_i) = 0.$$

Proof. The entries not associated with dual variables in $w_i - w_j$ are zero since $w_l = R^{(l)} w$ with $w \in \widetilde{W}$. Therefore, we have

$$I_{L_i}^{\mathcal{E}_{ij},(i)} D_{E_{ij},c}^{(j)}(w_i - w_j) = \sum_{k=1}^{L_i} x_k^{(i)} u_k^{(i)T}(w_{\Delta,i} - w_{\Delta,j}) = 0.$$

where $w_{\Delta,l}$ denotes the dual part of w_l, $l = i, j$. By an analogous argument, we conclude that $I_{L_j}^{\mathcal{E}_{ij},(j)} D_{E_{ij},c}^{(i)}(w_j - w_i) = 0$. □

For simplicity, we prove the next theorem only for the diffusion problem.

Theorem 4.5.3. *The condition number for our FETI-DP method with a scaling, as defined in Definition 4.5.1, with all vertices primal, and the coarse space enhanced with solutions of the eigenvalue problem (4.1), satisfies*

$$\kappa(\hat{M}^{-1}F) \leq C \left(1 + \log\left(\frac{\eta}{h}\right)\right)^2 \left(1 + \frac{1}{\eta \mu_{L+1}}\right),$$

where $\hat{M}^{-1} = M_{PP}^{-1}$ or $\hat{M}^{-1} = M_{BP}^{-1}$. Here, $C > 0$ is a constant independent of ρ, H, h, and η, and

$$\frac{1}{\mu_{L+1}} = \max_{l=1,\ldots,N} \left\{ \frac{1}{\mu_{L_k+1}^{(l)}} \right\}.$$

Proof. The proof is modeled on the proof of Theorem 4.4.1; see also [42]. With application of Lemma 4.5.2 and noting that the jump $w_i - w_j$ is zero in the endpoints of an edge we obtain for each edge $\mathcal{E}_{ij}$ in $|P_D w|_{\tilde{S}}^2$ the term

$$|I^h(\theta_{\mathcal{E}_{ij}} D^{(i)}(w_i - w_j))|_{S_i}^2 = |I^h(\theta_{\mathcal{E}_{ij}}((I - I_{L_i}^{\mathcal{E}_{ij},(i)}) D^{(i)}(w_i - w_j)))|_{S_i}^2.$$

Using Lemma 4.2.2 and Lemma 4.2.3, we obtain

$$
\begin{aligned}
&|I^h(\theta_{\mathcal{E}_{ij}} D^{(i)}(w_i - w_j))|^2_{S_i} = |I^h(\theta_{\mathcal{E}_{ij}}((I - I^{\mathcal{E}_{ij},(i)}_{L_i})D^{(i)}(w_i - w_j)))|^2_{S_i} \\
&\leq C\left(1 + \log\left(\frac{\eta}{h}\right)\right)^2 \left(|\mathcal{H}^{(i)}_{\mathcal{E}_{ij},c}\left((I - I^{\mathcal{E}_{ij},(i)}_{L_i})D^{(j)}_{E_{ij},c}(w_i - w_j)\right)|^2_{H^1_{\rho_i}(\widetilde{\Omega}_{i\eta})} \right. \\
&\qquad \left. + \frac{1}{\eta^2}||\mathcal{H}^{(i)}_{\mathcal{E}_{ij},c}\left((I - I^{\mathcal{E}_{ij},(i)}_{L_i})D^{(j)}_{E_{ij},c}(w_i - w_j)\right)||^2_{L^2_{\rho_i}(\widetilde{\Omega}_{i\eta})} \right) \\
&\leq C\left(1 + \log\left(\frac{\eta}{h}\right)\right)^2 \left(|\mathcal{H}^{(i)}_{\mathcal{E}_{ij},c}\left((I - I^{\mathcal{E}_{ij},(i)}_{L_i})D^{(j)}_{E_{ij},c}(w_i - w_j)\right)|^2_{H^1_{\rho_i}(\widetilde{\Omega}_{i\eta})} \right. \\
&\qquad \left. + \frac{1}{\eta}|| \left((I - I^{\mathcal{E}_{ij},(i)}_{L_i})D^{(j)}_{E_{ij},c}(w_i - w_j)\right)||^2_{L^2_{\rho_i}(\mathcal{E}_{ij})} \right) \\
&\leq C\left(1 + \log\left(\frac{\eta}{h}\right)\right)^2 \left(\left|\left((I - I^{\mathcal{E}_{ij},(i)}_{L_i})D^{(j)}_{E_{ij},c}(w_i - w_j)\right)\right|^2_{S^{(i)}_{\mathcal{E}_{ij},c,\rho_i}} \right. \\
&\qquad \left. + \frac{1}{\eta}\left|\left((I - I^{\mathcal{E}_{ij},(i)}_{L_i})D^{(j)}_{E_{ij},c}(w_i - w_j)\right)\right|^2_{M_{E_{ij}}} \right) \\
&\leq C\left(1 + \log\left(\frac{\eta}{h}\right)\right)^2 \left(1 + \frac{1}{\eta\mu^{(i)}_{L_i+1}}\right) \left|D^{(j)}_{E_{ij},c}(w_i - w_j)\right|^2_{S^{(i)}_{\mathcal{E}_{ij},c,\rho_i}} \\
&\leq C\left(1 + \log\left(\frac{\eta}{h}\right)\right)^2 \left(1 + \frac{1}{\eta\mu^{(i)}_{L_i+1}}\right) \left(|w_i|^2_{S^{(i)}_{\mathcal{E}_{ij},c,\rho_i}} + |w_j|^2_{S^{(j)}_{\mathcal{E}_{ij},c,\rho_j}}\right).
\end{aligned}
$$

Here, I denotes the identity operator. In the penultimate step, we have used Lemma 1.6.2 with $B = M_{E_{ij}}$, $x = D^{(j)}_{E_{ij},c}(w_i - w_j)$, $m = L_i$, $\Pi^B_M = I^{\mathcal{E}_{ij},(i)}_{L_i}$, and $A = S^{(i)}_{\mathcal{E}_{ij},c,\rho_i}$. For the last step, note that each column of A_{ij} in Definition 4.5.1 is in $\mathrm{Ker}\,(S^{(i)}_{\mathcal{E}_{ij},c,\rho_i} + S^{(j)}_{\mathcal{E}_{ij},c,\rho_j})$ and with the same argument as in the proof of Lemma 2.3.2, we have $\mathrm{Ker}\,(S^{(i)}_{\mathcal{E}_{ij},c,\rho_i} + S^{(j)}_{\mathcal{E}_{ij},c,\rho_j}) = \mathrm{Ker}\,(S^{(i)}_{\mathcal{E}_{ij},c,\rho_i}) \cap \mathrm{Ker}\,(S^{(j)}_{\mathcal{E}_{ij},c,\rho_j})$. Thus, we obtain $S^{(i)}_{\mathcal{E}_{ij},c,\rho_i} A_{ij} = 0$ and

$$
S^{(i)}_{\mathcal{E}_{ij},c,\rho_i} D^{(j)}_{E_{ij},c} = S^{(i)}_{\mathcal{E}_{ij},c,\rho_i} (S^{(i)}_{\mathcal{E}_{ij},c,\rho_i} + S^{(j)}_{\mathcal{E}_{ij},c,\rho_j})^+ S^{(j)}_{\mathcal{E}_{ij},c,\rho_j}.
$$

Applying Lemma 2.3.2 with $A = S^{(i)}_{\mathcal{E}_{ij},c,\rho_i}$, $B = S^{(j)}_{\mathcal{E}_{ij},c,\rho_j}$, and $D_A = D^{(j)}_{E_{ij},c}$ we obtain the estimate. □

Remark 4.5.4. *The constant in the condition number estimate in Theorem 4.5.3 depends on $N_{\mathcal{E}}^2$ in the same way as the condition number estimate for the first coarse space in Lemma 2.7.1 and as for the second coarse space in Lemma 3.3.1. Additionally, the constant depends on the constants in the weighted edge lemma (Lemma 4.2.2) and in the weighted Friedrichs inequality (Lemma 4.2.3); see also 4. in Remark 4.4.2.*

Remark 4.5.5. *As in Section 2.6, we can replace the matrices $S^{(l)}_{\mathcal{E}_{ij},c,\rho_l}$, $l = i, j$, by the economic version $S^{(l)}_{\mathcal{E}_{ij},c,\eta,\rho_l}$ in the scaling in Definition 4.5.1 and in the generalized Eigenvalue Problem 1.*

4.6 Numerical Results

4.6.1 FETI-DP with Projector Preconditioning or Balancing

In this section, we present numerical results for our algorithm with the adaptive coarse space defined in this chapter applied to scalar diffusion and linear elasticity problems using Eigenvalue Problem 1; see (4.1). We solve the eigenvalue problems in all experiments using the MATLAB function 'eig' which itself uses LAPACK. We always start with a FETI-DP coarse space using only vertices, often denoted as Algorithm A; cf. [82]. In this section, we choose the tolerance $\tau_\mu = 1$; see (4.9) and use *max-ρ-scaling* in this section. The numerical results are also published in [42]. Some of the results for elasticity are published in [36].

Diffusion Equation

We present numerical results for different coefficient distributions. We decompose the unit square into square subdomains and consider a coefficient distribution with different numbers of channels, cutting through subdomain edges; see Figures 4.4 and 4.5. All experiments for the diffusion equation are carried out with a homogeneous Dirichlet boundary condition on $\partial\Omega$ and a

constant right hand side $f = 1/10$. In Figure 4.6 the solutions for the diffusion equation with coefficient distributions from Figure 4.5 are shown. In case of one channel for each subdomain, we have a quasimonotone coefficient; cf. [72] and Definition 4.0.1. In this case, illustrated in Figure 4.4, on each interior edge the eigenvector corresponding to the eigenvalue zero is added to the coarse space. On interior edges, which do not intersect a channel with a high coefficient, the resulting constraint is a standard edge average. On interior edges intersecting a channel, the constraint is a weighted edge average, cf., also [45], up to a multiplicative constant. See also [67] for an analysis of the scalar elliptic case. This results in eight additional constraints; see Table 4.1. In case of two disjunct channels with a high coefficient on each edge, which intersects these channels, a maximum of two eigenvectors and in case of three channels, a maximum of three eigenvectors for each edge intersecting the channels are added to the coarse space; see Figure 4.5 for the coefficient distribution and Table 4.1 for the results. In Table 4.2, we see that the condition number of the algorithm with an enriched coarse space remains bounded if we change the contrast $\rho_2/\rho_1 \in \{1e3, 1e4, 1e5, 1e6\}$. Moreover, the number of adaptive constraints remains bounded. From Table 4.3 it can be seen that the number of adaptive constraints grows roughly in proportion to the number of subdomains and channels. Note that the adaptive algorithm chooses only constraints on subdomains where the Dirichlet boundary does not intersect the inclusions. In case of three channels on subdomains with Dirichlet boundary conditions that do not intersect the channels, six constraints, and on all inner subdomains, eight constraints are chosen. Linearly dependent constraints are detected using a singular value decomposition with a tolerance of $1e-6$ and afterwards removed. The additional constraints are implemented using balancing, i.e., M_{BP}. Alternatively, a transformation of basis could also be used. Our stopping criterion is the reduction of the preconditioned residual to $(1e-10)||z_0||_2+1e-16$, where z_0 is the preconditioned

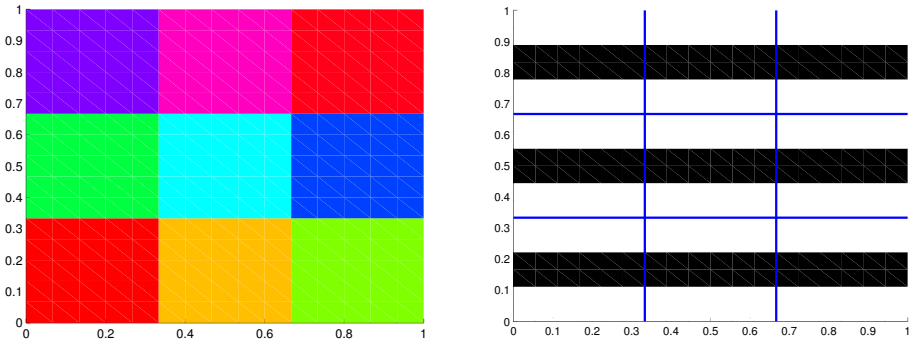

Figure 4.4: Domain decomposition in nine subdomains (left); coefficient distribution (right): One channel in black for each subdomain with high coefficient $\rho = \rho_2$ and $\rho = \rho_1 = 1$ in the white area; published in [42].

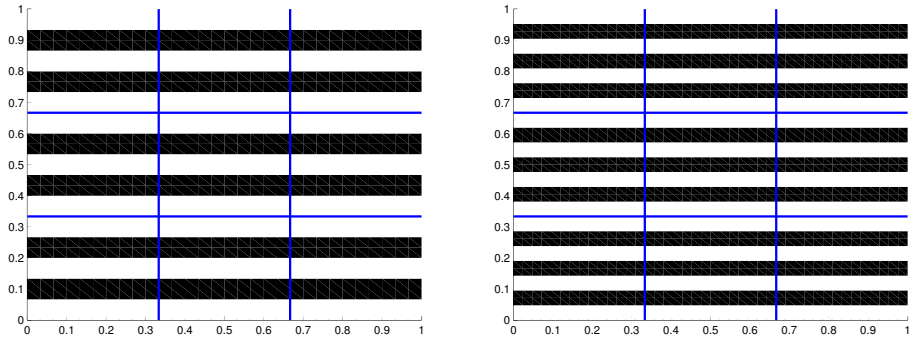

Figure 4.5: Coefficient distribution: Two channels for each subdomain (left), three channels for each subdomain (right). The black channels correspond to a high coefficient $\rho = \rho_2$, in the white area the coefficient is $\rho = \rho_1 = 1$; published in [42].

initial residual.

Elasticity with Discontinuous Coefficients

We test our algorithm for linear elasticity problems with certain distributions of varying coefficients inside subdomains. We impose homogeneous Dirichlet

# Channels		Algorithm A		**Adaptive Method**		# Adaptive constraints	# Dual Variables
	H/h	cond	# its	cond	# its	L	
1	6	9.55e4	7	**1.0412**	**3**	8	84
	12	1.20e5	7	**1.1547**	**4**	8	156
	18	1.33e5	7	**1.2519**	**4**	8	228
	24	1.44e5	8	**1.3325**	**4**	8	300
	30	1.52e5	8	**1.4011**	**5**	8	372
2	10	1.09e5	8	**1.0388**	**2**	14	132
	20	1.42e5	10	**1.1509**	**3**	14	252
	30	1.59e5	10	**1.2473**	**3**	14	372
	40	1.70e5	10	**1.3274**	**3**	14	492
	50	1.79e5	10	**1.3957**	**3**	14	612
3	14	39.21	6	**1.0387**	**2**	20	180
	28	1.34e5	10	**1.1507**	**3**	20	348
	42	1.39e5	11	**1.2471**	**3**	20	516
	56	1.84e5	14	**1.3272**	**3**	20	684
	70	1.93e5	13	**1.3954**	**3**	20	852

Table 4.1: One, two, and three channels for each subdomain; see Figure 4.4 (right) and Figure 4.5. Adaptive method using eigenvalue problem (4.1). We have $\rho_2 = 1e6$ in the channel and $\rho_1 = 1$ elsewhere. The number of additional constraints is clearly determined by the structure of the heterogeneity and independent of the mesh size. $1/H = 3$. TOL_μ=1; published in [42].

	Algorithm A		**Adaptive Method**		# Adaptive	# Dual
ρ_2/ρ_1	cond	# its	cond	# its	constraints L	Variables
$1e0$	$3.21e0$	5	**1.6377**	**5**	4	348
$1e1$	$5.58e0$	7	**1.5665**	**7**	4	348
$1e2$	$2.00e1$	9	**1.4599**	**7**	8	348
$1e3$	$1.59e2$	9	**1.1506**	**4**	20	348
$1e4$	$1.55e3$	11	**1.1507**	**2**	20	348
$1e5$	$1.54e4$	12	**1.1507**	**2**	20	348
$1e6$	$1.34e5$	10	**1.1507**	**3**	20	348

Table 4.2: Three channels for each subdomain; see Figure 4.5 (right). Adaptive method using eigenvalue problem (4.1). We have an increasing ρ_2 in the channels and $\rho_1 = 1$ elsewhere. $H/h = 28$. The number of additional constraints is bounded for an increasing contrast ρ_2/ρ_1. $1/H = 3$. TOL_μ=1; published in [42].

	Algorithm A		**Adaptive Method**		# Adaptive	# Dual
$1/H$	cond	# its	cond	# its	constraints L	Variables
2	$1.01e0$	4	**1.0100**	**1**	0	114
3	$1.34e5$	10	**1.1507**	**3**	20	348
4	$2.38e5$	16	**1.1507**	**3**	42	702
5	$3.02e5$	45	**1.1507**	**3**	72	1176
6	$3.55e5$	51	**1.1507**	**3**	110	1770

Table 4.3: Three channels for each subdomain; see Figure 4.5 (right). Increasing number of subdomains and channels. We have $\rho_2 = 1e6$ in the channel and $\rho_1 = 1$ elsewhere. $H/h = 28$. TOL_μ=1. The table was published in [42].

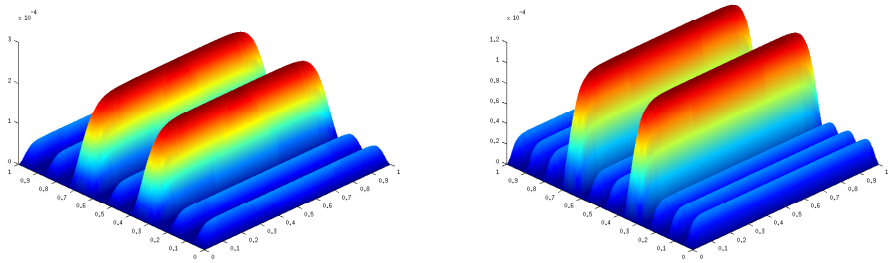

Figure 4.6: Solution of $-\text{div}\,(\rho\nabla u) = 1/10$ on $\Omega = (0,1)^2$, $u = 0$ on $\partial\Omega$ for the coefficient distributions given in Figure 4.5.

boundary conditions on the lower part of the boundary where $y = 0$ and a constant volume force $f = (1/10, 1/10)^T$. First, we run a set of experiments for the coefficient distribution above with three channels and with jumps in the Young modulus E. We use the balancing preconditioner M_{BP} or the projector preconditioner M_{PP} in our examples.

In our current strategy, we need to solve eigenvalue problems on all edges, i.e., also on edges where no heterogeneity appears and thus no additional constraints are necessary. A strategy to identify difficult edges, especially in the nonlinear context, may be desirable to reduce the computational cost. In Figure 4.8, the FETI-DP starting residual is plotted for the coefficient distribution depicted in Figure 4.5. Clearly, the difficult edges can be identified from the distribution of the residual on the interface Γ. An automatic strategy to identify the difficult edges may thus be developed in the future based on the residual. We have recently learned about a similar strategy for one-level FETI methods [77].

Elasticity with Discontinuous Coefficients and Using Eigenvalue Problem 1 and Eigenvalue Problem 2

In our examples considered in Section 4.6, we have only used Eigenvalue

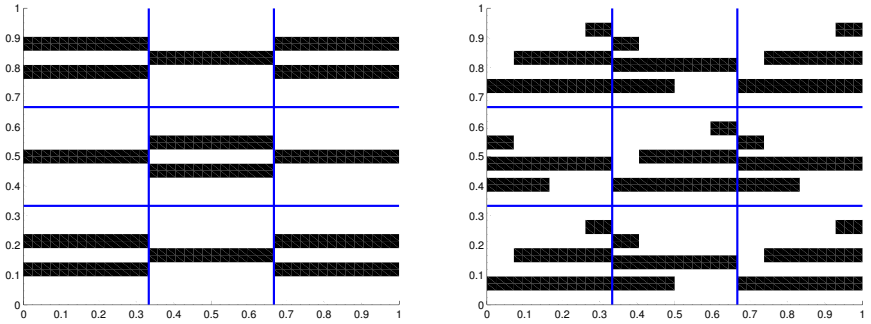

Figure 4.7: Test Problems with a coefficient distribution which is unsymmetric with respect to the edges for a 3x3 decomposition; see Table 4.5 (left) and Table 4.6 (right). Young's modulus $E = 1e6$ (black) and $E = 1$ (white); published in [42].

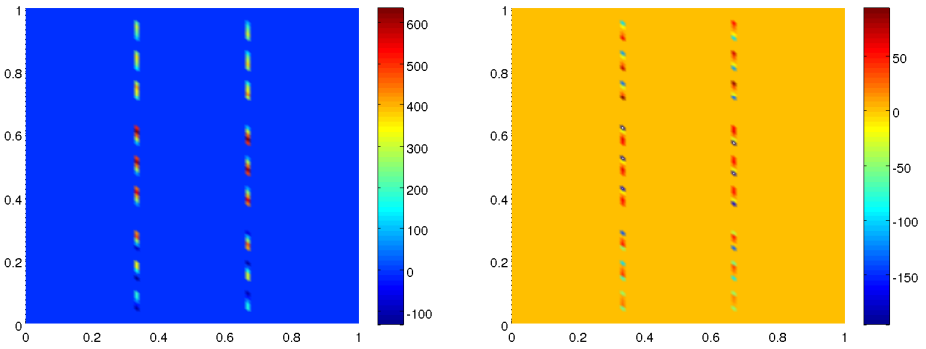

Figure 4.8: First (left) and second (right) component of the starting residuum of PCG in the test problem in Figure 4.5 (right) for linear elasticity with vertex constraints and $H/h = 28$. The oscillations of the residuum on the edges appear on the difficult edges and indicate additional constraints needed, e.g., from our eigenvalue problems; published in [42].

		M_{BP}		M_{PP}		# Adaptive	# Dual
E_2/E_1	H/h	cond	# its	cond	# its	constraints L	Variables
1	14	1.6744	11	1.6614	11	33	372
1	28	1.9208	12	1.8925	12	33	708
1	42	2.1022	13	2.0659	13	33	1044
$1e2$	14	2.7892	13	2.7734	13	54	372
$1e2$	28	2.3390	13	2.3227	13	62	708
$1e2$	42	2.2815	13	2.2678	14	62	1044
$1e4$	14	1.1701	8	1.1667	8	90	372
$1e4$	28	1.3431	9	1.3387	9	90	708
$1e4$	42	1.5064	11	1.5003	11	86	1044
$1e6$	14	1.1567	7	1.1703	8	114	372
$1e6$	28	1.3400	10	1.3363	10	114	708
$1e6$	42	1.5028	11	1.4974	11	114	1044

Table 4.4: Linear elasticity, three channels for each subdomain; see Figure 4.5 (right) with coefficient $E_2 = 1e6$ in the channels, outside the channels $E_1 = 1$, $\text{TOL}_\mu = 1$. The number of additional constraints is determined by the structure of the heterogeneity, independent of the mesh size and bounded for increasing contrast E_2/E_1; published in [42].

Problem 1, see (4.1), to enhance our coarse space. We will now consider coefficient distributions where this is not sufficient anymore and the additional Eigenvalue Problem 2, see (4.15), is necessary for the construction of a sufficient good coarse space. We test a coefficient distribution with jumps across and along the interfaces; see Figure 4.7. In these cases, it will be necessary to bound the extensions independently of the jumps in the coefficient; see also proof of Theorem 4.4.1. We use our strategy from Section 4.3. The numerical results are displayed in the Tables 4.5 and 4.6 for different tolerances for the eigenvalues $\overline{\nu}_k^{(i)}$ in Section 4.3. With a tolerance of "$-$", we denote the case where no additional constraints are chosen based on the respective eigenvalue

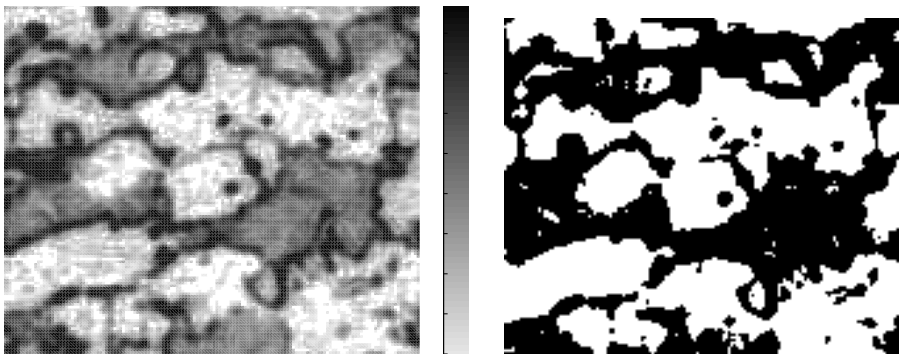

Figure 4.9: Microstructures obtained from electron backscatter diffraction (EBSD/FIB). Courtesy of Jörg Schröder, University of Duisburg-Essen, Germany, originating from a cooperation with ThyssenKrupp Steel. Left: gray scale image. Right: binary image. See Table 4.7 for the numerical results; published in [42].

problem, i.e., the tolerance is set to $-\infty$. We see from the results that we need both Eigenvalue Problems 1 and 2 to obtain a low condition number and iteration count.

Finally, we use a coefficient distribution obtained from a steel microsection pattern with 150×150 pixels; see Figure 4.9. We discretize the problem with $H/h = 50$ and $1/H = 3$; see Table 4.7 for the numerical results, which show the effectiveness of the adaptive algorithm now using both eigenvalue problems (4.1) and (4.15).

4.6.2 BDDC with a Transformation of Basis

We now present a few numerical examples that support our theory for the BDDC method using a transformation of basis to incorporate the adaptively computed constraints. We choose $\Omega = [0,1]^2$ with Dirichlet boundary conditions on $\partial\Omega$ and a constant right hand side $f = 1/10$. The coefficient distributions that we use in our BDDC experiments are depicted in Figure 4.10, 4.7 (right), and 4.5 (right). Algorithm A corresponds to a FETI-DP

Adaptive Method			M_{BP}		# Adaptive	# Dual
TOL_μ	TOL_ν	H/h	cond	# its	constraints $L+K$	Variables
–	–	14	$4.57e5$	> 250	0	372
–	–	28	$5.06e5$	> 250	0	708
–	–	42	$4.86e5$	> 250	0	1044
1	–	14	$2.21e5$	63	75	372
1	–	28	$2.75e5$	125	75	708
1	–	42	$3.05e5$	169	75	1044
1	1	14	1	1	312	372
1	1	28	1	1	648	708
1	1	42	1	1	984	1044
1	1/10	14	**1.1910**	**6**	160	372
1	1/10	28	**1.3816**	**8**	236	708
1	1/10	42	**1.5196**	**8**	308	1044
1	1/100	14	**1.1910**	**6**	156	372
1	1/100	28	**1.3820**	**8**	228	708
1	1/100	42	**1.5201**	**9**	300	1044

Table 4.5: Results for linear elasticity using the coefficient distribution for the heterogenous problem from the image in Figure 4.7 (left) with a Young modulus of $E_2 = 1e6$ (black) and $E_1 = 1$ (white) respectively. Decomposition into 3×3 subdomains. The first column refers to the tolerance for Eigenvalue Problem 1, see (4.1), the second column refers to the tolerance for Eigenvalue Problem 2, see (4.13). With a tolerance of "–" no additional constraints are chosen. L is the number of constraints from (4.1), K is the number of constraints from (4.13); published in [42].

Adaptive Method			M_{BP}		# Adaptive	# Dual
TOL_μ	TOL_ν	H/h	cond	# its	constraints $L+K$	Variables
–	–	14	3.00e5	>250	0	372
–	–	28	3.50e5	>250	0	708
–	–	42	3.73e5	>250	0	1044
1	–	14	2.24e5	81	93	372
1	–	28	2.79e5	192	93	708
1	–	42	3.13e5	>250	93	1044
1	1	14	1	2	312	372
1	1	28	1	2	648	708
1	1	42	1	2	984	1044
1	1/10	14	**1.2296**	**7**	156	372
1	1/10	28	**1.3876**	**9**	237	708
1	1/10	42	**1.5124**	**10**	297	1044
1	1/100	14	**1.2357**	**7**	152	372
1	1/100	28	**1.3921**	**10**	224	708
1	1/100	42	**1.5194**	**10**	284	1044

Table 4.6: Results for linear elasticity using the coefficient distribution for the heterogenous problem from the image in Figure 4.7 (right) with a Young modulus of $E_2 = 1e6$ (black) and $E_1 = 1$ (white) respectively. Decomposition into 3×3 subdomains. The first column refers to the tolerance for Eigenvalue Problem 1, see (4.1), the second column refers to the tolerance for Eigenvalue Problem 2, see (4.13). With a tolerance of "–" no additional constraints are chosen. L is the number of constraints from (4.1), K is the number of constraints from (4.13); published in [42].

.

	Adaptive Method					# Adaptive constraints	# Dual Variables
	TOL_μ	TOL_ν	H/h	cond	# its	$L+K$	
Fig. 4.9	1	–	50	$6.75e4$	> 250	89	1236
(left)	1	$1e-1$	50	**2.301**	**15**	237	1236
	1	$1e-2$	50	**6.5281**	**19**	218	1236
	1	$1e-3$	50	**8.5042**	**23**	213	1236
	–	–	50	$6.48e4$	> 250	0	1236
Fig. 4.9	1	–	50	$3.29e5$	> 250	135	1236
(right)	1	$1e-1$	50	**2.5552**	**14**	324	1236
	1	$1e-2$	50	**2.7634**	**15**	305	1236
	1	$1e-3$	50	**2.7645**	**16**	300	1236
	–	–	50	$5.52e5$	> 250	0	1236

Table 4.7: Results for linear elasticity using the coefficient distribution for the heterogenous problem from the gray scale image in Figure 4.9. We have set the coefficient $E_1 = 1$ for white and $E_2 = 1e6$ for black. An interpolated value is used for the different shades of gray. As above, TOL_μ is the tolerance for Eigenvalue Problem 1, see (4.1), TOL_ν is the tolerance for Eigenvalue Problem 2, see (4.13); published in [42].

method using only vertex constraints. In Table 4.8, we vary the number of elements for each subdomain. In Table 4.9, we vary the coefficient in the channels. In both cases, the coefficient distribution is symmetric with respect to the interface and thus the extension from Eigenvalue Problem 2 is not needed. Indeed, the results in Table 4.8 and 4.9 support that Eigenvalue Problem 1 is sufficient, here. Results for a varying number of subdomains are given in Table 4.10. We apply the adaptive method using Eigenvalue Problem 1 for the coefficient distribution in Figure 4.10 using standard ρ-scaling and deluxe scaling; see Table 4.11. The coefficient distribution is mildly unsymmetric and a good condition number is obtained using only Eigenvalue

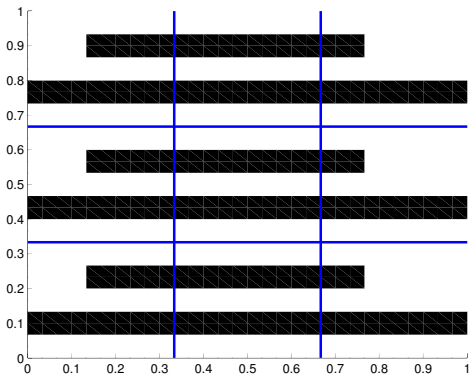

Figure 4.10: Coefficient distribution for a 3×3 domain decomposition with one channel connecting opposite boundaries and one shorter and off-centered channel per row of subdomains. Black corresponds to a high coefficient $\rho_2 = 1e6$, white corresponds to $\rho_1 = 1$; published in [41].

Problem 1. This is different for Figure 4.7 (right); see Table 4.12. Here, Eigenvalue Problem 2 seems to be necessary. It is interesting to note that, using deluxe scaling, results in a relatively low condition number when using Algorithm A; see Table 4.12. This is not the case in Table 4.11.

The numerical results presented here support our theory presented in this chapter. If the coefficient distribution is symmetric with respect to the interface or, at least has jumps only along but not across the interface, it is sufficient to use Eigenvalue Problem 1. If this is not the case both Eigenvalue Problems 1 and 2 should be used.

	Algorithm A Only vertices primal $\text{TOL}_\mu = -\infty$ $\text{TOL}_\nu = -\infty$			**Adaptive Method** EVP (4.1) $\text{TOL}_\mu = 1$			**Adaptive Method** EVP (4.1)+(4.13) $\text{TOL}_\mu = 1$ $\text{TOL}_\nu = 1e-1$		
H/h	cond	its	$\lvert\Pi\rvert$	cond	its	$\lvert\Pi\rvert$	cond	its	$\lvert\Pi\rvert$
14	$1.227e5$	13	4	**1.0387**	**2**	24	**1.0387**	**2**	24
28	$1.545e5$	17	4	**1.1507**	**3**	24	**1.1507**	**3**	24
42	$1.730e5$	16	4	**1.2471**	**3**	24	**1.2462**	**4**	28
56	$1.861e5$	16	4	**1.3272**	**3**	24	**1.3272**	**3**	24
70	$1.962e5$	16	4	**1.3954**	**3**	24	**1.3954**	**5**	28

Table 4.8: Three channels for each subdomain; see Figure 4.5 (right). We have $\rho_2 = 1e6$ in the channel and $\rho_1 = 1$ elsewhere. The number of additional constraints is clearly determined by the structure of the heterogeneity and independent of the mesh size. $1/H = 3$. The number of primal constraints is denoted by $|\Pi|$; published in [41].

	Algorithm A Only vertices primal $\text{TOL}_\mu = -\infty$ $\text{TOL}_\nu = -\infty$			**Adaptive Method** EVP (4.1) $\text{TOL}_\mu = 1$			**Adaptive Method** EVP (4.1)+(4.13) $\text{TOL}_\mu = 1$ $\text{TOL}_\nu = 1e-1$		
ρ_2/ρ_1	cond	# its	$\lvert\Pi\rvert$	cond	# its	$\lvert\Pi\rvert$	cond	# its	$\lvert\Pi\rvert$
$1e0$	3.207	5	4	**1.6376**	**5**	8	**1.6376**	**5**	8
$1e1$	5.581	7	4	**1.5663**	**7**	8	**1.5663**	**7**	8
$1e2$	$1.998e1$	9	4	**1.4599**	**7**	12	**1.4567**	**7**	16
$1e3$	$1.591e2$	10	4	**1.1505**	**4**	24	**1.1505**	**4**	32
$1e4$	$1.550e3$	13	4	**1.1507**	**3**	24	**1.1476**	**4**	31
$1e5$	$1.545e4$	15	4	**1.1507**	**3**	24	**1.1507**	**3**	28
$1e6$	$1.545e5$	17	4	**1.1507**	**3**	24	**1.1507**	**3**	24

Table 4.9: Three channels for each subdomain; see Figure 4.5 (right). Adaptive method using Eigenvalue Problems (4.1) and (4.13). We have ρ_2 in the channels and $\rho_1 = 1$ elsewhere. $H/h = 28$. The number of additional constraints is bounded for increasing contrast ρ_2/ρ_1. $1/H = 3$. The number of primal constraints is denoted by $|\Pi|$; published in [41].

	Algorithm A Only vertices primal $\text{TOL}_\mu = -\infty$ $\text{TOL}_\nu = -\infty$			**Adaptive Method** EVP (4.1) $\text{TOL}_\mu = 1$			**Adaptive Method** EVP (4.1)+(4.13) $\text{TOL}_\mu = 1$ $\text{TOL}_\nu = 1e-1$		
$1/H$	cond	# its	$\lvert\Pi\rvert$	cond	# its	$\lvert\Pi\rvert$	cond	# its	$\lvert\Pi\rvert$
2	1	1	1	**1.0000**	**1**	1	**1.0000**	**1**	1
3	$1.545e+05$	17	4	**1.1507**	**3**	24	**1.1507**	**3**	24
4	$2.734e+05$	26	9	**1.1507**	**3**	51	**1.1502**	**4**	59
5	$3.475e+05$	65	16	**1.1507**	**3**	88	**1.1507**	**3**	90
6	$4.078e+05$	65	25	**1.1507**	**3**	135	**1.1507**	**3**	152

Table 4.10: Three channels for each subdomain; see Figure 4.5 (right). Increasing number of subdomains and channels. We have $\rho_2 = 1e6$ in the channels and $\rho_1 = 1$ elsewhere. $H/h = 28$. The number of primal constraints is denoted by $|\Pi|$; published in [41].

	Algorithm A ($\text{TOL}_\mu = -\infty$, $\text{TOL}_\nu = -\infty$)					**Adaptive Method** EVP (4.1) ($\text{TOL}_\mu = 1$)				
	ρ-scaling		Deluxe			ρ-scaling		Deluxe		
H/h	cond	its	cond	its	$\lvert\Pi\rvert$	cond	its	cond	its	$\lvert\Pi\rvert$
10	6.201e4	25	6.200e4	20	4	**1.1480**	**6**	**1.1421**	**5**	24
20	7.684e4	25	7.683e4	20	4	**1.1978**	**7**	**1.1948**	**6**	24
30	8.544e4	25	8.544e4	23	4	**1.2630**	**7**	**1.2618**	**6**	24

Table 4.11: Adaptive method for the coefficient distribution in Figure 4.10. $1/H = 3$. Deluxe scaling and standard ρ-scaling are used. The number of primal constraints is denoted by $|\Pi|$; published in [41].

				Multiplicity-scaling		Deluxe-scaling		
	TOL_μ	TOL_ν	H/h	cond	# its	cond	# its	$\lvert\Pi\rvert$
Alg. A	$-\infty$	$-\infty$	42	$2.492e5$	161	24.4261	17	4
EVP 1	1	$-\infty$	42	$2.496e5$	128	$9.760e4$	40	24
EVP 1+2	1	1/10	42	**1.5184**	**10**	**1.4306**	**9**	126

Table 4.12: Adaptive method for the heterogenous problem with a coefficient distribution from the image in Figure 4.7 (right) with a coefficient of $\rho_2 = 1e6$ (black) and $\rho_1 = 1$ (white) respectively. $1/H = 3$. Either multiplicity or deluxe scaling are used. The number of primal constraints is denoted by $|\Pi|$; published in [41].

5 Comparison of the Coarse Spaces

In this chapter, we compare the adaptive coarse spaces presented in Chapters 2, 3, and 4. This chapter is based on [38] and organized as follows. In the first section, we briefly sketch the differences in computational cost of the different algorithms. We compare numerical results of the algorithms in Section 5.2. In the last section, we summarize the comparison and discuss advantages and disadvantages of the different approaches.

5.1 A Brief Comparison of Computational Cost

For the algorithm discussed in Section 2.4 (first coarse space), the matrices $S_{E_{ij}}^{(l)}$ and $S_{E_{ij},0}^{(l)}$, $l = i, j$ have to be computed. These matrices are usually dense. For their computation a Cholesky factorization of a sparse matrix is required and will usually need $\mathcal{O}((H/h)^3)$ floating point operations in two space dimensions, since the inverse involved in the Schur complement is of size $(H/h)^2 \times (H/h)^2$. If the Schur complements are computed explicitly, which might be necessary depending on the chosen eigensolver, a matrix-matrix multiplication, a matrix-matrix addition, and forward-backward substitutions for multiple right-hand sides with the Cholesky factorization have to be performed. If LAPACK (or MATLAB, which itself uses LAPACK) is used the matrices $S_{E_{ij}}^{(i)} : S_{E_{ij}}^{(j)}$ and $S_{E_{ij},0}^{(i)} : S_{E_{ij},0}^{(j)}$ are needed in explicit form. Otherwise, an application of the Schur complement needs a few matrix-vector multiplications and a forward-backward substitution. For $S_{E_{ij}}^{(i)} : S_{E_{ij}}^{(j)}$, depending on the kernel of $S_{E_{ij}}^{(i)} + S_{E_{ij}}^{(j)}$, a pseudoinverse or a Cholesky factor-

ization is needed. For the scaling matrices a factorization of $S^{(i)}_{E_{ij},0} + S^{(j)}_{E_{ij},0}$ has to be performed. If no deluxe scaling but ρ-scaling is used, the matrix $D^{(i)T}_{E_{ij}} S^{(j)}_{E_{ij},0} D^{(i)}_{E_{ij}} + D^{(j)T}_{E_{ij}} S^{(i)}_{E_{ij},0} D^{(j)}_{E_{ij}}$ has to be computed instead of $S^{(i)}_{E_{ij},0} : S^{(j)}_{E_{ij},0}$, which is much cheaper since no factorization of $S^{(i)}_{E_{ij},0} + S^{(j)}_{E_{ij},0}$ is needed. The computations of $S^{(l)}_{E_{ij},0,\eta}$ and $S^{(l)}_{E_{ij},\eta}$ need $(\eta/H)^{3/2}$ times as many floating point operations as the computations of $S^{(l)}_{E_{ij},0}$ and $S^{(l)}_{E_{ij}}$.

The eigenvalue problem described in Chapter 3.2 (second coarse space) is larger but sparser. The left-hand side is not dense because of the structure of the local jump operator $P_{D_{ij}}$ which contains only two non zero entries in each row. The right-hand side consists of two dense blocks and two zero blocks in the dual part. The size of the eigenvalue problem is determined by the number of degrees of freedom on $\Gamma^{(i)} \times \Gamma^{(j)}$ while the other algorithms are determined by the number of degrees of freedom on an edge $\mathcal{E}_{ij}$, e.g., in two dimensions it can be eight times larger. The computation of the left-hand side of the generalized eigenvalue problem in Section 3.2 also needs applications of the scaling matrices $D^{(i)}$ and $D^{(j)}$, which in case of deluxe scaling is more expensive than in case of multiplicity or ρ-scaling.

Eigenvalue Problem 1 discussed in Chapter 4 is completely local and needs no inter-subdomain communication but needs to be solved for two neighboring subdomains for each edge. For a chosen edge Eigenvalue Problem 2, presented in Chapter 4, has to be solved once for each subdomain sharing that edge but it needs inter-subdomain communication. While the algorithm in Chapter 2 needs to exchange the matrices $S^{(l)}_{E_{ij},0}$ and $S^{(l)}_{E_{ij}}$, $l = i, j$ and the scaling matrices, the algorithm in Section 3.2 needs to exchange $S^{(l)}$, the local jump matrices $B^{(l)}_E$, $l = i, j$, and the scaling matrices. Nonetheless, if ρ-scaling or deluxe scaling is used, the scaling data needs to be communicated for the construction of B_D in the FETI-DP algorithm anyways. The algorithm in Chapter 4 only needs to exchange $S^{(l)}_{\mathcal{E}_{ij},c,\rho_l}$, $l = i, j$. However, locally, in two dimensions, a one dimensional mass matrix has to be assembled

Coarse space in Chapter 2	First coarse space
Coarse space in Chapter 3	Second coarse space
Coarse space in Chapter 4	Third coarse space

Table 5.1: Short notation in the tables.

for each edge of a subdomain. Note that this matrix has tridiagonal form if piecewise linear finite element functions are used. This makes a Cholesky factorization very cheap.

A disadvantage of the algorithm in Chapter 4 (third coarse space) compared to the other algorithms is that no ρ-scaling with varying scaling weights inside of a subdomain can be used. In Section 5.2, we will see that using multiplicity scaling can lead to a large number of constraints. However, if the extension constant is nicely bounded, only local generalized eigenvalue problems with a tridiagonal mass matrix on the right-hand side need to be solved and the number of constraints remains bounded independently of H/h. This is the case, e.g., for coefficient distributions which are symmetric with respect to the subdomain interfaces (at least on slabs) and have jumps only along but not across edges. If the scaling in Section 4.5 is used, only the scaling matrices of neighboring subdomains have to be transferred. The eigenvectors in the first eigenvalue problem can be computed completely locally. The computation of the constraints includes an application of the mass matrix and the scaling matrix of a neighbor.

5.2 Numerical Examples

In this section, we will compare the different adaptive coarse spaces numerically. In Table 5.1, we introduce a short notation for the different coarse spaces. In all following numerical examples, we will remove linearly dependent constraints using a singular value decomposition of U. Constraints

related to singular values less then a drop tolerance of $1e-6$ are removed. In an efficient implementation this may not be feasible.

As a stopping criterion in the preconditioned conjugate gradient algorithm, we used $||r_k|| \leq 10^{-10}||r_0|| + 10^{-16}$, where r_0 is the preconditioned starting residual and r_k the preconditioned residual in the k-th iteration.

In our numerical experiments, whenever we need to compute a pseudoinverse of a symmetric matrix A, we first subdivide

$$A = \begin{pmatrix} A_{pp} & A_{rp}^T \\ A_{rp} & A_{rr} \end{pmatrix},$$

where A_{pp} is an invertible submatrix of A and A_{rr} is a small submatrix of A with a size of at least the dimension of the kernel of A. Then, we compute

$$A^+ = \begin{pmatrix} I & -A_{pp}^{-1}A_{rp}^T \\ 0 & I \end{pmatrix} \begin{pmatrix} A_{pp}^{-1} & 0 \\ 0 & S_{rr}^\dagger \end{pmatrix} \begin{pmatrix} I & 0 \\ -A_{rp}A_{pp}^{-1} & I \end{pmatrix}$$

using the Schur complement $S_{rr} = A_{rr} - A_{rp}A_{pp}^{-1}A_{rp}^T$. Here, $S_{rr}^\dagger$ denotes the Moore-Penrose pseudoinverse of S_{rr}. In the singular value decomposition of S_{rr}, we treat all singular values less then $(1e-3) \cdot \min(\text{diag}\,(A))$ as zero.

Throughout this section, we use *patch-ρ-scaling* whenever we write ρ-scaling.

We have considered different coefficient distributions. In Test Problem I (Figure 5.2), we consider the simple case of horizontal channels. In Test Problem II (Figure 5.3), the coefficient configuration is symmetric in a small neighborhood of vertical edges. In Test Problem III (Figure 5.4), the coefficient configuration is constructed with no symmetry with respect to the vertical edges. In Test Problem IV (Figure 5.6), we then have a challenging, randomly chosen coefficient distribution. Note that the coefficient distribution does not change when the meshes are refined. For our adaptive method, we therefore expect the number of constraints to remain bounded when H/h is increased. We attempt a fair comparison of the adaptive methods by using suitable tolerances for the different eigenvalues, i.e., we attemt to choose

tolerances such that all very large eigenvalues are removed but no more. Exemplarily, we present detailed spectra only for Test Problem IV; see Figure 5.6.

We present our numerical results in this chapter for FETI-DP methods, but they are equally valid for BDDC methods. The adaptive constraints are incorporated in the balancing preconditioner M_{BP}^{-1}, cf. equation (1.13), but other methods can also be used.

In Section 5.2.1, we first consider ρ-scaling, deluxe scaling and its economic variant for a standard case of constant coefficients on subdomains. In Section 5.2.2, we present numerical results for a scalar diffusion equation and Problems I-IV, using adaptive coarse spaces. In Section 5.2.3, we consider the problem of almost incompressible elasticity.

5.2.1 Comparison of Scalings

In Table 5.2, we consider ρ-, deluxe scaling, and an economic version of deluxe scaling (e-deluxe) for a compressible linear elasticity problem with a checker board distribution of the Young modulus; cf. Figure 5.1. We use a Young modulus of 10^6 for gray and of 1 for white subdomains and a constant Poisson ratio of $\nu = 0.3$. This is a standard, classic case with no jumps inside subdomains, which can successfully be treated by ρ-scaling. We observe no difference between the scalings in this situation.

5.2.2 Scalar Diffusion

First, we perform a comparison for our scalar diffusion problem with a variable coefficient for the first (Chapter 2 [68, 39]), second (Chapter 3 [59]) and third (Chapter 4 [42]) coarse spaces. We use homogenous Dirichlet boundary conditions on $\Gamma_D = \partial\Omega$ in all our experiments for scalar diffusion.

The first coefficient distribution is depicted in Figure 5.2 (Test Problem I; horizontal channels). This coefficient distribution is symmetric with respect

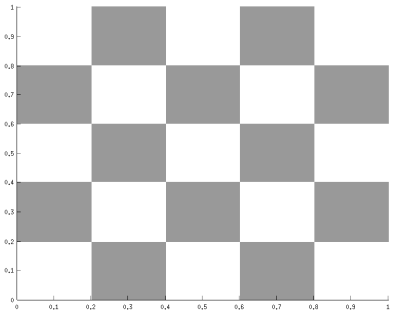

Figure 5.1: A simple checkerboard coefficient distribution with constant coefficients on subdomains is depicted for 5×5 subdomains; published in [38].

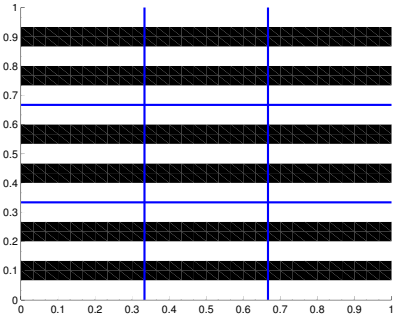

Figure 5.2: Test Problem I with a coefficient distribution consisting of two channels in each subdomain for a 3x3 decomposition. In case of diffusion the diffusion coefficient is 10^6 (black) and 1 (white). In case of elasticity the Young modulus is 10^3 (black) and 1 (white); published in [38].

		deluxe		e-deluxe		ρ	
$1/H$	H/h	cond	its	cond	its	cond	its
3	20	3.7701	4	3.7702	4	3.7702	4
3	30	4.2200	4	4.2200	4	4.2200	4
3	40	4.5409	4	4.5409	4	4.5409	4
5	20	3.5845	5	3.5845	5	3.5845	5
5	30	3.9855	5	3.9855	5	3.9855	5
5	40	4.2701	5	4.2701	5	4.2701	5

Table 5.2: Comparison of different scalings for linear elasticity using a simple checker board coefficient distribution for the Young modulus; see Figure 5.1. The table was published in [38].

to vertical edges. Since there are no jumps across the interface, the simple multiplicity scaling is sufficient, and $\rho-$scaling reduces to multiplicity scaling. The numerical results are presented in Table 5.3. The estimated condition numbers are identical for all cases and the number of constraints is similar.

In Table 5.4, we consider the coefficient distribution depicted in Figure 5.3 (Test Problem II; horizontal channels on slabs). Here, the coefficient distribution is symmetric on slabs with respect to vertical edges. Again, there are no coefficient jumps across subdomain interfaces, and multiplicity scaling is equivalent to ρ-scaling. We remark that in this test problem e-deluxe scaling with $H/\eta = 14$ is not equivalent to multiplicity scaling, since in the Schur complements $S^{(l)}_{E,0,\eta}$, $l = i, j$, the entries on $\partial\widetilde{\Omega}_{i\eta} \setminus (\partial\Omega_l \cap \partial\widetilde{\Omega}_{i\eta})$ are eliminated. In this case, the economic version of the extension scaling is equivalent to multiplicity scaling because the Schur complements $S^{(l)}_{E,\eta}$, $l = i, j$ are computed from local stiffness matrices on the slab. In Table 5.4, we report on multiplicity scaling, deluxe scaling, and e-deluxe scaling for the three cases. Using multiplicity scaling, the results are very similar, but not identical, for all three approaches to adaptive coarse spaces. The use of deluxe scaling can improve the results for the first two approaches. The use of extension scaling for the third approach has no significant impact. Where economic variants exist, e.g., versions on slabs, we also report on results using these methods. As should be expected using the economic versions of the eigenvalue problems yields worse results.

Next, we use the coefficient distribution depicted in Figure 5.4 (Test Problem III; unsymmetric channel pattern). The results are collected in Table 5.5. In this problem, coefficient jumps across the interface are present, in addition to the jumps inside subdomains. Therefore multiplicity scaling is not sufficient and all coarse space approaches are not scalable with respect to H/h, i.e., the number of constraints increases when H/h is increased; cf. Table 5.5 (left). Using ρ-scaling or deluxe/extension scaling yields the expected scala-

bility in H/h, i.e., the number of constraints remains bounded when H/h is increased. Where deluxe scaling is available, it significantly reduces the size of the coarse problem; cf. Table 5.5 (middle and right). The smallest coarse problem is then obtained for the combination of the second coarse space with deluxe scaling. Using extension scaling in the third coarse space approach yields smaller condition numbers and iteration counts for ρ-, deluxe-, or extension scaling but at the price of a much larger coarse space. In Table 5.6, we present results for Test Problem III using the slab variant of the first coarse space. Our results show that saving computational work by using the slab variants can increase the number of constraints significantly, namely, the number of constraints increases with decreasing η/H. On the other hand the condition numbers and iteration counts decrease. This implies that slab variants can be affordable if a good coarse space solver is available. The results may also indicate that scalability of the coarse space size with respect to H/h may be lost.

The results for Test Problem IV are collected in Table 5.7. Also for this difficult problem the number of constraints seems to remain bounded when H/h is increased although for $\rho-$scaling the number of constraints increases slightly with H/h. The smallest coarse problem, consisting of only four eigenvectors, is obtained when the second coarse space approach is combined with deluxe scaling although the difference between $\rho-$scaling and deluxe scaling is not as big as in Test Problem III. The third coarse space using extension scaling is scalable in H/h but, in this current version, yields the largest number of constraints. In Figure 5.5, we show the solutions for the coefficient distributions given in Figures 5.3 and 5.4 (Test Problems II and III).

The 50 largest eigenvalues appearing in the adaptive approaches for Test Problem IV using deluxe or extension scaling are presented in Figure 5.8. We can see that the tolerances chosen in Table 5.7 result in the removal of

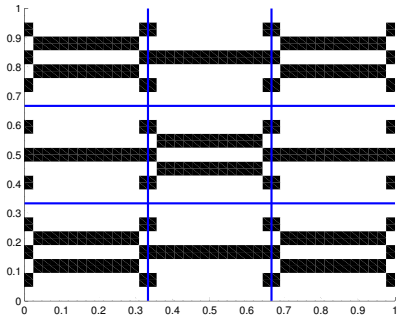

Figure 5.3: Test Problem II has a coefficient distribution symmetric in slabs with respect to the edges for a 3×3 decomposition. Diffusion coefficient 10^6 (black) and 1 (white). Domain decomposition in 3×3 subdomains, $H/\eta = 14$; published in [38].

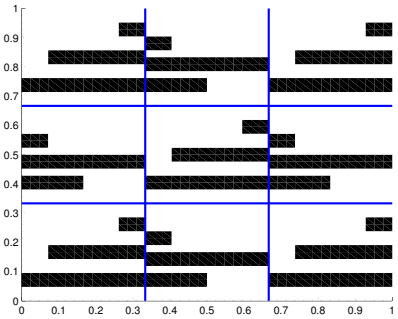

Figure 5.4: Test Problem III has a coefficient distribution which is unsymmetric with respect to the edges for a 3×3 decomposition. Diffusion coefficient 10^6 (black) and 1 (white); published in [38].

all large eigenvalues. We therefore believe that our comparison is fair.

For the third coarse space, we have also tested the combination of multiplicity scaling with both eigenvalue problems from [42] with $\text{TOL}_\mu = 1/10$ and $\text{TOL}_\nu = 1/10$. As in the other cases where we use multiplicity scaling, see Table 5.4, this leads to a small condition number but at the cost of a large number of constraints, and the approach thus is not scalable with respect to H/h.

Results for the slab variant of the third coarse space are presented in Table 5.8. In Table 5.7, we consider the distribution from Figure 5.6 for the different coarse space approaches. Note that we do not show the results for multiplicity scaling here, since the coarse space grows significantly with H/h, and this approach is therefore not recommended.

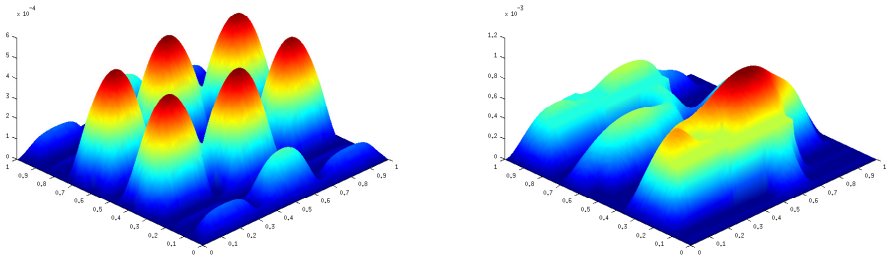

Figure 5.5: Solution of $-\mathrm{div}\,(\rho\nabla u) = 1/10$ on $\Omega = (0,1)^2$, $u = 0$ on $\partial\Omega$ for the coefficient distributions given in Figures 5.3 (Test Problem II, left) and 5.4 (Test Problem III, right).

	First coarse space with mult. scaling TOL $= 1/10$			Second coarse space with mult. scaling TOL $= 10$			Third coarse space with mult. scaling $\mathrm{TOL}_\mu = 1$, $\mathrm{TOL}_\nu = -\inf$			
H/h	cond	its	#EV	cond	its	#EV	cond	its	#EV	#dual
10	1.0388	2	14	1.0388	2	12	1.0388	2	14	132
20	1.1509	3	14	1.1509	3	12	1.1509	3	14	252
30	1.2473	3	14	1.2473	3	12	1.2473	3	14	372
40	1.3274	3	14	1.3274	3	12	1.3274	3	14	492

Table 5.3: Scalar diffusion. Test Problem I (see Figure 5.2); published in [38].

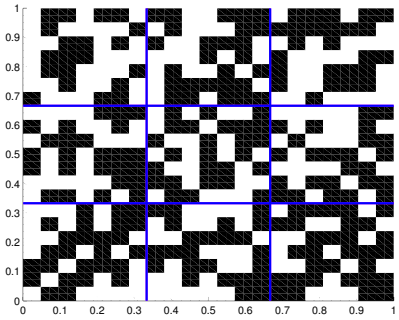

Figure 5.6: Test Problem IV has a random coefficient distribution which is constant on squares of size $1/21 \times 1/21$. Diffusion coefficient 10^6 (black) and 1 (white). Domain decomposition in 3×3 subdomains; published in [38].

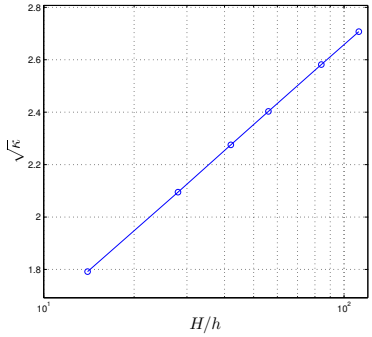

Figure 5.7: Plot of the square root of the condition number vs. H/h of the data given in Table 5.7 for the third coarse space with extension scaling using a logarithmic scale on the x-axis; published in [38].

	First coarse space with mult. scaling TOL = 1/10			Second coarse space with mult. scaling TOL = 10			Third coarse space with mult. scaling $\mathrm{TOL}_\mu = 1$, $\mathrm{TOL}_\nu = -\infty$			
H/h	cond	its	#EV	cond	its	#EV	cond	its	#EV	#dual
14	1.0469	5	20	1.0498	5	18	1.0467	6	20	180
28	1.1680	5	20	1.1710	5	18	1.1678	6	20	348
42	1.2696	6	20	1.2728	5	18	1.2695	6	20	516
56	1.3531	6	20	1.3564	6	18	1.3529	6	20	684
70	1.4238	6	20	1.4272	6	18	1.4237	7	20	852
	First coarse space on slabs with mult. scaling TOL = 1/10			Second coarse space			Third coarse space on slabs with mult. scaling $\mathrm{TOL}_\mu = 1$, $\mathrm{TOL}_\nu = -\infty$			
H/h	cond	its	#EV	cond	its	#EV	cond	its	#EV	#dual
14	1.0466	5	26				1.0465	6	24	180
28	1.1678	6	26		no		1.1677	6	24	348
42	1.2695	6	26		slab		1.2694	6	24	516
56	1.3530	6	26		variant		1.3529	6	24	684
70	1.4237	6	26				1.4236	6	24	852
	First coarse space with deluxe scaling TOL = 1/10			Second coarse space with deluxe scaling TOL = 10			Third coarse space with extension scaling $\mathrm{TOL}_\mu = 1$, $\mathrm{TOL}_\nu = -\infty$			
H/h	cond	its	# EV	cond	its	# EV	cond	its	# EV	# dual
14	1.2319	5	8	1.2510	6	6	1.0798	5	20	180
28	1.2948	6	8	1.3222	6	6	1.2170	5	20	348
42	1.4024	6	8	1.4403	6	6	1.3285	5	20	516
56	1.4906	6	8	1.5372	6	6	1.4189	6	20	684
70	1.5652	7	8	1.6188	7	6	1.4950	6	20	852

	First coarse space on slabs with e-deluxe scaling TOL = 1/10			Second coarse space			Third coarse space on slabs with extension scaling on slabs $\mathrm{TOL}_\mu = 1$, $\mathrm{TOL}_\nu = -\infty$			
H/h	cond	its	# EV	cond	its	# EV	cond	its	# EV	# dual
14	1.0256	5	22				1.0465	6	24	180
28	1.1218	6	26				1.1677	6	24	348
42	1.2143	6	26	no slab variant			1.2694	6	24	516
56	1.2945	6	26				1.3529	6	24	684
70	1.3645	6	26				1.4236	6	24	852

Table 5.4: Scalar diffusion. For the slab variants of the algorithms, we only consider the first and the third coarse space; see Sections 2 and 4. Test Problem II (see Figure 5.3), $H/\eta = 14$, $1/H = 3$; published in [38].

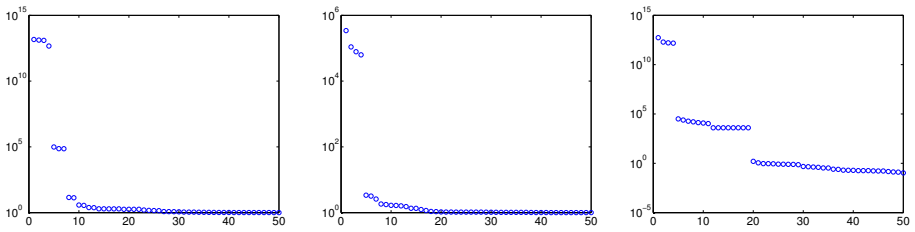

Figure 5.8: The 50 largest (inverse) eigenvalues of the generalized eigenvalue problems for Test Problem IV for $H/h = 28$; see Figure 5.6. First coarse problem using deluxe scaling, second coarse problem using deluxe scaling, and third coarse space using extension scaling (from left to right); cf. Table 5.7. The figure was published in [38].

Let us summarize our observations. The numerical results support the theory in Chapters 2, 3, and 4. For coefficient distributions that are symmetric with respect to the interface multiplicity scaling is sufficient and all coarse spaces have a similar size; see Table 5.3. In case of jumps both across

First coarse space, TOL = 1/10										
scal.	multiplicity			ρ			deluxe			
H/h	cond	its	#EV	cond	its	#EV	cond	its	#EV	#dual
14	1.2911	8	44	1.3874	9	15	4.8937	11	5	180
28	1.4148	9	74	1.5782	11	15	4.8672	12	5	348
42	1.5167	10	104	1.7405	11	15	4.8891	12	5	516
Second coarse space, TOL = 10										
scal.	multiplicity			ρ			deluxe			
H/h	cond	its	#EV	cond	its	#EV	cond	its	#EV	#dual
14	1.5013	9	42	1.5979	9	13	5.8330	11	3	180
28	1.6407	10	72	1.7351	11	13	5.8758	12	3	348
42	1.7413	10	102	1.8474	12	13	5.9296	13	3	516
Third coarse space, $\text{TOL}_\mu = 1$										
scal. TOL_ν	multiplicity $\text{TOL}_\nu = 1/10$			ρ			extension $\text{TOL}_\nu = -\infty$			
H/h	cond	its	#EV	cond	its	#EV	cond	its	#EV	#dual
14	1.2870	8	55	-			1.2498	8	20	180
28	1.4154	9	88	-			1.4238	9	20	348
42	1.5186	9	118	-			1.5525	10	20	516

Table 5.5: Scalar diffusion. Comparison of the coarse spaces for Test Problem III (see Figure 5.4); published in [38].

and along the interface, approaches with multiplicity scaling need a lot of constraints and the size of the coarse space depends on H/h. In case of ρ-, deluxe-, or extension-scaling this dependence is removed. Deluxe scaling yields the smallest coarse spaces in all our approaches but is also more expensive then ρ-scaling. The second approach equipped with deluxe scaling results in the smallest coarse space. The third coarse space with extension scaling is scalable with respect to H/h but yields more constraints than the first and second coarse space with deluxe scaling.

		First coarse space on slabs, e-deluxe scaling, TOL = 1/10			First coarse space on slabs, mult. scaling, TOL = 1/10			
η/h	H/h	cond	its	#EV	cond	its	#EV	#dual
1	14	1.1355	7	24	1.0776	6	52	180
1	28	1.1118	6	35	1.1831	7	89	348
1	42	1.1069	6	47	1.0881	7	133	516
2	14	1.1729	7	21	1.1552	7	48	180
2	28	1.2096	7	25	1.1867	7	82	348
2	42	1.1770	7	33	1.2897	8	116	516
3	14	1.3978	9	11	1.2912	8	44	180
3	28	1.2145	7	24	1.1865	7	82	348
3	42	1.3029	8	25	1.2941	8	112	516
5	14	1.4086	9	10	1.2911	8	44	180
5	28	1.3447	8	19	1.3021	8	78	348
5	42	1.2852	8	24	1.2927	8	112	516
10	14	2.6060	10	6	1.2911	8	44	180
10	28	1.4441	10	10	1.4148	9	74	348
10	42	1.5216	10	12	1.5171	9	105	516
14	14	4.8937	11	5	1.2911	8	44	180
28	28	4.8672	12	5	1.4148	9	74	348
42	42	4.8891	12	5	1.5167	10	104	516

Table 5.6: Test Problem III (see Figure 5.4). Results for the slab variant of Table 5.5; published in [38].

	First coarse space, TOL = 1/10						
scal.	ρ			deluxe			
H/h	cond	its	#EV	cond	its	#EV	#dual
14	7.3286	19	10	2.2748	11	7	180
28	8.8536	20	11	2.4667	10	9	348
42	6.4776	21	12	2.5994	10	9	516
56	7.0378	21	12	2.6947	11	9	684
84	7.8168	23	12	2.8302	11	9	1020
112	8.3651	24	13	2.9267	12	9	1356
	Second coarse space, TOL = 10						
scal.	ρ			deluxe			
H/h	cond	its	#EV	cond	its	#EV	#dual
14	7.4306	20	6	2.6263	12	4	180
28	9.0907	22	7	3.0782	13	4	348
42	8.3068	23	8	3.3914	13	4	516
56	9.0122	24	8	3.6362	14	4	684
84	7.8520	24	9	4.0141	15	4	1020
112	8.3651	24	10	4.3065	15	4	1356
	Third coarse space, $\text{TOL}_\mu = 1/10$, $\text{TOL}_\nu = -\infty$						
scal.	ρ			extension			
H/h	cond	its	#EV	cond	its	#EV	#dual
14				3.2109	12	19	180
28		no		4.3890	13	19	348
42		rho		5.1775	14	19	516
56		variant		5.7748	14	19	684
84				6.6648	15	19	1020
112				7.3288	16	19	1356

Table 5.7: Scalar diffusion. Test Problem IV (see Figure 5.6); published in [38].

Third coarse space Economic version of extension scaling					
H/h	η/h	cond	its	#EV	#dual
28	1	2.2478	11	50	348
28	2	1.9102	9	50	348
28	3	1.7047	9	50	348
28	4	1.5663	9	50	348
28	5	8.7645	13	33	348
28	6	7.4083	13	33	348
28	7	6.8836	13	33	348
28	8	6.6282	13	33	348
28	9	5.3208	13	29	348
28	10	5.2299	13	29	348
28	28	4.3890	13	19	348

Table 5.8: Scalar diffusion. Test Problem IV (see Figure 5.6). Third coarse space uses extension scaling with different η/h, see Definition 4.5.1 and Remark 4.5.5, only Eigenvalue Problem 1 with $\text{TOL}_\mu = 1/10$; also compare with the third coarse space in Table 5.7 for $H/h = 28$. On squares of four elements in each direction the coefficient is constant. Consequently, the number of constraints is reduced if the slab size η/h is increased such that a multiple of four is exceeded; published in [38].

5.2.3 Almost Incompressible Elasticity

In this section, we compare the algorithms for almost incompressible elasticity problems. First, we consider a problem with a constant coefficient distribution. Mixed displacement-pressure $\mathbb{P}2 - \mathbb{P}0$ elements are used for the discretization.

In the first test, we solve a problem with a Young modulus of 1 and a Poisson ratio of 0.499999. Zero Dirichlet boundary conditions are imposed on $\Gamma_D = \left\{(x, y) \in [0, 1]^2 | y = 0\right\}$. The results for the approach in Section 2.5.1 (first coarse space) with a tolerance 1/10 and varying H/h are presented in Table 5.9.

For constant $H/h = 20$ and varying Poisson ratio ν, see Table 5.10.

In the third case, we consider a distribution of Young's modulus from Figure 5.2 and a Poisson ratio of $\nu = 0.4999$. The result for the approach in Section 2.5.1 can be found in Table 5.11. For the related results of the algorithm in Chapter 3 (second coarse space [59]), see Tables 5.9, 5.10, and 5.11.

Note that the third coarse space algorithm is not suitable for this problem. Its eigenvalue problem is not based on a localization of the jump operator but designed to get constants in Korn-like inequalities and in an extension theorem that are independent of jumps in the coefficients. It therefore will not find the zero net flux condition which is necessary for a stable algorithm.

The first and second coarse space are reliable if the Poisson ratio ν approaches the incompressible limit; see Tables 5.9 and 5.10. With a constant Young modulus, the first coarse space needs approximately twice as many constraints as the second coarse space. However, if jumps in the Young modulus are present, the performance is similar; see Table 5.11.

	First coarse space mult. scal., TOL = 1/10			Second coarse space mult. scal., TOL = 10			
H/h	cond	its	#EV	cond	its	#EV	#dual var.
10	2.2563	12	32	6.3215	22	10	516
20	2.1821	14	34	5.4016	20	16	996
30	2.4743	15	34	5.1404	20	20	1476
40	2.6969	15	34	5.4856	20	22	1956

Table 5.9: Almost incompressible elasticity using a $\mathbb{P}2 - \mathbb{P}0$ finite elements discretization for 3×3 subdomains. Homogeneous coefficients with $E = 1$ and $\nu = 0.499999$; published in [38].

.

	First coarse space mult. scal., TOL = 1/10			Second coarse space mult. scal., TOL = 10			
ν	cond	its	#EV	cond	its	#EV	#dual var.
0.3	1.9078	12	34	7.7232	24	4	996
0.49	2.6715	14	34	5.1983	20	16	996
0.499	2.2745	14	34	5.3790	20	16	996
0.4999	2.1915	14	34	5.3993	20	16	996
0.49999	2.1830	14	34	5.4014	20	16	996
0.499999	2.1821	14	34	5.4016	20	16	996

Table 5.10: Almost incompressible elasticity using $\mathbb{P}2 - \mathbb{P}0$ finite elements and 3×3 subdomains. Homogeneous coefficients with $E = 1$. We vary ν, $H/h = 20$; published in [38].

5.3 Advantages and Disadvantages

We discuss some advantages and disadvantages of the algorithms presented here. This section is based on our work in [38]. For the first and second coarse space a condition number estimate is available for symmetric positive definite

	First coarse space mult. scal., TOL = 1/10			Second coarse space mult. scal., TOL = 10			
H/h	cond	its	#EV	cond	its	#EV	#dual var.
10	11.5279	25	50	11.3414	25	50	516
20	11.9831	23	54	11.8391	26	50	996
30	12.0786	23	54	11.9445	26	50	1476

Table 5.11: Almost incompressible elasticity using a $\mathbb{P}2-\mathbb{P}0$ finite elements discretization and 3×3 subdomains. Channel distribution with $E_1 = 1e3$ (black), $E_2 = 1$ (white) and $\nu = 0.4999$; cf. Figure 5.2. The table was published in [38].

problems in two dimensions; see Sections 2.4.2 and 2.5.1 for the first coarse space and Section 3.3 for the second coarse space, respectively. Also slab variants of the algorithms were provided, including proofs for the condition number bounds. A condition number estimate for the third coarse space, applied to scalar diffusion problems, can be found in Chapter 4 for constant $\rho-$scaling and for extension scaling. For this, a condition number estimate can be proven for linear elasticity using similar arguments and replacing H^1-seminorms by the elasticity seminorms. For all three coarse spaces, no theory exists yet for the three dimensional case but the second coarse space has been successfully applied to three dimensional problems in [60].

An advantage of the first and third coarse space is that the size of the eigenvalue problems depends only on the number of degrees of freedom on an edge. This has to be seen in comparison to the size of two local interfaces of two substructures in the second adaptive coarse space. In the eigenvalue problem for the first coarse space the involved matrices are dense while in the second coarse space the eigenvalue problem involves a sparse matrix on the left-hand side and a 2×2 block matrix with dense blocks on the right-hand side. However, the first coarse space needs the factorization of a matrix

on the left-hand side and possibly matrix-matrix multiplications with Schur complements if a direct eigensolver is used. The third coarse space needs the solution of two eigenvalue problems for each of two substructures sharing an edge with a dense matrix on the left-hand side and a tridiagonal matrix in case of piecewise linear elements on the right-hand side. It can be advantageous that these eigenvalue problems can be computed locally on one substructure and that for building the constraints, only in case of extension scaling, information of the neighboring substructure has to be used.

A multilevel BDDC variant for the second coarse space can be found in [76].

All coarse spaces require an additional factorization with matrix-matrix multiplications or multiple forward-backward substitutions if deluxe scaling is used. In case of multiplicity scaling and a nonsymmetric coefficient the size of all coarse spaces can depend on the size of the substructures H/h as can be seen in Section 5.2.

Bibliography

[1] W. N. Anderson, Jr. and R. J. Duffin. Series and parallel addition of matrices. J. Math. Anal. Appl., 26:576–594, 1969.

[2] L. Beirão da Veiga, L. F. Pavarino, S. Scacchi, O. B. Widlund, and S. Zampini. Isogeometric BDDC preconditioners with deluxe scaling. SIAM J. Sci. Comput., 36(3):A1118–A1139, 2014.

[3] Petter Bjørstad, Jacko Koster, and Piotr Krzyzanowski. Domain decomposition solvers for large scale industrial finite element problems. In Applied Parallel Computing. New Paradigms for HPC in Industry and Academia, volume 1947 of Lecture Notes in Comput. Sci., pages 373–383. Springer, Berlin, 2001.

[4] Petter Bjørstad and Piotr Krzyzanowski. A flexible 2-level Neumann-Neumann method for structural analysis problems. In Parallel Processing and Applied Mathematics, volume 2328 of Lecture Notes in Comput. Sci., pages 387–394. Springer, Berlin, 2002.

[5] Dietrich Braess. Finite elements. Cambridge University Press, Cambridge, third edition, 2007. Theory, fast solvers, and applications in elasticity theory, Translated from the German by Larry L. Schumaker.

[6] Susanne C. Brenner and L. Ridgway Scott. The mathematical theory of finite element methods, volume 15 of Texts in Applied Mathematics. Springer, New York, third edition, 2008.

[7] Franco Brezzi and Michel Fortin. Mixed and hybrid finite element methods, volume 15 of Springer Series in Computational Mathematics. Springer-Verlag, New York, 1991.

[8] Xiao-Chuan Cai. The use of pointwise interpolation in domain decomposition methods with nonnested meshes. SIAM J. Sci. Comput., 16(1):250–256, 1995.

[9] Juan G. Calvo. A BDDC algorithm with deluxe scaling for H(curl) in two dimensions with irregular subdomains. New York University Computer Science Technical Report TR2014-965, 2014.

[10] Carsten Carstensen and Roland Klose. Elastoviscoplastic finite element analysis in 100 lines of Matlab. J. Numer. Math., 10(3):157–192, 2002.

[11] Tony F. Chan, Barry F. Smith, and Jun Zou. Overlapping Schwarz methods on unstructured meshes using non-matching coarse grids. Numer. Math., 73(2):149–167, 1996.

[12] Eric T. Chung and Hyea Hyun Kim. A deluxe FETI-DP algorithm for a hybrid staggered discontinuous Galerkin method for H(curl)-elliptic problems. Internat. J. Numer. Methods Engrg., 98(1):1–23, 2014.

[13] Jean-Michel Cros. A preconditioner for the Schur complement domain decomposition method. In Domain Decomposition Methods in Science and Engineering, pages 373–380. National Autonomous University of Mexico (UNAM), Mexico City, Mexico, 2003. Proceedings of the 14th International Conference on Domain Decomposition Methods in Science and Engineering; http://www.ddm.org/DD14.

[14] Clark R. Dohrmann. A preconditioner for substructuring based on constrained energy minimization. SIAM J. Sci. Comput., 25(1):246–258, 2003.

[15] Clark R. Dohrmann, Axel Klawonn, and Olof B. Widlund. Domain decomposition for less regular subdomains: overlapping Schwarz in two dimensions. SIAM J. Numer. Anal., 46(4):2153–2168, 2008.

[16] Clark R. Dohrmann and Clemens Pechstein. Constraints and weight selection algorithms for BDDC. Talk at 21st International Conference on Domain Decomposition Methods, Rennes, France, June 25-29, 2012, http://www.numa.uni-linz.ac.at/~clemens/dohrmann-pechstein-dd21-talk.pdf.

[17] Clark R Dohrmann and Olof B Widlund. Some recent tools and a BDDC algorithm for 3D problems in H(curl). volume 91, pages 15–25. LNCSE series, Springer-Verlag, 2013.

[18] Clark R Dohrmann and Olof B Widlund. A BDDC Algorithm with Deluxe Scaling for three-dimensional H (Curl) Problems. Comm. Pure Appl. Math. (electronic), 2015.

[19] Victorita Dolean, Frédéric Nataf, Robert Scheichl, and Nicole Spillane. Analysis of a two-level Schwarz method with coarse spaces based on local Dirichlet-to-Neumann maps. Comput. Methods Appl. Math., 12(4):391–414, 2012.

[20] Zdeněk Dostál. Conjugate gradient method with preconditioning by projector. International Journal of Computer Mathematics, 23(3-4):315–323, 1988.

[21] Maksymilian Dryja, Marcus V. Sarkis, and Olof B. Widlund. Multilevel Schwarz methods for elliptic problems with discontinuous coefficients in three dimensions. Numer. Math., 72(3):313–348, 1996.

[22] Yalchin Efendiev, Juan Galvis, Raytcho Lazarov, and Joerg Willems. Robust domain decomposition preconditioners for abstract symmetric positive definite bilinear forms. ESAIM Math. Model. Numer. Anal., 46(5):1175–1199, 2012.

[23] Charbel Farhat, Michael Lesoinne, and Kendall Pierson. A scalable dual-primal domain decomposition method. Numer. Linear Algebra Appl., 7(7-8):687–714, 2000.

[24] Charbel Farhat, Michel Lesoinne, Patrick LeTallec, Kendall Pierson, and Daniel Rixen. FETI-DP: A dual-primal unified FETI method - part i: A faster alternative to the two-level FETI method. Internat. J. Numer. Methods Engrg., 50:1523–1544, 2001.

[25] Charbel Farhat, Kendall Pierson, and Michel Lesoinne. The second generation FETI methods and their application to the parallel solution of large-scale linear and geometrically non-linear structural analysis problems. Comput. Methods Appl. Mech. Engrg., 184(24):333 – 374, 2000.

[26] Yannis Fragakis and Manolis Papadrakakis. The mosaic of high performance domain decomposition methods for structural mechanics: Formulation, interrelation and numerical efficiency of primal and dual methods. Computer Methods in Applied Mechanics and Engineering, 192(3536):3799 – 3830, 2003.

[27] Juan Galvis and Yalchin Efendiev. Domain decomposition preconditioners for multiscale flows in high-contrast media. Multiscale Model. Simul., 8(4):1461–1483, 2010.

[28] Juan Galvis and Yalchin Efendiev. Domain decomposition preconditioners for multiscale flows in high contrast media: reduced dimension coarse spaces. Multiscale Model. Simul., 8(5):1621–1644, 2010.

[29] Sabrina Gippert, Axel Klawonn, and Oliver Rheinbach. Analysis of FETI-DP and BDDC for linear elasticity in 3D with almost incompressible components and varying coefficients inside subdomains. SIAM J. Numer. Anal., 50(5):2208–2236, 2012.

[30] Pierre Gosselet, Daniel Rixen, François-Xavier Roux, and Nicole Spillane. Simultaneous FETI and block FETI: Robust domain decomposition with multiple search directions. Internat. J. Numer. Methods Engrg., 2015.

[31] Weimin Han and B. Daya Reddy. Plasticity, volume 9 of Interdisciplinary Applied Mathematics. Springer, New York, second edition, 2013. Mathematical theory and numerical analysis.

[32] A. Heinlein, U. Hetmaniuk, A. Klawonn, and O. Rheinbach. The approximate component mode synthesis special finite element method in two dimensions: Parallel implementation and numerical results. J. Comput. Appl. Math., 289:116–133, 2015.

[33] Marta Jarošová, Axel Klawonn, and Oliver Rheinbach. Projector preconditioning and transformation of basis in FETI-DP algorithms for contact problems. Math. Comput. Simulation, 82(10):1894–1907, 2012.

[34] C. T. Kelley. Iterative methods for linear and nonlinear equations, volume 16 of Frontiers in Applied Mathematics. Society for Industrial and Applied Mathematics (SIAM), Philadelphia, PA, 1995.

[35] Hyea Hyun Kim and Eric T. Chung. A BDDC algorithm with enriched coarse spaces for two-dimensional elliptic problems with oscillatory and high contrast coefficients. Multiscale Model. Simul., 13(2):571–593, 2015.

[36] Axel Klawonn, Martin Lanser, Patrick Radtke, and Oliver Rheinbach. On an adaptive coarse space and on nonlinear domain decomposition. In Domain Decomposition Methods in Science and Engineering XXI, volume 98, pages 71–83. Springer-Verlag, Lecture Notes in Computational Science and Engineering, 2014. Proceedings of the 21st International Conference on Domain Decomposition Methods, Rennes, France, June 25-29, 2012. See also http://dd21.inria.fr/pdf/klawonna_plenary_3.pdf .

[37] Axel Klawonn, Luca F. Pavarino, and Oliver Rheinbach. Spectral element FETI-DP and BDDC preconditioners with multi-element subdomains. Comput. Methods Appl. Mech. Engrg., 198(3-4):511–523, 2008.

[38] Axel Klawonn, Patrick Radtke, and Oliver Rheinbach. A comparison of adaptive coarse spaces for iterative substructuring in two dimensions. Submitted for publication to ETNA. Preprint available online at http://tu-freiberg.de/sites/default/files/media/fakultaet-fuer-mathematik-und-informatik-fakultaet-1-9277/prep/2015-05_fertig.pdf.

[39] Axel Klawonn, Patrick Radtke, and Oliver Rheinbach. FETI-DP with different scalings for adaptive coarse spaces. PAMM - Proceedings in Applied Mathematics and Mechanics, 14(1):835–836, December 2014. http://dx.doi.org/10.1002/pamm.201410398.

[40] Axel Klawonn, Patrick Radtke, and Oliver Rheinbach. A Newton-Krylov-FETI-DP Method with an Adaptive Coarse Space applied to Elastoplasticity. In Domain Decomposition Methods in Science and Engineering XXII. LNCSE series, Springer-Verlag, 2015. Accepted for publication. Submitted January 31, 2014. Revised version May, 2014, to appear September 14, 2015. Proceedings of the 22nd Conference on Domain Decomposition Methods in Science and Engineering, Lugano, Switzerland, September 16-20, 2013. Available as a preprint at http://www.mi.uni-koeln.de/numerik/file/DD22_elastoplas.pdf.

[41] Axel Klawonn, Patrick Radtke, and Oliver Rheinbach. Adaptive coarse spaces for BDDC with a transformation of basis. In Domain Decomposition Methods in Science and Engineering XXII. LNCSE series, Springer-Verlag, 2015. Accepted for publication. Submitted January 2014, revised July 2014, to appear September 14, 2015. Proceedings of the 22nd Conference on Domain Decom-

position Methods in Science and Engineering, Lugano, Switzerland, September 16-20, 2013. Available as a preprint at http://www.mi.uni-koeln.de/numerik/file/DD22_bddc_Homepage_1.pdf.

[42] Axel Klawonn, Patrick Radtke, and Oliver Rheinbach. FETI-DP methods with an adaptive coarse space. SIAM J. Numer. Anal., 53(1):297–320, 2015.

[43] Axel Klawonn and Oliver Rheinbach. A parallel implementation of dual-primal FETI methods for three-dimensional linear elasticity using a transformation of basis. SIAM J. Sci. Comput., 28(5):1886–1906 (electronic), 2006.

[44] Axel Klawonn and Oliver Rheinbach. Inexact FETI-DP methods. Internat. J. Numer. Methods Engrg., 69(2):284–307, 2007.

[45] Axel Klawonn and Oliver Rheinbach. Robust FETI-DP methods for heterogeneous three dimensional elasticity problems. Comput. Methods Appl. Mech. Engrg., 196(8):1400–1414, 2007.

[46] Axel Klawonn and Oliver Rheinbach. Highly scalable parallel domain decomposition methods with an application to biomechanics. ZAMM Z. Angew. Math. Mech., 90(1):5–32, 2010.

[47] Axel Klawonn and Oliver Rheinbach. Deflation, projector preconditioning, and balancing in iterative substructuring methods: connections and new results. SIAM J. Sci. Comput., 34(1):A459–A484, 2012.

[48] Axel Klawonn, Oliver Rheinbach, and Olof B. Widlund. An analysis of a FETI-DP algorithm on irregular subdomains in the plane. SIAM J. Numer. Anal., 46(5):2484–2504, 2008.

[49] Axel Klawonn and Olof B. Widlund. Dual-primal FETI methods for linear elasticity. Comm. Pure Appl. Math., 59(11):1523–1572, 2006.

[50] Axel Klawonn, Olof B. Widlund, and Maksymilian Dryja. Dual-primal FETI methods for three-dimensional elliptic problems with heterogeneous coefficients. SIAM J. Numer. Anal., 40(1):159–179 (electronic), 2002.

[51] Jong Ho Lee. A Balancing Domain Decomposition by Constraints Deluxe Method for Reissner–Mindlin Plates with Falk–Tu Elements. SIAM J. Numer. Anal., 53(1):63–81, 2015.

[52] Jing Li. A dual-primal FETI method for incompressible Stokes equations. Numer. Math., 102(2):257–275, 2005.

[53] Jing Li and Olof Widlund. BDDC algorithms for incompressible Stokes equations. SIAM J. Numer. Anal., 44(6):2432–2455, 2006.

[54] Jing Li and Olof B. Widlund. FETI–DP, BDDC, and Block Cholesky Methods. Internat. J. Numer. Methods Engrg., 66(2):250–271, 2006.

[55] Jing Li and Olof B. Widlund. On the use of inexact subdomain solvers for BDDC algorithms. Comput. Methods Appl. Mech. Engrg., 196(8):1415–1428, 2007.

[56] Jan Mandel and Clark R. Dohrmann. Convergence of a balancing domain decomposition by constraints and energy minimization. Numer. Linear Algebra Appl., 10:639–659, 2003.

[57] Jan Mandel, Clark R. Dohrmann, and Radek Tezaur. An algebraic theory for primal and dual substructuring methods by constraints. Appl. Numer. Math., 54(2):167–193, 2005.

[58] Jan Mandel and Bedřich Sousedík. Adaptive coarse space selection in the BDDC and the FETI-DP iterative substructuring methods: Optimal face degrees of freedom. Springer, LNCSE, Domain decomposition methods in science and engineering XIX, 2007.

[59] Jan Mandel and Bedřich Sousedík. Adaptive selection of face coarse degrees of freedom in the BDDC and the FETI-DP iterative substructuring methods. Comput. Methods Appl. Mech. Engrg., 196(8):1389–1399, 2007.

[60] Jan Mandel, Bedřich Sousedík, and Jakub Šístek. Adaptive BDDC in three dimensions. Math. Comput. Simulation, 82(10):1812–1831, 2012.

[61] Jan Mandel and Radek Tezaur. On the convergence of a dual-primal substructuring method. Numer. Math., 88(3):543–558, 2001.

[62] Sujit Kumar Mitra and Madan Lal Puri. On parallel sum and difference of matrices. J. Math. Anal. Appl., 44:92–97, 1973.

[63] Reinhard Nabben and Cornelis Vuik. A comparison of deflation and the balancing preconditioner. SIAM J. Sci. Comput., 27(5):1742–1759, 2006.

[64] Roy A. Nicolaides. Deflation of conjugate gradients with applications to boundary value problems. SIAM J. Numer. Anal., 24(2):355–365, 1987.

[65] Duk-Soon Oh, Olof B. Widlund, and Clark R. Dohrmann. A BDDC algorithm for Raviart-Thomas vector fields. New York University Computer Science Technical Report TR2013-951, 2013.

[66] Luca F. Pavarino, Olof B. Widlund, and Stefano Zampini. BDDC preconditioners for spectral element discretizations of almost incompressible elasticity in three dimensions. SIAM J. Sci. Comput., 32(6):3604–3626, 2010.

[67] Clemens Pechstein. On iterative substructuring methods for multiscale problems. Proceedings of the 21st International Conference on Domain Decomposition Methods, LNCSE series, Springer-Verlag, available at http://dd21.inria.fr/pdf/pechstein_plenary.pdf, 2012.

[68] Clemens Pechstein and Clark R. Dohrmann. in Clemens Pechstein, Modern domain decomposition solvers - BDDC, deluxe scaling, and an algebraic approach. Slides to a talk at NuMa Seminar, JKU Linz, December 10th, 2013, http://people.ricam.oeaw.ac.at/c.pechstein/pechstein-bddc2013.pdf.

[69] Clemens Pechstein, Marcus Sarkis, and Robert Scheichl. New theoretical coefficient robustness results for FETI-DP. Domain Decomposition Methods in Science and Engineering XX, LNCSE series, Springer-Verlag, 2011.

[70] Clemens Pechstein and Robert Scheichl. Analysis of FETI methods for multiscale PDEs. Numer. Math., 111(2):293–333, 2008.

[71] Clemens Pechstein and Robert Scheichl. Analysis of FETI methods for multiscale PDEs. Part II: interface variation. Numer. Math., 118(3):485–529, 2011.

[72] Clemens Pechstein and Robert Scheichl. Weighted Poincaré inequalities. IMA J. Numer. Anal., 33(2):652–686, 2013.

[73] Oliver Rheinbach. Parallel scalable iterative substructuring: Robust exact and inexact FETI-DP methods with applications to elasticity. PhD thesis, Department of Mathematics, University of Duisburg-Essen, 2006.

[74] Daniel J. Rixen and Charbel Farhat. A simple and efficient extension of a class of substructure based preconditioners to heterogeneous structural mechanics problems. Internat. J. Numer. Methods Engrg., 44(4):489–516, 1999.

[75] J. C. Simo and T. J. R. Hughes. Computational inelasticity, volume 7 of Interdisciplinary Applied Mathematics. Springer-Verlag, New York, 1998.

[76] Bedřich Sousedík, Jakub Šístek, and Jan Mandel. Adaptive-multilevel BDDC and its parallel implementation. Computing, 95(12):1087–1119, 2013.

[77] Nicole Spillane. Oral Presentation. 22nd International Conference on Domain Decomposition Methods, Lugano, Switzerland, September 16-20, 2013.

[78] Nicole Spillane. Adaptive Multi Preconditioned Conjugate Gradient: Algorithm, Theory and an Application to Domain Decomposition. https://hal.archives-ouvertes.fr/hal-01170059, 2015.

[79] Nicole Spillane, Victorita Dolean, Patrice Hauret, Frédéric Nataf, Clemens Pechstein, and Robert Scheichl. A robust two-level domain decomposition preconditioner for systems of PDEs. Comptes Rendus Mathématique, 349(23):1255–1259, 2011.

[80] Nicole Spillane, Victorita Dolean, Patrice Hauret, Frédéric Nataf, Clemens Pechstein, and Robert Scheichl. Abstract robust coarse spaces for systems of PDEs via generalized eigenproblems in the overlaps. Numerische Mathematik, 126(4):741–770, 2014.

[81] Nicole Spillane and Daniel J. Rixen. Automatic spectral coarse spaces for robust finite element tearing and interconnecting and balanced domain decomposition algorithms. Internat. J. Numer. Methods Engrg., 95(11):953–990, 2013.

[82] Andrea Toselli and Olof Widlund. Domain decomposition methods—algorithms and theory, volume 34 of Springer Series in Computational Mathematics. Springer-Verlag, Berlin, 2005.

[83] Benoit Vereecke, Henri Bavestrello, and David Dureisseix. An extension of the FETI domain decomposition method for incompressible

and nearly incompressible problems. Computer Methods in Applied Mechanics and Engineering, 192(3132):3409 – 3429, 2003.

Erklärung

Ich versichere, dass ich die von mir vorgelegte Dissertation selbständig angefertigt, die benutzten Quellen und Hilfsmittel vollständig angegeben und die Stellen der Arbeit - einschließlich Tabellen, Karten und Abbildungen -, die anderen Werken im Wortlaut oder dem Sinn nach entnommen sind, in jedem Einzelfall als Entlehnung kenntlich gemacht habe; dass diese Dissertation noch keiner anderen Fakultät oder Universität zur Prüfung vorgelegen hat; dass sie - abgesehen von unten angegebenen Teilpublikationen - noch nicht veröffentlicht worden ist, sowie, dass ich eine solche Veröffentlichung vor Abschluss des Promotionsverfahrens nicht vornehmen werde. Die Bestimmungen der Promotionsordnung sind mir bekannt. Die von mir vorgelegte Dissertation ist von Prof. Dr. Klawonn betreut worden.

Ort, Datum Unterschrift

Nachfolgend genannte Teilpublikationen liegen vor:

Klawonn, A., Radtke, P. and Rheinbach, O., “A Comparison of adaptive coarse spaces for iterative substructuring in two dimensions”, submitted for publication to Electronic Transactions on Numerical Analysis. Preprint available online at
`http://tu-freiberg.de/sites/default/files/media/fakultaet-fuer-mathematik-und-informatik-fakultaet-1-9277/prep/2015-05_fertig.pdf`

Klawonn, A., Radtke, P. and Rheinbach, O., “FETI-DP Methods with an Adaptive Coarse Space”, SIAM J. Numer. Anal., 53 (1), p. 297–320, 2015.

Klawonn, A., Radtke, P. and Rheinbach, O., “Adaptive coarse spaces for BDDC with a transformation of basis”, LNCSE, Springer, Proceedings of the 22nd Conference on Domain Decomposition Methods in Science and Engineering, Lugano, Switzerland, Submitted January 2014, revised July 2014, to appear September 14, 2015.

Klawonn, A., Radtke, P. and Rheinbach, O., “A Newton-Krylov-FETI-DP Method with an Adaptive Coarse Space Applied to Elastoplasticity”, LNCSE, Springer, Proceedings of the 22nd Conference on Domain Decomposition Methods in Science and Engineering, Lugano, Switzerland, Submitted January 31, 2014. Revised version May, 2014, to appear September 14, 2015.

Klawonn, A., Lanser, M., Radtke, P. and Rheinbach, O., “On an adaptive coarse space and on nonlinear domain decomposition”, LNCSE, Springer, 98, p.71-83, Proceedings of the 21st Conference on Domain Decomposition Methods in Science and Engineering, Rennes, France, published version 2014.

Klawonn, A., Radtke, P. and Rheinbach, O., ”FETI-DP with different scalings for adaptive coarse spaces“, PAMM - Proceedings in Applied Mathematics and Mechanics, 14 (1), p. 835–836, December 2014.